



Dissertations

Theses and Dissertations

1993

Effect of solvent on 1,3-dipolar cycloaddition transition states

Sheila Louise Celsor
Loyola University Chicago

Follow this and additional works at: https://ecommons.luc.edu/luc_diss

 Part of the [Chemistry Commons](#)

Recommended Citation

Celsor, Sheila Louise, "Effect of solvent on 1,3-dipolar cycloaddition transition states" (1993).

Dissertations. 3013.

https://ecommons.luc.edu/luc_diss/3013

This Dissertation is brought to you for free and open access by the Theses and Dissertations at Loyola eCommons. It has been accepted for inclusion in Dissertations by an authorized administrator of Loyola eCommons. For more information, please contact ecommons@luc.edu.



This work is licensed under a [Creative Commons Attribution-Noncommercial-No Derivative Works 3.0 License](#).
Copyright © 1993 Sheila Louise Celsor

LOYOLA UNIVERSITY OF CHICAGO

**EFFECT OF SOLVENT ON
1,3-DIPOLAR CYCLOADDITION
TRANSITION STATES**

**A DISSERTATION SUBMITTED TO
THE FACULTY OF THE GRADUATE SCHOOL
IN CANDIDACY FOR THE DEGREE OF
DOCTOR OF PHILOSOPHY
DEPARTMENT OF CHEMISTRY**

BY

SHEILA LOUISE CELSOR

CHICAGO, ILLINOIS

MAY 1993

Copyright by Sheila L. Celsor, 1993
All rights reserved

TABLE OF CONTENTS

LIST OF ILLUSTRATIONS	iv
LIST OF TABLES	vi
LIST OF ABBREVIATIONS	ix
CHAPTER I	1
INTRODUCTION	1
CHAPTER II	7
HISTORY	7
CHAPTER III	37
RESULTS	37
1. Overall yields of mono-pyrazoline adducts.	37
2. Relative yields of mono-pyrazoline adducts and product ratios.	37
3. Rate of formation of monoadducts in n-hexane.	42
4. Rate of formation of monoadducts in acetonitrile.	53
5. Rate of disappearance of diphenyldiazomethane in hexane.	58
6. Rate of disappearance of diphenyldiazomethane in acetonitrile.	62
7. NMR analysis of mono- and bis-adducts.	67
CHAPTER IV	71
DISCUSSION	71
1. Overall yields of mono-pyrazoline adducts.	71
2. Relative yields and product ratios of monopyrazoline adducts.	73
3. Rate of formation of monoadducts in n-hexane.	75
4. Rate of formation of monoadducts in acetonitrile.	76

5. Rate of disappearance of diphenyldiazomethane in n-hexane.	77
6. Rate of disappearance of diphenyldiazomethane in acetonitrile.	77
7. Correlations with empirical solvent parameters.	77
8. Multiple linear regression analysis.	82
 CHAPTER V	 98
EXPERIMENTAL	98
1. General information.	98
2. Preparation of diphenyldiazomethane.	99
3. Reaction of diphenyldiazomethane with 7- <i>tert</i> -butoxynornadiene.	99
4. Isolation of mono- and bis-pyrazoline adducts.	100
5. Determination of HPLC response factors for mono- and bis-pyrazoline adducts.	105
6. HPLC analysis of mono- and bis-pyrazoline adducts.	106
7. Determination of residual diphenyldiazomethane.	106
8. Determination of rate of reaction between 7- <i>tert</i> -butoxynornadiene and diphenyldiazomethane in n-hexane and acetonitrile.	107
 APPENDIX	 109
 SPECTRA	 118
 REFERENCES	 138

LIST OF ILLUSTRATIONS

Figure	Page
1. Rate of disappearance of 7- <i>tert</i> -butoxynorbornadiene in 25 mL hexane solution. (×) are experimental data points and line is the quadratic regression curve	50
2. Rate of disappearance of 7- <i>tert</i> -butoxynorbornadiene in 50 mL hexane solution. (*) are experimental data points and line is the quadratic regression curve.	50
3. Rate of disappearance of 7- <i>tert</i> -butoxynorbornadiene in 25 mL CH ₃ CN solution. (×) are experimental data points and line is the quadratic regression curve.	57
4. Rate of disappearance of 7- <i>tert</i> -butoxynorbornadiene in 50 mL CH ₃ CN solution. (*) are experimental data points and line is the quadratic regression curve.. . . .	57
5. Plot of 1/c vs. time in 25 mL in hexane solution. (×) are experimental data points and line is the linear regression curve. The slope is k_{obs} for the apparent 2 nd order rate of Ph ₂ CN ₂ disappearance.	65
6. Plot of 1/c vs. time in 50 mL in hexane solution. (*) are experimental data points and line is the linear regression curve. The slope is k_{obs} for the apparent 2 nd order rate of Ph ₂ CN ₂ disappearance.	65
7. Plot of 1/c vs. time in 25 mL in CH ₃ CN solution. (×) are experimental data points and line is the linear regression curve. The slope is k_{obs} for the apparent 2 nd order rate of Ph ₂ CN ₂ disappearance.	66
8. Plot of 1/c vs. time in 50 mL in CH ₃ CN solution. (*) are experimental data	

- points and line is the linear regression curve. The slope is k_{obs} for the apparent 2nd order kinetics of Ph₂CN₂ disappearance. 66
9. Plot of $\log(\text{syn}/\text{anti})$ vs. solvent polarity scale, π^* . Open error bars (I) represent aprotic solvents, closed error bars (□) represent protic solvents, and the line is the linear regression curve for the aprotic solvents. 90
10. Cohesive energy density (δ_H^2) versus $\Sigma\text{syn}/\Sigma\text{anti}$ product ratio. The three straight lines are the linear regression curves when treating nonpolar, protic, and polar aprotic solvents separately 96

LIST OF TABLES

Table	Page
1. Partial rate factors of cycloaddition with 7-substituted norbornadienes	29
2. Product distribution of hexachlorocyclopentadiene cycloaddition	30
3. Stereochemistry of 1,3-dipolar cycloaddition of some 1,3-dipoles to 7-substituted norbornadienes	32
4. Overall yield of monoadduct	39
5. Relative percentages of monoadducts in selected solvents	40
6. Syn/Anti and Exo/Endo monoadduct ratios	41
7. Molar concentrations of monoadducts formed over time in 25 mL hexane solution ([7-TBN] = 0.502 M)	43
8. Molar concentrations of monoadducts formed over time in 50 mL hexane solution ([7-TBN] = 0.251 M)	44
9. Estimation of rate constants in a 25 mL hexane solution	46
10. Estimation of rate constants in a 50 mL hexane solution	46
11. Rate of disappearance of 7-TBN in a 25 mL n-hexane solution	48
12. Rate of disappearance of 7-TBN in a 50 mL n-hexane solution	49

13. Molar concentrations of monoadducts formed over time in a 25 mL CH ₃ CN solution ([7-TBN] = 0.502 M)	51
14. Molar concentrations of monoadducts formed over time in 50 mL CH ₃ CN solution ([7-TBN] = 0.251 M)	52
15. Estimate of rate constants in a 25 mL acetonitrile solution	53
16. Estimate of rate constants in a 50 mL acetonitrile solution	53
17. Rate of disappearance of 7-TBN in a 25 mL acetonitrile solution	55
18. Rate of disappearance of 7-TBN in a 50 mL acetonitrile solution	56
19. Determination of k_{obs} for the disappearance of Ph ₂ CN ₂ in a 25 mL hexane solution	60
20. Determination of k_{obs} for the disappearance of Ph ₂ CN ₂ in a 50 mL hexane solution	61
21. Determination of k_{obs} for the disappearance of Ph ₂ CN ₂ in a 25 mL CH ₃ CN solution	63
22. Determination of k_{obs} for the disappearance of Ph ₂ CN ₂ in a 50 mL CH ₃ CN solution	64
23. Single parameter correlations with log(Σ Syn/ Σ Anti)	79
24a. Analysis of variance for the Koppel-Palm equation	84
24b. Analysis of variance for the SSPA equation	86

24c. Analysis of variance for the AKT equation	88
25. Solvent parameters for the Koppel-Palm equation	110
26. Swain's acidity-basicity parameters, dielectric constants and refractive indices	111
27. Solvent parameters for the Abraham-Kamlet-Taft equation	113

LIST OF ABBREVIATIONS

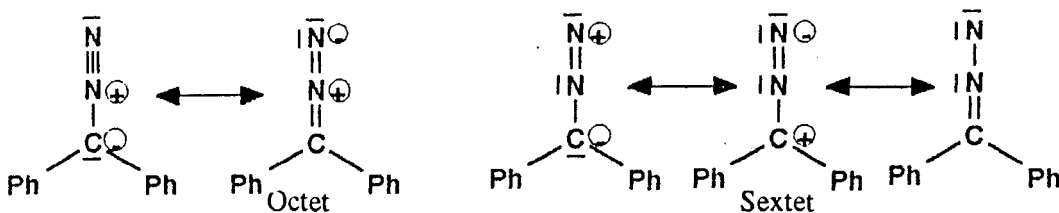
A	Absorbance
Å	angstroms
°C	degrees Celsius
δ	nuclear magnetic resonance chemical shift units, ppm
DMSO	Dimethylsulfoxide
F	Response factor (HPLC analysis)
ΔG	Gibbs free energy change
<i>h</i>	Planck's constant, 6.6256×10^{-34} J·s
ΔH _v ^o	Heat of vaporization, kcal/mol
<i>k'</i>	Boltzmann's constant, 1.3805×10^{-23} J/K
K	Temperature, Kelvin
LFER	Linear free energy relationship
LSER	Linear solvation free energy relationship
log	Base 10 logarithm
M	Molar concentration, mole/Liter
MO	Molecular Orbital
N	Number of data sets
Psi	Pounds per square inch
R	Gas Constant, 0.08206 L·atm/mol·K
R ²	Pearson correlation coefficient
R	Square root of Pearson correlation coefficient
s	Standard deviation
T	Temperature, Kelvin
7-TBN	7- <i>tert</i> -butoxynorbornadiene
TCNE	Tetracyanoethylene
THF	Tetrahydrofuran
TMS	Tetramethylsilane

CHAPTER I

INTRODUCTION

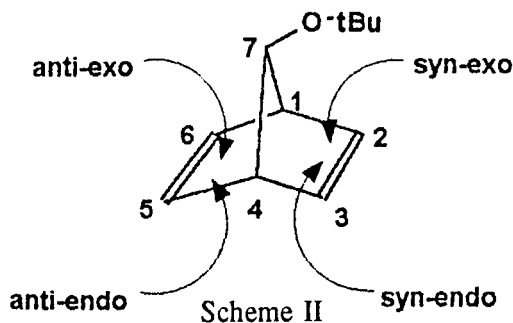
Cycloadditions such as the Diels-Alder and the 1,3-dipolar cycloaddition reactions have been firmly established as concerted processes. The necessary absence of a charged intermediate might imply the lack of specific solvation effects from such reactions. Indeed, the absence of significant or consistent solvent-induced rate enhancement data on a given reaction is taken as an indicator of its concertedness.¹ However, within the past two decades, there has been some research that would suggest that solvation has some control over the stereochemistry of concerted reactions.²⁻⁸ Just what solvent properties are responsible for these observations still is not universally agreed upon, although many ideas have been forwarded.

Huisgen first recognized that a collection of similar reactions could be classified into what is now known as 1,3-dipolar cycloadditions.⁹ His classification scheme facilitated the prediction of outcome of reactions which had not yet been studied. Cyclization takes place by simultaneous bond formation of two σ bonds and breakage of two π bonds when the two reactant molecules -- the 1,3-dipole and dipolarophile -- are oriented together in parallel planes in the transition state complex. The 1,3-dipole is a charge separated species in which formal positive and negative charges are distributed across three linearly connected atoms when resonance structures are invoked. Using diphenyldiazomethane as an example, both octet and sextet structures can be drawn to describe its charge distribution (Scheme I). Sustmann further classified dipoles into three types to explain orientation effects by FMO theory.¹⁰



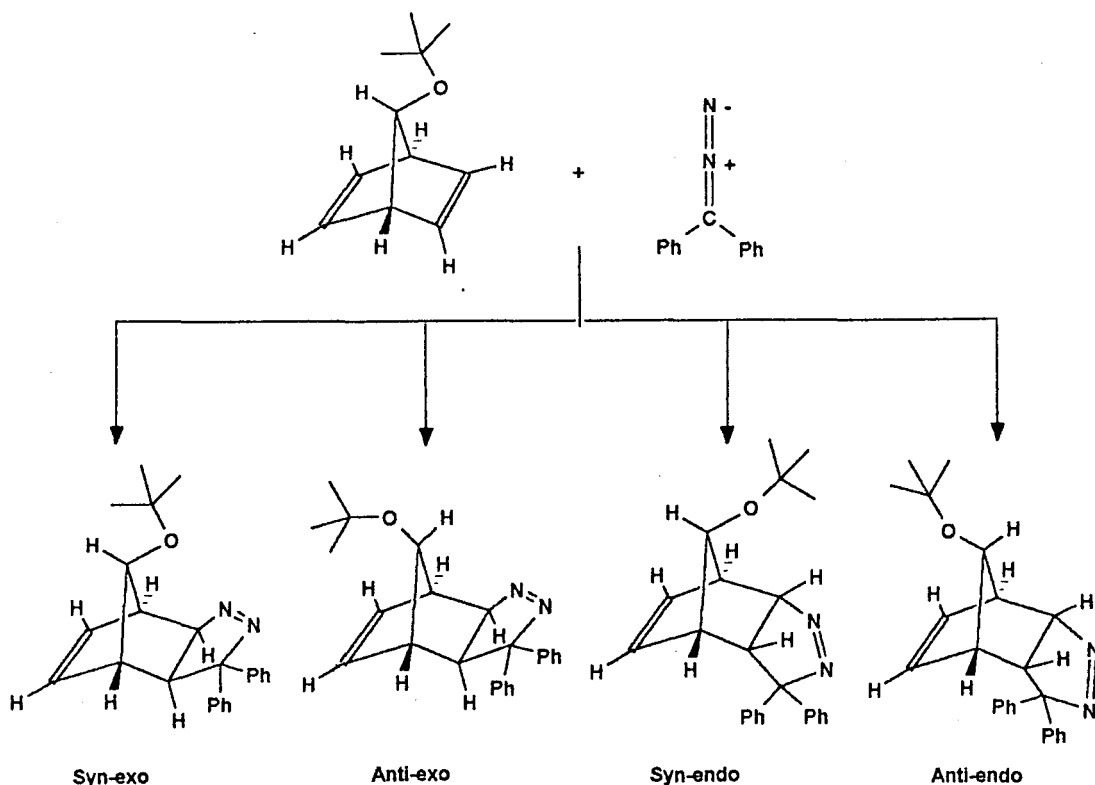
The dipolarophile is a doubly bonded species, usually, but not necessarily, an alkene. Norbornene and its derivatives make excellent dipolarophiles for two reasons. First, the rigidity of the norbornene structure permits the stereochemistry of heterocycles to be analyzed without the added complication of rotational considerations. Second, a large amount of ring strain in norbornene is reduced when the π bond is broken upon cyclization with the dipole.¹¹ The release of ring strain translates into sizeable rate enhancements in comparison to other alkenes, such as cyclohexene. Any 1,3-dipolar cycloadditions with norbornene produce only the *exo* isomer.¹² When norbornadiene is used as a dipolarophile, the *endo* as well as the major *exo* adduct is observed.¹³ Formation of *endo* adduct was facilitated because the olefinic hydrogens on the second double bond are nearly "planar" with carbons 1, 4, 5, and 6 thus relieving steric hindrance on the *endo* face of norbornadiene.

When a substituent is introduced at the 7-position, the possibility arises that a total of four monoadducts may form. The usual *syn-anti*, *exo-endo* nomenclature is demonstrated in Scheme II.



In the reaction between diphenyldiazomethane and 7-*tert*-butoxynorbornadiene chosen for this

In the reaction between diphenyldiazomethane and 7-*tert*-butoxynorbornadiene chosen for this study, all four monoadducts form (Scheme III).



Scheme III

This reaction had previously been studied by Wilt and Sullivan in the absence of solvent and under pseudo 1st order conditions.¹⁴ The primary directive influences in isomer formation are thought to be electronic and steric. Electronic influences are the result of through-space interaction of *tert*-butoxy oxygen electron pairs with the π orbitals of the underlying double bond.¹⁴ This makes the *endo-anti* site more reactive toward cycloaddition than the other sites. The steric contribution dictates a larger *endo* product overall, since the *endo* direction of approach is least sterically hindered. Formation of the *syn-exo* adduct is least favored.

electrostatic attraction, this direction of approach is hindered by the combined bulk of the tert-butoxy substituent and the 1,3-dipole molecule.

The present study was conducted in order to determine whether solvation (i.e., solvent properties) has an influence on 1,3-dipolar cycloadditions, and if so, what is the probable mode of reaction-solvent interaction. When the latter part of the question is addressed, it may be possible to improve our understanding of the fine details of cycloaddition transition states. During the study it was observed that the relative yields of the four monoadducts varied significantly in the presence of various solvents. An explanation for this outcome has been sought by attempting to identify the specific solvent properties responsible for the influence(s) by comparison with bulk solvent properties and empirical parameters. Once a set of solvent parameters closely correlating with product yield data has been identified, a rationale for the solvent interaction can be surmised.

Of the numerous solvation models available in the literature, relatively few appropriately explain this solvent effect. Many single solvent parameters have been tested, with limited success. Multiple parameter relationships, in which distinct solvent parameters are additively combined to describe a complex solvation model, were also tested and fared better. Among these, the Abraham-Kamlet-Taft (AKT) relationship seems most suitably designed to describe a unique set of solvent-solute interactions.¹⁵ Gajewski, et al. have applied the AKT expression and a modified AKT expression to concerted Claisen rearrangements and Diels-Alder cycloaddition reactions, with excellent results.⁸

When the results of the AKT expression were interpreted, it appeared that solvent polarity, solvent hydrogen-bond donor ability, and cohesive energy density were important to the outcome of the reaction depicted in Scheme III. The latter parameter is uniquely applicable to concerted processes and merits some detail. In the process of solvating a single solute

molecule, a cavity must form in bulk solvent. This is an energy demanding process, since all solvent-solvent interactions need to be overcome at the cavity site. Cohesive energy density (c) describes the amount of energy required to overcome those forces within a given volume.

$$c = (\Delta H_v^\circ - RT)/V_M \quad (1)$$

Where ΔH_v° is heat of vaporization, R is the ideal gas constant, T is Kelvin temperature, and V_M is molar volume. Larger cavities require more energy for their formation. Since cohesive energy density acts upon cavity formation, it will augment any process that gives rise to a solute transition state requiring a smaller cavity. Concerted reactions are distinct among all reaction types in that they have large negative activation volumes, ΔV^\ddagger , in the range of -25 to -40 cm^3 . In the present case, ΔV^\ddagger results from constriction of the 1,3-dipole and dipolarophile in the transition state, creating a net volume reduction (Equation 2).

$$-\Delta V^\ddagger = V_{M,A} + V_{M,B} - V_{M,A-B}^\ddagger \quad (2)$$

$V_{M,A}$ and $V_{M,B}$ are the molar volumes of reactants A and B, respectively, and $V_{M,A-B}^\ddagger$ is the molar volume of the transition state complex. In the model reaction shown in Scheme III, a distinct transition state gives rise to each of the monoadducts. Given that each of the four transition states has a different ΔV^\ddagger , it would be expected that the cohesive energy density of a given solvent would favor formation of some adducts and disfavor formation of others. The reaction in Scheme III has been run in 26 solvents. Yields of the four monoadducts have been quantified by reversed phase HPLC using an internal standard method. Best results were obtained when the log *syn/anti* ratio was correlated with single and multiple parameter relationships. The log

exo/endo ratios did not correlate as well. Results were evaluated in terms of the physical requirements of the transition state(s).

CHAPTER II

HISTORY

An early solvation model in which the solvent played other than a passive role in solution chemistry was that of Kirkwood in 1934.¹⁶ His model was purely electrostatic, placing a spherical zwitterionic solute molecule having a dipole, μ and radius, r_M , in a solvent of dielectric constant ϵ . Although the model made no allowance for specific solvent interactions, it did provide a quantitative measure of the effect of a single solvent property on a reaction process. One form of the Kirkwood expression is given in Equation 3, where μ_{chem} is the

$$\mu_{\text{chem}} = -(\mu^2/r_M^3) [(\epsilon - 1)/(2\epsilon + 1)] \quad (3)$$

chemical potential, $(\epsilon - 1)/(2\epsilon + 1)$ is the solvent dielectric function. Equation 3 has found application to numerous chemical systems. Laidler and Eyring extended the expression to describe free energy changes occurring in and reaction rates and equilibria in solution.¹⁷ Kwart and Lilley¹⁸ used the Laidler-Eyring equation to describe the free energy of activation in terms of μ_{chem} of the cycloaddition of tetracyanoethylene to enol ethers in aprotic solvents.¹⁹

Solvent cohesion had also been considered as a driving force in reactions. In 1929, Richardson and Soper,²⁰ and later Glasstone,²¹ considered the influence of cohesion of reactants, products, and solvent on reaction rates. They noted that a solvent's cohesiveness was a determining factor in the acceleration or deceleration of a reaction, depending upon the relative

cohesiveness of reactants and products. Hildebrand²² and Scatchard²³ introduced a solvation model to account for non-electrostatic types of solvation. Making the supposition that van der Waals interactions are the only interactions occurring between solute and solvent, they developed Equation 4 for a solute molecule *i* dissolved in a solvent *s*.

$$RT \cdot \ln f_i = V_{m,i} \cdot (\delta_i - \delta_s)^2 \quad (4)$$

In Equation 4, f_i is the activity coefficient of the nonelectrolyte solute, and δ_i and δ_m are the Hildebrand solubility parameters for solute and solvent, respectively. The δ term was defined as the square root of cohesive energy density, $((\Delta H_v^\circ - RT)/V_M)^{1/2}$. For a bimolecular reaction between A and B, such that $A + B \rightleftharpoons (AB)^\ddagger$, the rate constant could be expressed in the form $\ln k = \ln k_0 + \ln f_A + \ln f_B - \ln f_\ddagger$, where k_0 is the rate constant in an ideal solution. Since reaction rate constants could be expressed as activity coefficients, rate constants could in turn be correlated to the Hildebrand solubility parameter. In 1970, Wong and Eckert observed a good correlation of relative rate constants of the Diels-Alder condensation of maleic anhydride with 1,3-butadiene in different solvents using the Hildebrand-Scatchard equation.²⁴

Aware of the limited ability of intrinsic solvent polarity indices (ie., dielectric constant, dipole moment) to correlate with reaction free energy terms, numerous researchers sought to develop empirical polarity scales having improved predictive capabilities. The earliest empirical scale was devised in 1914 by Meyer when he noticed that the equilibrium constants of numerous tautomerizations varied proportionately in the same set of solvents.²⁵

$$[\text{enol}]/[\text{diketo}] = L \cdot E \quad (5)$$

L is the enolization power of the solvent, and E is a property of the ketone. In 1966, Gutmann developed the donor number, DN, as a measure of the electron donating ability of a solvent.²⁶ DN was measured calorimetrically as the enthalpy of the equilibrium resulting from coordination of SbCl_5 with solvent molecules in dilute 1,2-dichloroethane solution. Several other polarity scales have been developed based upon reaction equilibria or physical equilibria (ie., liquid-liquid partitioning).²⁷⁻³³ In 1988, Abraham and coworkers introduced the solvophobicity parameter, Sp, whose use was intended to be distinct from solvent polarity.³² The scale was derived from the free energy of transfer values of solutes transferred from one solvent to another according to Equation 6. The parameters M and D are solvent related, and R_T is related to

$$\Delta G_i^\circ (\text{to solvent}) = MR_T + D \quad (6)$$

solute volume. The parameters for each solute-solvent system were subjected to a computerized iterative procedure until constant values were obtained. Sp values could then be obtained from Equation 7. The scale was fixed by setting Sp=1 for water and Sp=0 for hexadecane.

$$Sp = 1 - M/M(\text{hexadecane}) \quad (7)$$

Solvent polarity scales have been developed from reaction kinetics. An early single parameter polarity scale was the Y scale developed by Grunwald and Winstein in 1948.³⁴ The Y scale was based on the relative reaction rate of solvolysis of *t*-butyl chloride in various solvent mixtures versus the reaction rate in 80% ethanol in water. These rates were observed to increase with increasing solvent polarity. A linear free energy relationship was devised to correlate different reaction rates with Y values.

$$\log(k_s/k_0) = mY \quad (8)$$

In Equation 8, m is a coefficient measuring the reactant's sensitivity to changes in solvent ionizing power, k_s is the solvolytic rate constant in a given solvent and k_0 is the corresponding rate constant in a 80% ethanol/water solution. Winstein later expanded the relationship to include a solvent nucleophilicity parameter, N .³⁵ Schleyer also expanded the Winstein Equation to include an adjustable parameter, Q , using methyl tosylate as the S_N2 model and substituting 2-adamantyl tosylate for *t*-butyl chloride as the S_N1 mechanistic extreme of solvolysis.³⁶ Swain also expanded the Winstein relationship to four parameters to include two solvent parameters, d_1 and d_2 , and two compound parameters, c_1 and c_2 . These parameters were derived from an iterative computational program combining 146 available $\log(k/k_0)$ values.³⁷ Peterson and coworkers demonstrated the usefulness of the aforementioned Swain-Mosely-Bown parameters by transforming them into the desired form of the Winstein parameters, Y and N .³⁸ In 1961, Winstein introduced $\log k_1$,³⁹ an entirely different parameter using the rate of ionization of methylnephyl tosylate as a reference reaction which could be used in a wider variety of organic solvents than the *t*-butyl chloride solvolysis. In 1969, Drougard and Decroocq similarly introduced $\log k_2$ of the Menschutkin reaction as being a good solvent sensitive reaction model.⁴⁰ Other scales patterned after the original Grunwald-Winstein equation have been suggested.⁴¹

Numerous solvation parameters have been derived from the spectral shifts of specific organic indicator compounds or (groups of compounds). Parameters developed from UV-visible spectra have a general feature in common. The indicator dyes employed undergo a specific electronic transition in which either the ground state or excited state forms a distinct charge-separated species which is highly sensitive to changes in solvent polarity. If the charge-separated species is in the ground state, the observed spectral shift will be progressively hypsochromic with

increasing solvent polarity, corresponding to solvent stabilization of the ground state relative to the excited state. Conversely, bathochromic shifts occur when the charge-separated excited state is stabilized by polar solvents.

In 1958, Kosower introduced the Z scale based upon the charge transfer UV absorption band of 1-ethyl-4-methoxycarbonyl pyridinium iodide going to form a radical pair excited state.⁴² Hypsochromic shifts were observed in solvents of increasing polarity attributable to increased stabilization of the ion-pair ground state. In 1960, Brownstein incorporated the Z scale as a standard reference process into a linear free energy relationship and generated two new parameters, R and S.⁴³

$$\log(k_{\text{solv}}/k_{\text{EtOH}}) = SR \quad (S=0 \text{ in EtOH}) \quad (9)$$

The S parameter is solvent-dependent, and R is process-dependent.

Dimroth and coworkers developed the $E_T(30)$ solvent scale in 1963.⁴⁴ This scale was derived from the longest-wavelength visible-range absorption band of the pyridinium-N-phenoxide betaine dye and of its polysubstituted tert-butyl derivative. The E_T scale was later normalized by setting tetramethylsilane as the lower limit (at 0.0) and water as the upper limit (at 1.0), and this revised scale was renamed E_T^N .^{44c} In 1965, Brooker used the bathochromic shifts of the $\pi \rightarrow \pi^*$ transition of a meropolymethine dye in his χ_R scale. The hypsochromic shifts of a second dye were used for a second scale, χ_B .⁴⁵ Several more scales have been proffered as indices of solvent polarity or as Lewis acidity/basicity based upon UV-visible absorption shifts.⁴⁶⁻⁵¹

Solvent parameters have also been designed around shifts in position or intensity of other emission or absorption spectra. In 1959, Zelinski developed a scale from the fluorescence

maxima of 4-amino-N-methylphthalimide.⁵² Another fluorescence scale was introduced by Dong and Winnik.⁵³ The 'Py' scale was derived from the ratio of intensities of two vibrational bands, I and III, of pyrene in different solvents. Of the existing solvent scales based upon infrared absorption, all are modeled on the Lewis basicity power of the solvent rather than on polarity.⁵⁴⁻⁵⁸ NMR chemical shifts have been employed to develop polarity scales. Taft's P scale was introduced in 1972.⁵⁹ The P scale was based on ¹⁹F chemical shifts of 4-fluoronitrosobenzene in various solvents relative to the shift in cyclohexane. The acceptor number, AN, proposed by Gutmann in 1975 was a measure of Lewis acidity of organic solvents.⁶⁰ Gutmann *et al.* developed the scale from ³¹P chemical shift values of triethylphosphine oxide in equilibrium with its solvent adduct relative to the ³¹P shifts of triethylphosphine oxide in equilibrium with its SbCl₅ adduct. Finally, Knauer and Napier drew upon the fact that the nitrogen hyperfine splitting constants of nitroxides in esr spectra were sensitive to solvent polarity to prepare their A_N scale.⁶¹

Single solvent parameter relationships often do not adequately correlate with observed reaction quantities or with spectral data. Several research groups have proposed multiple parameter linear free energy relationships that are generalized enough to treat a wide variety of free energy and spectral trends. Each parameter is a measure of a distinct solvent property (and therefore a specific solvent interaction) and is, ideally, noncollinear with all other parameters in the relationship. In 1971, Katritzky tested the viability of combinations of empirical and intrinsic solvent parameters (eg., E_T(30), f(ε), f(η)).⁶² In the same year, Koppel and Palm developed a multiple parameter approach combining two specific and two nonspecific parameters.⁶³

$$A = A_0 + y \cdot Y + p \cdot P + e \cdot E + b \cdot B \quad (10)$$

Y is the Kirkwood dielectric function, $(\epsilon - 1)/(2\epsilon + 1)$, or $(\epsilon - 1)/(\epsilon + 1)$, and is the polarization

parameter. P is the solvent refractive index, $(n^2 - 1)/(2n^2 + 1)$ or $(n^2 - 1)/(n^2 + 2)$, and serves as the polarizability parameter. E and B are described as electrophilic solvating power and nucleophilic solvating power, respectively. Coefficients y , p , e , and b indicate the sensitivity of the reaction free energy process, A , to their corresponding parameters. E is Dimroth's $E_T(30)$ parameter and B is based on the O-D infrared stretching frequency band of CH_3OD .

In 1975, Krygowski and Fawcett introduced a 2-parameter relationship employing $E_T(30)$ and DN .⁶⁴ This treatment considered only specific solvent-solute interactions, assuming that nonspecific interactions are constant. The multiple parameter equation presented by Abraham, Kamlet, Taft, and Abboud was introduced in a piecewise fashion beginning in 1976, and was fully realized in 1988.¹⁵

$$\text{XYZ} = \text{XYZ}_0 + s(d\delta + \pi^*) + a\alpha + b\beta + h\delta_H^2 + e\xi \quad (11)$$

XYZ is a reaction free energy function or spectral shift. The solvent parameters π^* , α , and β are empirical values determined from averaged solvatochromic data of numerous indicator dyes. The π^* value is a solvent polarity/polarizability parameter, α represents solvent hydrogen bond donor acidity, and β is solvent hydrogen bond acceptor basicity. The δ and ξ terms are correction terms for solvent polarizability and for $\text{X}=\text{O}$ ($\text{X} = \text{C}, \text{P}, \text{or S}$) functional groups (if present), respectively. The δ_H^2 term is cohesive energy density, as mentioned earlier. Buncel and Rajagopal have recently suggested the creation of a new π^* scale, which they have called π_{zo}^* , using a collection of merocyanine dyes in place of the (mostly) nitrobenzene derivatives used by Taft *et al.* when developing the original π^* scale. This substitution, they believe, would improve the general applicability of the π^* scale.⁶⁵

Mayer introduced a multiple parameter correlation in 1978 specifically directed toward

the free energy change associated with cavitation.⁶⁶

$$\Delta G^S - \Delta G^R = a \cdot (DN^S - DN^R) + b \cdot (AN^S - AN^R) + c \cdot (\Delta G_{vap}^{oS} - \Delta G_{vap}^{oR}) \quad (12)$$

$$\Delta \Delta G = a \Delta DN + b \Delta AN + c \Delta \Delta G_{vap}^o$$

In Equation 12, DN and AN are Gutmann's donor number and acceptor number, respectively. The ΔG_{vap}^o term is free energy of vaporization, and S and R are solvent and acetonitrile reference solvent, respectively. The coefficients a and b are the donor and acceptor strengths of the reaction partners relative to the reference compounds $SbCl_5$ and $Et_3P=O$, respectively. Swain and coworkers put forward a multiple parameter treatment in 1983.⁶⁷ Single solvent parameter data were culled from the literature and combined via a nonlinear least-squares computer program. The end result was a 2-parameter equation:

$$A = A_0 + a_i \cdot A_j + b_i \cdot B_j \quad (13)$$

In Equation 13, A_j is solvent anion-solvating ability and B_j is cation-solvating ability, and a_i and b_i are regression coefficients.

A few other multiple parameter relationships have been introduced, but are somewhat more specific in their intended use.⁶⁸⁻⁷²

Two single-parameter solvent scales exist which were tailored to concerted processes. In 1962, Berson *et al.* developed a linear free energy relationship using a Diels-Alder reaction between methyl acrylate and cyclopentadiene as a reference reaction for the new parameter, Ω .

$$\Omega = \log(Endo/Exo) \quad (14)$$

In Equation 14, $\log(\textit{Endo}/\textit{Exo})$ is the logarithm of the *Endo/Exo* isomeric product ratio of the cycloaddition. The value of Ω became increasingly positive as solvent polarity increased for three cycloadditions studied. Berson rationalized the finding by suggesting that the net dipoles of *endo* and *exo* transition states are dissimilar, so that the transition state of the adduct having the larger net dipole will be preferentially stabilized by polar solvents.² In 1981, Nagai and coworkers developed the D_{π} parameter based upon the relative rate constants of the cycloaddition reaction between diphenyldiazomethane and tetracyanoethylene (TCNE), to be used in a linear free energy relationship.⁷³

$$\log k = mD_{\pi} + Q_0 \quad (15)$$

$\log k$ represents rate process being studied, and m and Q are slope and intercept, respectively. These researchers attributed the observed decrease in second order rate constant with increasing solvent basicity to hard-soft acid-base interactions between TCNE and donor solvents.

In 1980, Huisgen used the relative rates of three cycloaddition reactions in a range of solvents to argue a mechanism for each.⁷⁴ The 2+2 cycloaddition between TCNE and enol ethers was long thought to involve a zwitterionic intermediate, and rate constant data in various solvents supported the theory. The rate constant varied linearly with solvent polarity, from 140 L/mol·sec in nonpolar cyclohexane to 6.29×10^5 L/mol·sec in acetonitrile for the cycloaddition of TCNE and ethyl isobutenyl ether. Rate constants were linear with Dimroth's E_T parameter when alcohol solvents were excluded ($R^2 = 0.93$ to 0.97) and were linear when the alcohol solvents were included and the Koppel-Palm relationship⁶³ employed ($R^2 = 0.990$). The high sensitivity to solvent polarity reflected an increased stabilization of the zwitterionic intermediate

with increasing solvent polarity. Conversely, the marginal sensitivity of certain other cycloadditions supported the view that such reactions were strictly concerted. Hence, the cycloaddition of TCNE and anthracene ($k_2^{74b}(\text{o-xylene}) = 0.09 \text{ L/mol}\cdot\text{sec}$, $k_2(\text{1,2-dichloroethane}) = 4.69 \text{ L/mol}\cdot\text{sec}$) in various solvents was not as dramatic, nor was the reaction between styrene and hexachlorocyclopentadiene ($k_2(\text{toluene}) = 6.6 \times 10^5 \text{ L/mol}\cdot\text{sec}$, $k_2(\text{DMF}) = 11.1 \times 10^5 \text{ L/mol}\cdot\text{sec}$) or styrene and 3,6-diphenyl-1,2,4,5-tetrazine ($k_2(\text{toluene}) = 4.4 \times 10^4 \text{ L/mol}\cdot\text{sec}$, $k_2(\text{DMF}) = 10.6 \times 10^4 \text{ L/mol}\cdot\text{sec}$). Of the 1,3-dipolar cycloadditions, the reaction between phenyldiazomethane and norbornene showed no solvent sensitivity at all. The 1,3-dipolar cycloaddition rate of N-methyl-C-phenylnitron and ethyl acrylate showed some sensitivity to solvent polarity, but the correlation to E_T was acceptable ($R^2 = 0.930$) and the slope was negative with increasing polarity. The negative slope was rationalized as an overall loss of polarity in the transition state relative to reactants.

Some researchers have observed Diels-Alder rate accelerations in aqueous medium. In 1980, Breslow and coworkers attributed such rate enhancement to hydrophobic association of diene to dienophile.⁷⁵ They reported a 700-fold increase in the Diels-Alder cycloaddition between cyclopentadiene and methyl vinyl ketone in water compared with the rate in 2,2,4-trimethylpentane. Other reactions showing a hydrophobic effect were cycloadditions between cyclopentadiene and acrylonitrile and between anthracene-9-carbinol and N-ethylmaleimide.⁷⁶ In 1983, these same researchers observed shifts in *endo/exo* product ratios in Diels-Alder reactions of cyclopentadiene and ascribed this effect to hydrophobicity as well.^{77,78} The need to minimize transition state surface area in water is met by a preference for formation of the isomer with the smaller surface area. Also in 1983, Grieco and coworkers noted both rate enhancement and isomeric selectivity in Diels-Alder reactions when the solvent was changed from pure organic to pure water and water mixtures. Their observations were likewise attributed to

hydrophobic interactions which they dubbed "micellar catalysis".⁷⁹

They also noted that, in studying Diels-Alder reactions between dienophiles (eg., dimethylbenzoquinones, methoxymethylbenzoquinones, methyl (acetoxymethyl)acrylate, acrolein, methacrolein) and the dienes sodium 4-methyl-3,5-hexadienoate, sodium 3,5-hexadienoate, and sodium 4,6-heptadienoate, additions of water soluble cosolvents (eg., methanol, dioxane and THF) greatly reduced the dramatic hydrophobicity effect.⁸⁰ Grieco and coworkers attributed the rate accelerations and stereoselectivity of a series of Diels-Alder reactions in 5.0 M LiClO₄/ether solution to a heightened internal solvent pressure of the lithium perchlorate-ether medium, similar to that of water.^{81a} Dailey and Forman have observed that some Diels-Alder reactions are not affected by the LiClO₄/ether medium and suggest that rate accelerations are due to Lewis acid catalysis.^{81b} Breslow and Guo, in 1988, pointed to the likelihood that a generalized solvophobic interaction was acting upon Diels-Alder reactions in polar media.⁸² The observed rate enhancements and *endo/exo* selectivities were, however, far less dramatic than those observed in aqueous solution. The *endo/exo* product ratio from reaction of cyclopentadiene with methyl vinyl ketone was found to be 25.0 in aqueous solution, but ranged from 3.85 in neat cyclopentadiene to 10.4 in ethylene glycol.

In 1987, Schneider and Sangwan³ observed good linear correlation between $\log(\textit{endo/exo})$ for the Diels-Alder cycloaddition of cyclopentadiene and the monoethyl ester of maleic acid and Abrahams solubility parameter, Sp .³ The cycloaddition took place in binary solvent mixtures of increasing water content. In 1989, Schneider and Sangwan measured the rates of 19 different dienophiles with (mostly) cyclopentadiene in a range of solvents. Derivatives of fumaric, maleic, and acrylic acids with alkyl ester groups were used as dienophiles. Definite rate increases with increasing solvophobicity was observed according to Equation 16.

$$\log k = a \cdot Sp + \log k_0 \quad (16)$$

The sensitivity coefficient a showed that rate acceleration due to solvophobicity varied by 3 orders of magnitude. If a multiple parameter treatment were used, including E_T^N ^{44c} (Equation 17), no significant improvement in fit was observed over the single parameter treatment (Equation 16).⁴

$$\log k = a \cdot Sp + m \cdot E_T^N + \log k_0 \quad (17)$$

In 1990, Cativiela *et al.* tested the applicability of the Sp scale³² to Diels-Alder rate accelerations and selectivity using the reaction of cyclopentadiene and methyl (E) α -cyanocinnamate in several water/dioxane and water/acetone mixtures as a model. They obtained excellent linear correlations of $\log (Endo/Exo)$ with Sp ($R = 0.99$) when the acetone/water and dioxane/water series were treated separately. They also obtained good linear correlations of $\log k$ with Sp when the acetone and dioxane mixtures were treated together ($R = 0.9939$).⁵ Again in 1991, these same researchers studied the reaction of cyclopentadiene with methyl acrylate in numerous pure solvents and solvent mixtures and found a good correlation with Sp and E_T^N ^{44c} with $\log k$.

$$\log k = -3.195 + 2.075(\pm 0.824)Sp + 0.904(\pm 0.746)E_T^N \quad (18)$$

$$N = 19 \quad R = 0.942 \quad s = 0.180$$

Since the reaction also showed high *endo/exo* selectivity, another correlation was also found:

$$\log(k_{\text{Endo}}/k_{\text{Exo}}) = 0.457 + 0.356(\pm 0.149)Sp + 0.399(\pm 0.135)E_T^N \quad (19)$$

$$N = 19 \quad R = 0.970 \quad s = 0.033$$

The authors admit that there is an intrinsic collinearity between Sp and E_T^N ($R = 0.747$) which makes a clear physiochemical explanation difficult. Both $\log k_{\text{Endo}}$ and $\log k_{\text{Exo}}$ increase with increasing solvophobicity.⁶

In 1969, Kadaba combined substituent and solvent effects on the rate of 1,3-dipolar cycloaddition reactions between diazomethane and substituted benzalanilines (anils) to form triazolines. Kadaba noted that rate accelerations could not be attributed to solvent polarity. He suggested instead that observed rate increases (particularly in water and DMF) could be explained in terms of the specific solvent interactions of hydrogen bonding and polarizability.

Small anions are solvated to a large extent by hydrogen-bonded interactions with protic solvents. Larger anions experience a decrease in H-bonding interactions but, at the same time, undergo mutual polarizability interactions with dipolar aprotic solvents such as DMF. In a similar manner, the charged transition state of the cycloaddition of diazomethane and benzalaniline is solvated largely through hydrogen bonding with small amounts of water. The transition state of diazomethane and benzal-p-nitroaniline, on the other hand, experiences charge delocalization due to resonance with the nitro substituent. Such a delocalization is synonymous with polarizability, and the rate increases seven-fold on going from "inert" dioxane to dipolar aprotic DMF.⁸³

As part of a larger 1975 study, Stevens *et al.* determined the activation enthalpies and reaction rates of a series of Diels-Alder reactions of N-substituted triazolinediones with different dienes in benzene, dioxane, and ethyl acetate solvents. Increases in rate constant and activation enthalpies were attributed to increased solvation of the triazolinedione dienophile. Increases in

solvation, in turn, were attributed to increases in solvent polarity. In particular, changes in the relative reactivities of the dienophiles toward a given diene was explained on the basis of differing sensitivity of N-substituents to solvent polarity.⁸⁴

Schuster and Sauer, in 1986, found that Diels-Alder cycloaddition reactions of acrylonitrile, ethyl acrylate, butyl acrylate and styrene as dienophiles and hexachlorocyclopentadiene and cyclopentadiene as dienes exhibited rate increases of 2 orders of magnitude in micelles (produced by addition of sodium dodecylsulfate) compared with the rate in dioxane. Additionally, $\log(\textit{endo/exo})$ of the cycloadducts forming from reaction of cyclopentadiene with acrylonitrile and butyl acrylate in micellar conditions in 14 solvents were linearly correlated with Dimroth's E_T parameter.⁴⁴ In the case of the cyclopentadiene-acrylonitrile reaction, E_T correlations were good only when the polar and nonpolar solvents were considered separately.⁷ Their findings suggested that the reactions take place at the solvent-micellar interface and are thus highly influenced by solvent polarity.

In 1979, Huisgen *et al.* pointed to the differences in 1,3-dipolar cycloaddition reaction pathways between diazomalonate and 1-pyrrolidinocyclopentene or 1-pyrrolidinocyclohexene as evidenced by their respective solvent dependencies.⁸⁵ The $k_2(\text{DMSO})/k_2(\text{decalin})$ ratio for 1-pyrrolidinocyclopentene, known to occur via a zwitterionic intermediate, is 1540. The same ratio for 1-pyrrolidinocyclohexene is 41, pointing toward a concerted mechanism. The authors suggest that the reaction with 1-pyrrolidinocyclohexene also occurs by an azo coupling equilibrium, but that the slow competing concerted cycloaddition ultimately dominates.

Beginning in 1973 with a series of articles,⁸⁶ Firestone *et al.* expounded the vibrational activation theory that the microscopic viscosity environment of a solvent affected reactions involving bond formation (such as the Diels-Alder and Claisen rearrangement) by promoting reactant vibrational energy and discouraging reactant translational motion. Solvent density and

viscosity were taken as rough indices of the viscosity of the microscopic reactant environment, since all of the solvents were of the same family (tetraglyme and polymonomethyl ethers). Jorgensen and Blake investigated the phenomenon of Diels-Alder rate accelerations in water via Monte Carlo simulations in 1991.⁸⁷ They used as a reaction model the reaction between cyclopentadiene and methyl vinyl ketone. Their findings discount micellar formation and instead favor the view that enhanced polarization of the transition state allows for stronger hydrogen bonding at the carbonyl oxygen of the ketone.

Bond formation of pericyclic reactions is accompanied by overall volume contraction of an unusually large magnitude. Pressure induced Diels-Alder rate accelerations often reveal that the volume of activation (ΔV^\ddagger) in fact exceeds the volume of reaction ($\Delta \bar{V}$).⁸⁸ This being the case, the measurement of volume changes during the course of reaction is a methodology employed by investigators seeking to establish the concertedness of reaction. In 1973, McCabe and Eckert performed high pressure kinetic studies to determine volumes of activation of a variety of Diels-Alder reactions. The magnitudes of these activation volumes were in turn used as positive evidence in support of a concerted mechanism.⁸⁹ The effect of externally applied pressure on 1,3-dipolar cycloaddition reactions was studied by von Jouanne and Kelm in 1983.⁹⁰ Volumes of activation and of reaction were experimentally determined for the reaction between diphenyldiazomethane and four different dipolarophiles in four solvents. These volume profiles were used, along with other experimental and calculational evidence to argue the feasibility of different reaction pathways. Two possibilities could not be distinguished as more reasonable where volume profiles alone were considered: a diradical mechanism and a concerted mechanism having an early transition state. The authors also found good correlation of rate data with cohesive energy density, $E_T(30)$, and $(\epsilon - 1)/(2\epsilon - 1)$, but cautioned that such rate changes were small and possibly negligible.

Since concerted processes have large, negative activation volumes, application of high external pressures might be expected to increase the reaction rate or yield by encouraging transition state formation. Raistrick, Newitt and Sapiro in 1939⁹¹ and Walling and Peisach in 1958⁹² used the negative ΔV^\ddagger values obtained from external pressure studies to distinguish between diradical and concerted mechanisms in the dimerization of isoprene and cyclopentadiene, respectively. Both groups favored the diradical pathway, since the ΔV^\ddagger values obtained were 21-23 cc/mol smaller than $\Delta \bar{V}$ for dimerization of isoprene and 11.6 cc/mol smaller for dimerization of cyclopentadiene. Dauben and Kozekowski in 1974 reported some success in increasing yields and reaction times of sluggish, thermally unstable Diels-Alder cycloadditions of enamines, dienamines, and dienophiles by applying high external pressures (8 - 20 kbars).⁹³ Issacs and Rannala conducted pressure studies on cycloaddition reactions of diphenylketene, dimethylketene, TCNE, and diethyl diazocarbonylate and on a 1,3-dipolar cycloaddition to determine whether the reactions are concerted. Increases in rates of reaction with increasing pressure indicated concertedness. The 1,3-dipolar cycloaddition between diphenyldiazomethane and 5,6-bisethoxycarbonyl-5,6-diazabicyclo[2.2.1]hept-2-ene also showed increased reaction rate with increased pressure. However, it was noted that the measured activation volumes of multistep (non-concerted) cycloadditions (eg., TCNE with dihydropyran and 2-ethoxy-2,3-dihydro(4H)pyran) were as large or larger than activation volumes for concerted reactions. This finding was attributed to other effects, ie., the effect of solvent organization or electrostriction by a dipolar transition state. They concluded that measured activation volumes were not a clear criterion for the assignment of a concerted mechanism.⁹⁴

Gajewski and coworkers evaluated the effect of internal solvent pressure on a number of reactions, including concerted Diels-Alder reactions and Claisen rearrangements.⁸ They found internal pressure to be strongly linearly correlated to both rate constants and *Endo/Exo* product

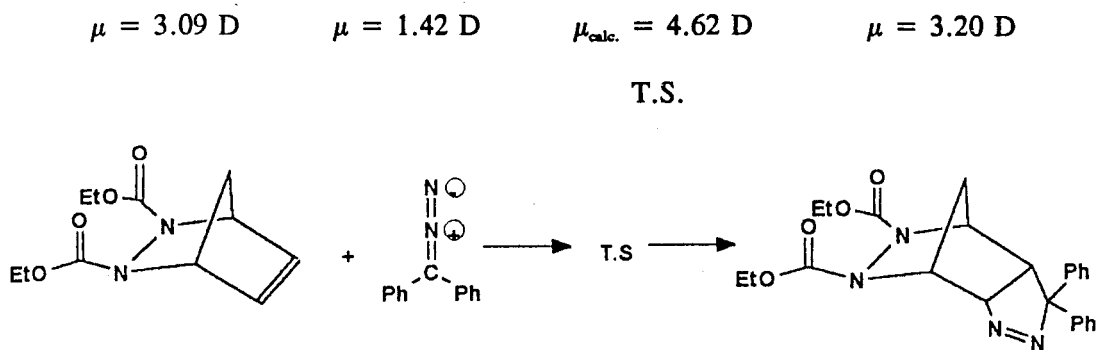
ratios. Ouellette and Williams studied the effect of internal solvent pressure on the conformational equilibria of 4,4-dimethyl-2-silapentane and 2,3-dimethyl-2-silabutane. Their supposition that an increased solvent pressure will increase the population of the conformer with the smallest molar volume was tested using NMR coupling constant data.⁹⁵ Snyder and Harpp suggested that the good correlation between internal solvent pressure and the rate of nitrogen extrusion of diaza compounds—a cycloreversion—was supportive of a concerted process as opposed to a diradical intermediate process.⁹⁶

In a 1963 review article, Huisgen discussed the mechanism of 1,3-dipolar cycloadditions in terms of solvent effect.¹ The zwitterionic pathway is rejected, since the rate of reaction in increasingly polar solvents would correspondingly increase if a zwitterionic intermediate were involved.⁹⁷ On the other hand, the loss of formal charge of the 1,3-dipole in the transition state of a concerted process might be expected to display an inverse solvent dependence. In actuality, 1,3-dipoles possess low to moderate dipole moments due to the multiple resonance structures which distribute the formal charges. The dipole moment of diphenyldiazomethane is, therefore, 1.42 D instead of the expected 6-7 D of a single resonance structure. Huisgen rationalized the absence of solvent influence on the concerted process by evoking the following version of the Kirkwood expression for the condition of zero solvent dependence.

$$\frac{\mu^2 \text{ 1,3-dipole}}{\text{MV 1,3-dipole}} + \frac{\mu^2 \text{ dipolarophile}}{\text{MV dipolarophile}} = \frac{\mu^2 \text{ transition state}}{\text{MV transition state}} \quad (20)$$

In Equation 20, μ is the dipole moment and MV is molar volume. The dipole moment of the transition state can be estimated in this way by assuming that it resembles the orientation complex which precedes the transition state. Then, if no solvent dependence is exhibited, the calculated

transition state dipole should be approximately equal to the sum of reactant dipole moments. Such calculations did fulfill expectation, as with the example in Scheme IV:



Scheme IV

Firestone used the same calculation argument to discredit the concerted pathway in favor of the spin-paired diradical pathway.⁹⁸ Firestone asserted that solvent polarity effects should be manifested if the mechanism were truly concerted. He maintained that, while it was reasonable for Huisgen to employ Equation 20, Huisgen had not used it properly. Since dipole moments have a directional component, the vector sum accounting for the alignment of the dipoles of the two reactants in the orientation complex required by Equation 20 should have been used instead of the direct sum. When the transition state dipole moment is calculated in this way for the above example of the reaction between diphenyldiazomethane and N,N-dicarbethoxy-1,2-diazanorbornene, the transition dipole moment becomes 3.4 D, far below the sum of the reactant dipoles. Firestone maintained that this new value better reflects the charge dispersal that would be expected to take place in the concerted transition state. An inverse solvent dependence should be, but is not, evident if the mechanism were concerted. Since no inverse solvent dependence is evident, the mechanism cannot be concerted. Huisgen countered Firestone's solvent effect argument by stating that the magnitude of observed solvent effects was far more

consistent with a concerted pathway than with a diradical pathway.⁹⁹

Eduard Buchner was the first to report a 1,3-dipolar cycloaddition reaction in 1888. Buchner studied the reactions of ethyl diazoacetate with unsaturated carboxylic esters, but his conception of the molecular structures of reactant diazo compound and cycloadduct was incorrect.¹⁰⁰ In 1938, Smith published a comprehensive review of 1,3-additions involving compounds containing "pentavalent" nitrogen as the middle atom.¹⁰¹ A zwitterionic intermediate for the 1,3-dipolar cycloaddition was proposed by different researchers.¹⁰² Huisgen subsequently developed a generalized classification scheme for such reactions, allowing new reactions to be predicted and carried out. Huisgen's group first proposed the concerted mechanism for this series of reactions in which two π bonds are broken and two new σ bonds are formed.⁹ The Woodward-Hoffmann selection rules for concerted cycloadditions (1965) were consistent with the mechanism proposed by Huisgen.¹⁰³ Frontier Molecular Orbital calculations, such as those discussed by Houk,¹⁰⁴ are in keeping with experimental observation. In particular, FMO calculations have been employed to address the problems of regio- and stereoselectivity in 1,3-dipolar cycloadditions.¹⁰ Orientation effects have been most readily explained in terms of HOMO-LUMO frontier molecular orbital considerations.¹⁰⁵

Recently, Morokuma and coworkers conducted an ab initio molecular orbital study of the addition reaction between norbornene and BH_3 , a reaction having a cyclic 4-centered transition state, in an effort to elucidate the reasons behind high *exo* selectivity (*exo/endo* = 200:1).¹⁰⁶ Upon breaking down reactant deformation and interaction energies into strain, steric, and torsional energy components, *endo* deformability was found to be the greatest contributor to energy of activation differences between *exo* and *endo* reactivity. *Endo* deformation is evident in the optimized norbornene structure, wherein the olefinic C(2)-H and C(3)-H bonds are bent from C(1)-C(2)-C(3)-C(4) planarity by 4.8° toward the *endo* face of the molecule. This bending

hinders the *endo* orientation of addition and likewise enhances *exo* addition. Although the difference in calculated energy between the "bent" and "planar" norbornene structures is small (0.2 kcal/mol), it is translated into a large difference in activation energies (ΔE_a (*exo*, *endo*) = -8.8 to -6.8 kcal/mol). Turner, Meador and Winkler in 1957 determined that additions across the double bonds of norbornene and norbornadiene brought about a relief of angle strain, as evidenced by their unusually large heats of hydrogenation of -33.13 kcal/mol for norbornene and -68.11 kcal/mol for norbornadiene, as compared to -27.1 kcal/mol for cyclohexene.¹¹

In 1935, Alder and Stein,¹⁰⁷ and later Huisgen¹⁰⁸ found that the addition of azides to norbornene occurred on the less hindered *exo* face. Bis adducts likewise possessed *exo*, *exo* stereochemistry. DeMicheli and Gandolfi studied the effects of chloro-substitution on the norbornadiene skeleton upon *exo*, *endo* selectivity¹⁰⁹ during cycloaddition reactions with 1,3-dipoles benzonitrile oxide, diphenylnitrilimine and 2-diazopropane.¹¹⁰ Of particular note was the complete *endo* selectivity when chlorine was present at the bridgetop position *syn* to the reactive (unsubstituted) double bond, attributed to steric shielding of the *exo* direction of approach of the 1,3-dipole by the chlorine atom. It was also noted that a large decrease in *exo* isomer formation was brought about by chlorine substitution at the bridgetop position of 1,2,3,4-tetrachloronorbornadiene *anti* to the reactive double bond. This was thought to occur because of increased deflection of the methylene bridge toward the *exo* position of the double bond, thus causing increased steric shielding.

In 1959, Findlay, Roy and McLean were the first to report *endo* adduct formation from cycloaddition of phenylazide and norbornadiene in addition to the major *exo* adduct.¹³ They also reported two *exo*, *exo* and two *exo*, *endo* bis adducts formed either by reaction of norbornadiene with excess phenyl azide or by reaction of phenyl azide with *exo* or *endo* monoadducts. In 1966, Klumpp and Bickelhaupt studied the cycloaddition of phenylazide to 7-*tert*-

butoxynorbornadiene and to both isomers of 7-*tert*-butoxynorbornene.¹¹¹ It was found that cycloaddition of the isomeric 7-*tert*-butoxynorbornene dipolarophiles afforded only *exo* adducts. The triazoline adducts resulting from cycloaddition with 7-*tert*-butoxynorbornadiene were produced in relative compositions of 30% *exo-anti*, 55% *endo-syn*, and 15% *exo-syn*. No *endo-anti* adduct was reported to have formed. The triazolines were not considered stable enough for direct isolation, and were isolated instead as reduced aziridine compounds (formed by treatment with H₂ and light, causing elimination of N₂). Bis adducts were recovered which suggested further reaction of *syn-endo* monoadduct to form the *syn-endo*, *anti-exo* bis adduct. *Syn-exo* and *anti-exo* monoadducts formed *exo*, *exo* bis adduct. The Alder-Stein *exo* rule¹⁰⁷ was credited for the formation of *exo* adduct, while the steric favorability of the *endo* position was held responsible for the predominant formation of *endo-syn* adduct. The *syn* double bond was assumed to be more reactive because of electronic interaction with the 7-*tert*-butoxy substituent. Halton and Woolhouse repeated the reaction first reported by Klumpp and Bickelhaupt between 7-*tert*-butoxynorbornadiene and phenylazide, and were successful in isolating the triazolines by preparative thin-layer chromatography. They obtained a somewhat different product distribution of 56% *syn-endo*, 9.2% *anti-endo*, and a 1.4% mixture of *syn-exo* + *anti-exo*.¹¹²

In 1975, Wilt and Sullivan studied the "neat" reaction of diphenyldiazomethane with 7-*tert*-butoxynorbornadiene.¹⁴ Four monoadducts and one bis adduct were quantified and characterized. The relative yields were in the order 36.5% *exo-anti*, 36% *endo-syn*, 25% *endo-anti*, 2.5% *exo-syn*, and trace *exo*, *exo* bis adduct. This outcome was significantly different from that of Klumpp and coworkers. The reason given was that diphenyldiazomethane is a bulky reagent as compared to phenyl azide, making steric hindrance a more important factor in the diphenyldiazomethane reaction. The authors also noted that the Alder-Stein *exo* rule was not adhered to in this reaction. Franck-Neumann and Sedrati,¹¹³ and Wilt and Peeran¹¹⁴ found that

diazomethane and diazoethane add to 7-chloro, iodo, bromo, and hydroxy substituted norbornadiene compounds giving rise to *endo* monoadducts, the *endo-anti* isomers being produced to a much larger extent than *endo-syn* adducts. Franck-Neuman and Sedrati rationalized their findings as an orbital interaction between the highest-occupied π orbital of norbornadiene and the low-lying antibonding σ^* orbital of the C-X bond, rendering the anti-double bond electron-poor, thus influencing orientation of reaction. Wilt and Peeran found that reaction of diazoethane with 7-*tert*-butoxynorbornadiene produced three monoadducts; 16% *endo-syn*, 63% *exo-anti*, and 21% *endo-anti*, with at least one bis adduct (*exo-anti*, *endo-syn*). In 1978 Wilt and Roberts acknowledged that no stereospecificity was evident in the reaction between diphenyldiazomethane and 7-chloronorbornadiene.¹¹⁵ The three monoadducts were formed in the proportions 58% *endo-anti*, 16% *endo-syn*, and 26% *exo-anti*. Saito and Motoki reported that *exo* monoadducts alone were formed in the 1,3-dipolar cycloaddition between thione S-imides and norbornene and norbornadiene in 1979.¹¹⁶ Likewise, Wilt and Malloy obtained exclusively *exo* monoadduct and *exo*, *exo* bis adduct from the cycloaddition of diphenyldiazomethane and norbornadiene.¹¹⁷ Filipescu and DeMember obtained the *exo* monoadducts alone in high yield upon reaction of 9-diazofluorene with either norbornene or norbornadiene under thermal or photochemical conditions.¹¹⁸ McLean and Findlay performed the cycloaddition between phenylazide and norbornadiene and recovered both the *exo* and *endo* monoadducts in a ratio of 11:1.¹¹⁹ They were additionally able to identify four of the six possible bis adducts in the product mixture. The *endo*, *endo* bis adducts were not formed. In 1959, Stille and Frey observed only *exo* addition of cyclopentadiene to norbornadiene,¹²⁰ as did Lidlov, Delacey and Kennard in the cycloaddition of hexachlorocyclopentadiene to norbornadiene.¹²¹ This was believed to be the case because the *exo* position was the least hindered site of attack. Fliege and Husigen studied cycloadditions between 1,3-dipoles

diphenylnitrilimine and benzonitrile oxide and dipolarophiles norbornene and 7,7-dimethylnorbornene.¹²² They attribute exclusive *exo* preference to torsional effect and steric hindrance by *endo* 5,6-norbornene hydrogens.

Battiste and coworkers reported similar findings for Diels-Alder cycloadditions between 7-substituted norbornadienes and hexachlorocyclopentadiene.¹²³ The authors note that a large formation of the *endo-syn* isomer coincides with the presence of an oxo group (eg., OAc, OCOPh, O-t-Bu) in the 7-substituent, while other non-oxo 7-substituents (eg., methyl) afford little or no *syn-endo* adduct. A comparison of partial rate factors (relative to standard norbornadiene) of 7-*tert*-butoxynorbornadiene and 7-norbornadienyl benzoate was an indication to the authors of the sensitivity of cycloaddition to the inductive effect of the oxygen bound to C-7. Since the *endo-syn* mode of cycloaddition was taken to be most sensitive to electron density of C-7 bound oxygen, the relative rate factor decrease on substituting the benzoyl group for O-tBu should be most dramatic for *endo-syn*, as was confirmed by the data in Table 1.

Table 1. Partial rate factors of cycloaddition with 7-substituted norbornadienes

	<i>endo-syn</i>	<i>endo-anti</i>	<i>exo-anti</i>	<i>exo-syn</i>
Norbornadiene		1.0		16.9
7- <i>tert</i> -butoxy	1.65	0.78	0.42	--
7-benzoyl	0.32	0.28	0.20	--

In 1974, Byrne, Rye, and Wege reported on a series of 7-substituted norbornadiene cycloadditions with hexachlorocyclopentadiene.¹²⁴ Their data are summarized in Table 2.

Table 2. Product distribution of hexachlorocyclopentadiene cycloaddition

	<i>anti-endo</i>	<i>syn-endo</i>	<i>anti-exo</i>
Norbornadiene		4%	96%
7- <i>tert</i> -butoxy		86%*	
7-Acetoxy	28%	47%	25%
7-Methyl	9%	4%	87%

* The remaining 14% was not identified, but was comprised of a single component.

With norbornadiene, predominant, but not stereospecific, addition to form the *exo* adduct is consistent with their expectation, as was the "normal" cycloaddition with 7-methylnorbornadiene. The amount of total *endo* formation increases from 13% for the 7-methyl substituent to 75% for the 7-acetoxy substituent to "predominately" for 7-*tert*-butoxy. One explanation for these observations was that the increase in size of the 7-substituent pushes the H-7 towards the *anti* double bond, thus allowing *endo* addition to become competitive. Additionally, electron activation of the *syn* double bond by the bound oxygen at the 7-position (as suggested by Klumpp and coworkers) was also suggested for the increased appearance of *syn-endo* adducts in 7-O-*t*Bu and 7-OAc substituted norbornadienes.

Houk and coworkers reported the rates and product ratios from reaction of hexachlorocyclopentadiene with 7-substituted norbornadienes in 1980,¹²⁵ and seven additional 7-substituted norbornadienes in 1990.¹²⁶ The rates of *exo* adduct formation were slowed upon substitution at the 7-position of increasingly electronegative substituents to a much greater extent than *endo* adduction. Additionally, 7-alkoxy substituents appeared to facilitate *endo-syn* adduction more than *endo-anti* adduction. Houk employed MO calculations to explain these observations. His explanation arises from the finding that the *endo* transition state partial bond

formation eclipses with the norbornadienyl allylic bonds, resulting in closed-shell repulsions. The *exo* transition state does not encounter similar repulsions, because the partially formed bonds are in a staggered conformation with the allylic bonds. While both *exo-anti* and *endo-anti* attack of electrophiles are decelerated by electron-withdrawing 7-substituents by lowering π -HOMO energy, *endo* attack is compensated somewhat by reduced closed-shell repulsive interactions. Electron-releasing 7-substituents produce the opposite effect of that just described. The increased production of *endo-syn* adduct compared to *endo-anti* adduct in the presence of 7-alkoxy substituents was attributed to through space interaction. Houk also mentions that the olefinic norbornadienyl C-H bonds were calculated as being distorted 2° from planarity in the *endo* direction.¹²⁷

DeMicheli, Gandolfi, Houk, and coworkers were interested in developing a general scheme to explain the means by which the electronegativities of 7-substituents on norbornadiene influence the stereochemistries of adducts observed.¹²⁸ They conducted 1,3-dipolar cycloaddition reactions between mesonitrile oxide and a series of nine 7-substituted norbornadienes and determined the relative percentages of each of the four possible monoadducts. They came to the conclusion that electron release by the 7-substituent increases the rate of *exo*-attack by electrophilic species, because electron rich allylic σ bonds are *anti* to electron deficient partial bonds in the transition state. Conversely, electron-withdrawal by the 7-substituent decreases the rate of electrophilic attack at the *exo* face to a greater extent than at the *endo* face. A *syn-endo* versus *anti-endo* preference was not observed.

Freeman compiled data that indicated that 7-substituents *syn* to the double bond of 7-substituted norbornenes greatly reduce the rate of *exo* additions involving cyclic transition states relative to unsubstituted norbornenes.¹²⁹ The rate reductions were attributed to both the size of the 7-substituent and the size of the addend.¹³⁰ Baird and Surridge observed either complete

failure to react or formation of *endo* products (in lieu of *exo*) in the addition reactions of syn-7-*tert*-butylnorbornadiene involving cyclic transition states. The combined bulk of the *tert*-butyl group and addends was made to account for the observed selectivity.¹³¹

Table 3. Stereochemistry of 1,3-dipolar cycloaddition of some 1,3-dipoles to 7-substituted norbornadienes

Substituent	Dipole	% Adduct				Ref.
		<i>exo-anti</i>	<i>endo-anti</i>	<i>endo-syn</i>	<i>exo-syn</i>	
	-diazomethane					
H	Dimethyl	100(exo)				110
H	Diphenyl	100(exo)				117
OH	Methyl	70	--	30	--	113
O- <i>t</i> Bu	Methyl	--	--	--	100	113
O- <i>t</i> Bu	Diphenyl	36.5	25	36	2.5	14
Cl	--	--	100	--	--	113
Cl	Methyl	--	100	--	--	113
Cl	Diphenyl	26	58	16	--	115
CH ₃	Diphenyl	100	--	--	--	132
Phenyl	Diphenyl	86.8	4.7	8.5	--	132
	-azide					
H	Phenyl	92(exo)	8(endo)			119
O- <i>t</i> Bu	Phenyl	30	--	55	15	111
CH ₃	Phenyl	64	14	23.6	--	132
Phenyl	Phenyl	57.6	32.2	10.2	--	132
Cl	Phenyl	31.4	39.1	29.5	--	132

Table 3 provides a summary of data given in the literature of product distributions of

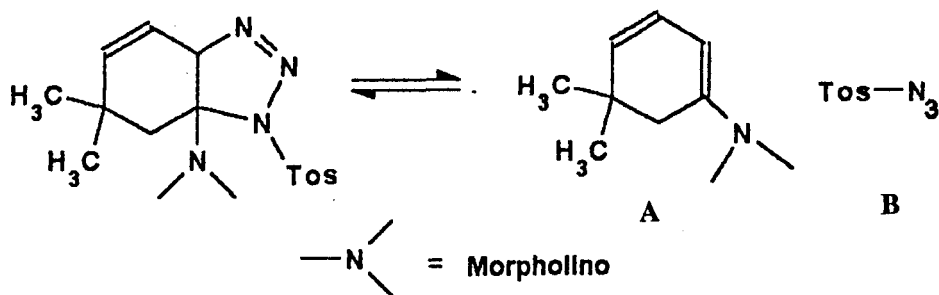
1,3-dipolar cycloadditions between 7-substituted norbornadienes and derivatives of azides and diazomethane dipoles. Several 1,3-dipolar cycloadditions between 7-substituted norbornadienes and phenylazide derivatives bearing electron withdrawing and releasing substituents have also been tested, but the inductive effect on the dipole has been shown to be insignificant.¹³²

In 1981, Cieplak proposed a model that would explain the stereochemical outcome of bimolecular reactions in which two specific interactions tended to oppose one another.¹³³ The first is steric hindrance, a destabilizing interaction which favors one direction of approach of a reactant species to the substrate molecule. The second is a two-electron stabilizing interaction between non-reacting vicinal occupied orbitals (σ) with the unoccupied antibonding orbitals of the incipient bonds (σ^*), and tends to favor the opposite direction of approach. Cieplak developed his model from reduction reactions with cyclohexanone derivatives, but suggested that the model had wide general application. Cieplak additionally suggested that solvation may affect stereoselectivity through electron-donor interactions with incipient σ^* orbitals. In 1992, le Noble and Hahn invoked Cieplak's model to explain the dramatic E/Z ratio of 20 - 25 for the reduction of 5-aza-2-adamantanone and its N-substituted derivatives.¹³⁴

Most recently, diphenyldiazomethane has been used in a 1,3-dipolar cycloaddition with buckminsterfullerene, C_{60} , producing spherical expansion compounds dubbed fulleroids; Ph_2C_{61} , Ph_4C_{62} , Ph_6C_{63} , Ph_8C_{64} , $Ph_{10}P_{65}$, $Ph_{12}C_{66}$.¹³⁵

A number of 1,3-dipolar cycloreversions have been reported. A review article by Bianchi, DeMicheli, and Gandolfi cites numerous examples of 1,3-dipolar cycloreversions in which the cycloadduct undergoes ring fission and small molecule extrusion processes.¹³⁶ Triazolines, such as the cycloadducts formed from reaction of phenyl azide and β -piperidinomethacrylonitrile,^{137,138} undergo cycloreversions to azides and alkenes, and to diazoalkanes and azomethines.¹³⁹⁻¹⁴⁶ In 1965, Huisgen *et al.* noted a thermal cycloreversion of

exo-monoadduct of norbornadiene and phenylazide to give a retro-Diels-Alder reaction to form cyclopentadiene and 1-phenyl-1,2,3-triazole.¹⁴⁷ Other cycloreversions lead to diazoalkanes and C=O¹⁴⁸⁻¹⁵¹, C=Se¹⁵², C=S¹⁵³, and N=P¹⁵⁴ double bonds. Paulisson was the first to report a cycloreversion of a 1,3-dipole adduct obtained from a diazoalkane. When the cycloaddition between norbornadiene and ethyl diazoacetate was allowed to proceed in the presence of Fe(CO)₅ catalyst, only cycloreversion products 3-ethylpyrazole carboxylate and cyclopentadiene were present.¹⁵⁵ Fewer examples exist of thermally or photochemically induced equilibria in which the original reactant molecules are reformed from cycloadduct.¹⁵⁶⁻¹⁵⁸ The cycloaddition between A and B (Scheme V) is an equilibrium process.¹⁵⁹



Scheme V

Smets and L'abbé reported a series of cycloreversions in 1973. Cycloreversions of 1,3-dipolar cycloadducts were found to occur with the ethoxy ester of 1-hexyl-4-carboalkoxy- Δ^2 -tetrazolin-5-one and several 1-alkyl-4-sulfonyl- Δ^2 -tetrazolin-5-ones at elevated temperatures, decomposing to starting materials. The cycloreversions were thought to have a concerted mechanism and to be in equilibrium with the cycloaddition process.¹⁶⁰ Grashey and Adelsberger reported a series of 1,3-dipolar cycloadditions between azomethine imines of the 3,4-dihydroisoquinoline series and other carbonyl compounds to form 5-membered rings called oxadiazolidines, but these are thermally unstable and undergo cycloreversion to starting

compounds.¹⁶¹ These researchers also observed thermolability of cycloadducts formed from reaction of the same azomethine imines with Schiff bases and azines, although to a lesser extent.¹⁶²

In summary, a full complement of empirical solvent parameters has been presented. All have been developed to improve on the comparison of observed solvent effects (on physical and chemical processes) to a well defined set of solvent parameters. Some of these parameters were designed for a narrow application (eg., Berson's Ω , Abraham's Sp , Winstein's Y) while others were intended for general use (eg., Dimroth's E_T polarity scale, multiple parameter equations). When considering an empirical parameter to be used in correlation with an observed physical or chemical process, it is essential that the parameter in question was derived from a compatible physicochemical process. If this were not the case, there could be no logical interpretation of the correlation, regardless of the goodness of fit. Inclusion of most of the parameters in this chapter--whether their application in this study is viable or not--is a statement that they have all been considered to some extent.

The study of solvent effect on concerted reactions has been approached from numerous directions. In studies involving pure solvents, Diels-Alder rate enhancements have been attributed to solvent polarity⁸⁴, "solvophobic interaction",⁸² viscosity,⁸⁶ and have been correlated to E_T and the Koppel-Palm equation.⁷⁴ Some 1,3-dipolar cycloaddition rate accelerations were attributed to solvent hydrogen-bonding and polarizability interactions.⁸³ Diels-Alder *endo/exo* stereoselectivity and rate enhancements have been observed in pure solvents and binary water mixtures as having occurred by micellar catalysis^{7, 79, 80} and were correlated to E_T .⁷ *Endo/exo* stereoselectivity and rate enhancement of Diels-Alder reactions in aqueous media (ie., binary solvent mixtures or pure water) has been investigated^{3-6, 76-78} and was attributed to "hydrophobicity"⁷⁶⁻⁷⁸ and correlated to Sp and a two-parameter combination of $Sp + E_T^N$.³⁻⁶ Very

little investigation of solvent effect on 1,3-dipolar cycloadditions has been done, possibly because this class of reactions is more complicated than Diels-Alder reactions due to the charge-separation of the reacting species. As a consequence, while the particulars of the transition state complex are understood, the details of solvent interaction with the complex are not. The results of this research may help to clarify this interaction.

CHAPTER III

RESULTS

1. Overall yields of mono-pyrazoline adducts.

A total of 26 solvents have been used in this study. The solvents were chosen based upon the following criteria:

- a) The reactants must be completely soluble in the solvent.
- b) Chosen solvents must be inert toward both reactants. Carbon disulfide, trifluoroethanol, and all carboxylic acids and olefins were eliminated as possible solvents for this reason.
- c) The solvents must be miscible with methanol if they are high boiling, since methanol is used both as an HPLC cosolvent and for sample preparation for HPLC analysis.
- d) Sufficient solvent parameter data must be available for the chosen solvents.

Table 4 provides a listing of the total monoadduct yield in millimoles and as percent yields from limiting reagent *7-tert*-butoxynorbornadiene and from reacted diphenyldiazomethane. The moles of monoadduct in each case was obtained from HPLC analysis against internal standard *E*-stilbene. Diphenyldiazomethane data were obtained by spectrophotometric analysis of the reaction mixture. The entries have been grouped into solvent "families" for ease of comparison.

2. Relative yields of mono-pyrazoline adducts and product ratios.

The relative percentages of each monoadduct obtained from reaction in pure solvents for 30 ± 2 days are given in Table 5. Table 6 also provides a listing of (*syn-endo* + *syn-*

exo)/(*anti-endo* + *anti-exo*) ratios and (*syn-exo* + *anti-exo*)/(*syn-endo* + *anti-endo*) ratios, and their corresponding \log_{10} values. Standard deviations have been calculated for the $\Sigma\text{syn}/\Sigma\text{anti}$ product ratios and their \log_{10} values. Since all four monoadducts are inextricable and should be considered simultaneously, we have used the option of summing the pairs of like isomers (ie., *syn-exo* + *syn-endo*, *anti-exo* + *anti-endo*, etc.) and have used the ratios of these sums instead of ratios of single isomers. Compared to the $\Sigma\text{syn}/\Sigma\text{anti}$ values, deviations from the overall trend of the $\Sigma\text{exo}/\Sigma\text{endo}$ calculation are enhanced, because the two typically smallest quantities--*syn-exo* and *anti-exo*--are both in the numerator. In the $\Sigma\text{syn}/\Sigma\text{anti}$ calculation, however, the *syn-exo* and *anti-exo* quantities are distributed in the numerator and denominator, so that modest deviations are effectively averaged out. The $\Sigma\text{exo}/\Sigma\text{endo}$ values will not be used further.

The $\log(\Sigma\text{syn}/\Sigma\text{anti})$ and $\log(\Sigma\text{exo}/\Sigma\text{endo})$ treatments can be related to free energy differences in the reaction, as argued by Berson.² A free energy relationship can provide a physical meaning for observed solvent effects. Given that all four isomeric products are under kinetic control, it can be assumed that formation of each isomer in a given solvent follows a 2nd order rate law.¹⁶³ Therefore, it may be assumed that the product ratio of *syn/anti* or *exo/endo* is equal to the ratios of their specific rate constants, $k_{\text{syn}}/k_{\text{anti}}$ or $k_{\text{exo}}/k_{\text{endo}}$, respectively. Since the reactants giving rise to each isomeric transition state are identical, the $\log(k_{\text{syn}}/k_{\text{anti}})$ or $\log(k_{\text{exo}}/k_{\text{endo}})$ is proportional to the free energy difference of the *syn* and *anti* (or *exo* and *endo*) transition states, according to Equation 21, where h is Planck's constant and k' is Boltzmann's constant.

$$\Delta G^\ddagger = -2.303RT(\log k + \log h/k'T) \quad (21)$$

Table 4. Overall yield of monoadduct

Entry	Solvent	mmole 7-TBN (LmRe) [†]	mmole Ph ₂ CN ₂ Consumed	mmole Adduct total	Adduct Yield @ Ph ₂ CN ₂	Adduct Yield @ 7-TBN
1	Neat	1.01	0.880	0.405	46.3	40.1
2	CCl ₄	1.00	0.651	0.220	33.8	19.6
3	CHCl ₃	1.01	0.411	0.192	46.7	19.0
4	CH ₂ Cl ₂	1.02	0.404	0.157	38.9	15.4
5	n-Octanol	1.03	0.664	0.269	40.6	26.1
6	t-Butanol	1.00	0.597	0.309	51.7	30.9
7	n-Butanol	1.01	0.436	0.250	57.3	24.6
8	2-Propanol	0.988	0.434	0.243	56.1	24.4
9	Ethanol	0.994	0.385	0.223	57.7	22.4
10	Methanol	1.03	0.324	0.197	60.8	19.1
11	Ethyl Acetate	0.996	0.378	0.209	55.4	21.0
12	Acetone	1.00	0.344	0.186	53.9	18.4
13	Ethyl ether	1.00	0.436	0.242	55.6	24.1
14	Tetrahydrofuran	0.996	0.499	0.268	53.7	26.9
15	Dioxane	1.06	0.452	0.242	53.7	22.9
16	n-Hexane	1.00	0.449	0.231	51.4	23.0
17	Cyclohexane	1.02	0.462	0.311	67.4	30.6
18	Decalin	0.995	0.409	0.267	65.2	26.9
19	Benzene	1.06	0.380	0.258	67.9	24.4
20	Nitrobenzene	0.996	0.407	0.256	63.7	25.7
21	Nitromethane	1.05	0.606	0.209	34.5	19.9
22	Propionitrile	1.08	0.601	0.201	33.4	18.7
23	Benzonitrile	1.02	0.401	0.227	56.8	22.4
24	Acetonitrile	1.02	0.581	0.182	31.4	17.9
25	HCON(CH ₃) ₂	1.01	0.669	0.304	45.4	30.1
26	Sulfolane	1.00	0.841	0.267	31.9	26.6
27	CH ₃ SOCH ₃	0.993	0.808	0.406	50.2	40.9

[†]7-*tert*-butoxynorbornadiene (7-TBN) is the limiting reagent

Table 5. Relative percentages of monoadducts in selected solvents

Entry	Solvent	<i>Anti-Endo</i> %	<i>Anti-Exo</i> %	<i>Syn-Exo</i> %	<i>Syn-Endo</i> %
1	Neat	42.2 ± 2.4	27.1 ± 1.7	2.0 ± 0.3	28.7 ± 2.6
2	CCl ₄	33.1 ± 0.3	27.5 ± 1.2	6.0 ± 0.5	33.5 ± 0.9
3	CHCl ₃	42.8 ± 2.0	31.4 ± 0.5	2.2 ± 0.2	23.7 ± 1.8
4	CH ₂ Cl ₂	42.1 ± 2.0	31.6 ± 2.3	2.6 ± 0.6	23.8 ± 0.8
5	1-Octanol	34.6 ± 1.9	30.2 ± 1.7	3.9 ± 0.2	31.4 ± 3.3
6	<i>t</i> -Butanol	38.8 ± 1.0	28.4 ± 1.4	3.6 ± 0.3	29.2 ± 0.7
7	<i>n</i> -Butanol	36.8 ± 1.0	31.8 ± 2.1	2.9 ± 0.1	28.5 ± 2.6
8	2-Propanol	38.3 ± 0.9	30.5 ± 0.6	3.4 ± 0.7	27.8 ± 1.0
9	Ethanol	38.2 ± 0.6	31.8 ± 0.5	3.3 ± 0.3	27.0 ± 0.8
10	Methanol	39.8 ± 1.0	35.6 ± 0.0	2.4 ± 0.4	22.3 ± 0.6
11	Ethyl Acetate	35.4 ± 1.4	30.8 ± 0.4	4.2 ± 0.2	29.5 ± 1.5
12	Acetone	36.5 ± 1.4	29.0 ± 1.4	4.2 ± 0.4	30.4 ± 2.2
13	Ethyl ether	34.7 ± 1.4	28.5 ± 0.8	5.1 ± 0.9	31.8 ± 1.5
14	Tetrahydrofuran	35.4 ± 1.7	29.1 ± 0.9	4.2 ± 0.5	31.4 ± 1.4
15	Dioxane	33.2 ± 1.0	31.6 ± 1.8	3.8 ± 0.2	31.5 ± 1.4
16	Hexane	33.3 ± 1.1	26.6 ± 1.2	6.2 ± 0.5	33.9 ± 0.6
17	Cyclohexane	33.0 ± 1.0	25.1 ± 1.1	5.2 ± 0.6	36.7 ± 1.9
18	Decalin	33.0 ± 0.7	23.6 ± 0.5	6.1 ± 0.2	37.4 ± 0.9
19	Benzene	36.4 ± 1.0	30.4 ± 1.8	3.9 ± 0.8	29.3 ± 2.6
20	Nitrobenzene	40.5 ± 1.3	32.0 ± 2.5	3.1 ± 0.4	24.4 ± 1.5
21	Nitromethane	41.4 ± 0.9	37.6 ± 1.6	2.2 ± 0.2	18.8 ± 1.5
22	CH ₃ CH ₂ CN	40.1 ± 2.2	30.0 ± 1.3	4.6 ± 0.8	25.4 ± 1.8
23	Benzonitrile	43.5 ± 2.1	29.6 ± 1.5	3.0 ± 0.4	23.9 ± 1.2
24	Acetonitrile	38.4 ± 1.2	36.6 ± 1.2	2.2 ± 0.3	22.9 ± 2.0
25	HCON(CH ₃) ₂	39.0 ± 0.6	33.8 ± 1.1	2.6 ± 0.5	24.8 ± 1.2
26	Sulfolane	40.0 ± 1.2	31.9 ± 0.9	2.6 ± 0.2	25.6 ± 0.6
27	CH ₃ SOCH ₃	41.4 ± 3.0	31.8 ± 2.6	2.0 ± 0.5	25.0 ± 5.2

Table 6. Syn/Anti and Exo/Endo monoadduct ratios

Entry	Solvent	$\Sigma\text{Syn}/\Sigma\text{Anti}$	$\log(\Sigma\text{Syn}/\Sigma\text{Anti})$	$\Sigma\text{Exo}/\Sigma\text{Endo}$	$\log(\Sigma\text{Exo}/\Sigma\text{Endo})$
1	Neat	0.445 ± 0.057	-0.354 ± 0.052	0.410	-0.387
2	CCl_4	0.651 ± 0.036	-0.187 ± 0.024	0.651	-0.186
3	CHCl_3	0.349 ± 0.035	-0.460 ± 0.440	0.505	-0.297
4	CH_2Cl_2	0.359 ± 0.018	-0.446 ± 0.021	0.519	-0.285
5	1-Octanol	0.548 ± 0.088	-0.266 ± 0.066	0.517	-0.287
6	t-Butanol	0.488 ± 0.010	-0.312 ± 0.009	0.471	-0.327
7	n-Butanol	0.459 ± 0.053	-0.340 ± 0.052	0.531	-0.275
8	2-Propanol	0.455 ± 0.030	-0.343 ± 0.028	0.513	-0.290
9	Ethanol	0.431 ± 0.022	-0.367 ± 0.022	0.537	-0.270
10	Methanol	0.326 ± 0.017	-0.487 ± 0.023	0.612	-0.213
11	Ethyl Acetate	0.509 ± 0.037	-0.294 ± 0.031	0.539	-0.268
12	Acetone	0.530 ± 0.058	-0.278 ± 0.050	0.496	-0.305
13	Ethyl ether	0.585 ± 0.049	-0.234 ± 0.036	0.505	-0.297
14	THF	0.552 ± 0.040	-0.259 ± 0.031	0.499	-0.302
15	Dioxane	0.546 ± 0.038	-0.264 ± 0.030	0.547	-0.262
16	Hexane	0.668 ± 0.011	-0.175 ± 0.007	0.488	-0.312
17	Cyclohexane	0.722 ± 0.054	-0.143 ± 0.033	0.435	-0.362
18	Decalin	0.768 ± 0.029	-0.115 ± 0.017	0.422	-0.375
19	Benzene	0.498 ± 0.062	-0.306 ± 0.054	0.522	-0.282
20	Nitrobenzene	0.381 ± 0.034	-0.421 ± 0.038	0.541	-0.267
21	Nitromethane	0.266 ± 0.025	-0.576 ± 0.042	0.661	-0.214
22	$\text{CH}_3\text{CH}_2\text{CN}$	0.428 ± 0.022	-0.370 ± 0.022	0.528	-0.277
23	Benzonitrile	0.369 ± 0.026	-0.433 ± 0.030	0.484	-0.315
24	Acetonitrile	0.335 ± 0.034	-0.477 ± 0.045	0.633	-0.199
25	$\text{HCO}(\text{NH}_3)_2$	0.375 ± 0.032	-0.427 ± 0.037	0.571	-0.243
26	Sulfolane	0.393 ± 0.015	-0.406 ± 0.016	0.526	-0.279
27	CH_3SOCH_3	0.373 ± 0.107	-0.438 ± 0.127	0.509	-0.293

3. Rate of formation of monoadducts in n-hexane.

The rate of formation of three of the four possible monoadducts in hexane solution at two different concentrations was monitored by HPLC and the concentration values are listed in Tables 7 and 8. Due to the large error associated with very small HPLC peak areas (especially during the earlier part of the experiments), the *syn-exo* monoadduct concentrations were not monitored. The experiment represented by the data in Table 8 was conducted under conditions similar to that of the Table 7 data, except that it was carried out at twice (50 mL instead of 25 mL) the dilution.

Errors in Tables 7 and 8 expressed in \pm percentage for each monoadduct and total monoadduct were obtained by converting the standard deviations for individual and total monoadduct yields (in molar concentration, M) that were determined in the solvent study for hexane (see section 2 of Results). The error bars in Figures 1 and 2 are based on these \pm percentage values.

Reaction of Ph_2CN_2 with 7-TBN (7-t-butoxynorbornadiene) is expressed in Equation 22.



The 2nd order (1st order in both reactants) rate expression for the formation of monoadducts is given in Equation 23.

$$d[\text{Ph}_2\text{CN}_2]/dt = d[7\text{-TBN}]/dt = -k_1[\text{Ph}_2\text{CN}_2][7\text{-TBN}] \quad (23)$$

If the reaction is as simple as it appears in Equation 22, the 2nd order rate constant for this reaction could be obtained from the linear Equation 24, where a and b are initial concentrations

**Table 7. Molar concentrations of monoadducts formed over time
in a 25 mL hexane solution ([7-TBN] = 0.502 M)**

Day	[<i>endo-anti</i>]	[<i>exo-anti</i>]	[<i>endo-syn</i>]	[Total]
1	0.00104	0.00080	0.00135	0.00319
2	0.00206	0.00166	0.00277	0.00649
4	0.00496	0.00351	0.00488	0.0134
6	0.00670	0.00633	0.00849	0.0210
9	0.0105	0.00707	0.0124	0.0300
11	0.00985	0.00790	0.0125	0.0303
13	0.0102	0.00886	0.0125	0.0315
16	0.0147	0.0106	0.0166	0.0419
18	0.0146	0.0121	0.0159	0.0426
20	0.0149	0.0114	0.0178	0.0441
22	0.0160	0.0131	0.0193	0.0485
24	0.0191	0.0142	0.0198	0.0531
27	0.0216	0.0192	0.0249	0.0657
29	0.0204	0.0178	0.0228	0.0607
31	0.0193	0.0157	0.0218	0.0567
35	0.0254	0.0189	0.0264	0.0706
56	0.0321	0.0250	0.0365	0.0936
66	0.0402	0.0321	0.0461	0.1184
99	0.0506	0.0359	0.0543	0.1408
134	0.0571	0.0373	0.0528	0.1472

Errors are: [*endo-anti*] 13%; [*exo-anti*] 7%, [*endo-syn*] 1%, [Total Adduct] 10.0%

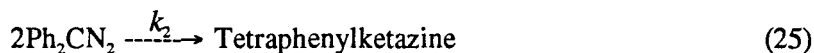
**Table 8. Molar concentrations of monoadducts formed over time
in a 50 mL hexane solution ([7-TBN] = 0.251 M)**

Day	[<i>endo-anti</i>]	[<i>exo-anti</i>]	[<i>endo-syn</i>]	[Total]
2	0.00071	0.00038	0.00076	0.00185
4	0.00116	0.00092	0.00142	0.00350
7	0.00161	0.00124	0.00257	0.00542
15	0.00286	0.00241	0.00386	0.00913
21	0.00531	0.00463	0.00649	0.0164
28	0.00659	0.00520	0.00842	0.0202
35	0.00796	0.00756	0.00914	0.0248
42	0.0124	0.00954	0.0123	0.0342
49	0.0125	0.00910	0.0132	0.0348
56	0.0113	0.00806	0.0128	0.0321
63	0.0145	0.0111	0.0166	0.0423
72	0.0165	0.0122	0.0191	0.0479
77	0.0175	0.0126	0.0192	0.0493
86	0.0175	0.0118	0.0200	0.0492
91	0.0168	0.0139	0.0196	0.0502
98	0.0176	0.0155	0.0208	0.0538
105	0.0168	0.0140	0.0211	0.0519
112	0.0170	0.0115	0.0205	0.0491
119	0.0174	0.0151	0.0209	0.0534
126	0.0198	0.0163	0.0229	0.0589

Errors are: [*endo-anti*] 13%, [*exo-anti*] 7%, [*endo-syn*] 1%, [Total Adduct] 10%

$$\{1/(a - b)\} \ln b(a - x)/a(b - x) = kt \quad (24)$$

of reactants and x is the amount of reactant consumed. Equation 24 is valid only when the decrease in both reactants over time is equivalent. In the present study, however, the competing condensation reaction of Ph_2CN_2 (Equation 25) ensures that the rate of disappearance of Ph_2CN_2 exceeds that of 7-TBN.



The rate expression for Equation 25 is given in Equation 26.

$$d[\text{Ph}_2\text{CN}_2]/dt = -k_2[\text{Ph}_2\text{CN}_2]^2 \quad (26)$$

The overall rate of disappearance of Ph_2CN_2 is expressed by combining Equations 23 and 26 into Equation 27.

$$d[\text{Ph}_2\text{CN}_2]/dt = -k_1[\text{Ph}_2\text{CN}_2][7\text{-TBN}] - k_2[\text{Ph}_2\text{CN}_2]^2 \quad (27)$$

Rearranging Equation 27 to equal zero and dividing both sides by $k_2[\text{Ph}_2\text{CN}_2]$ gives Equation 28.

$$(1/k_2)d\ln[\text{Ph}_2\text{CN}_2]/dt + k_1/k_2[7\text{-TBN}] + [\text{Ph}_2\text{CN}_2] = 0 \quad (28)$$

Using Equations 23 and 28, an iterative computer BASIC program (see appendix) was written

in which rate constants k_1 and k_2 were obtained simultaneously, adjusted to optimize the fit to experimental $[\text{Ph}_2\text{CN}_2]_t$ values. The k_1 values thus obtained are listed in Tables 9 and 10.

Table 9: Estimation of rate constants in a 25 mL hexane solution

	<i>endo-anti</i>	<i>exo-anti</i>	<i>endo-syn</i>	total adduct
k_1 (L/mol·min) =	1.45×10^{-6}	1.18×10^{-6}	1.64×10^{-6}	$4.27(\pm 0.23) \times 10^{-6}$

Table 10: Estimation of rate constants in a 50 mL hexane solution

	<i>endo-anti</i>	<i>exo-anti</i>	<i>endo-syn</i>	total adduct
k_1 (L/mol·min) =	1.18×10^{-6}	1.03×10^{-6}	1.44×10^{-6}	$3.65(\pm 0.17) \times 10^{-6}$

The rate of disappearance of 7-TBN was also monitored. Since 7-TBN is assumed to be unreactive toward any species other than Ph_2CN_2 , its concentration at time, t , can be found by subtracting total monoadduct concentration from the initial 7-TBN concentration. These values are given in Tables 11 and 12. The rate of disappearance of 7-TBN is depicted in Figures 1 and 2.

Rates of monoadduct formation at time, t , were determined by Equation 23 and using the k_1 values in Tables 9 and 10, $[\text{7-TBN}]_t$ values in Tables 11 and 12, and $[\text{Ph}_2\text{CN}_2]_t$ values in Tables 19 and 20. In 25 mL hexane, the initial rate ($t = 0$) is;

$$d[\text{Ph}_2\text{CN}_2]/dt = 4.27 \times 10^{-6} \text{ M}^{-1}\text{min}^{-1}(0.502 \text{ M})(0.600 \text{ M}) = 1.28 \times 10^{-6} \text{ M}\cdot\text{min}^{-1}$$

and in 50 mL hexane, the initial rate is;

$$d[\text{Ph}_2\text{CN}_2]/dt = 3.65 \times 10^{-6} \text{ M}^{-1}\text{min}^{-1}(0.251 \text{ M})(0.316 \text{ M}) = 2.90 \times 10^{-7} \text{ M}\cdot\text{min}^{-1}$$

After 29 days (the interval at which the solvent study was conducted; see section 2 of Results), the rate decreases in 25 mL hexane to;

$$d[\text{Ph}_2\text{CN}_2]/dt = 4.27 \times 10^{-6} \text{ M}^{-1}\text{min}^{-1}(0.441 \text{ M})(0.490 \text{ M}) = 9.23 \times 10^{-7} \text{ M}\cdot\text{min}^{-1}$$

And after 28 days in 50 mL hexane, the rate decreases to;

$$d[\text{Ph}_2\text{CN}_2]/dt = 3.65 \times 10^{-6} \text{ M}^{-1}\text{min}^{-1}(0.231 \text{ M})(0.287 \text{ M}) = 2.42 \times 10^{-7} \text{ M}\cdot\text{min}^{-1}$$

Rate constants for individual monoadducts were estimated by multiplying the relative percentage yield of each monoadduct (at 30 days) with the rate constant determined for total monoadduct. These data are listed in Tables 9 and 10.

Table 11: Rate of disappearance of 7-TBN in a 25 mL n-hexane solution

Time minutes	[Adduct] M	[7-TBN] M
0	0	0.502
1440	0.0032	0.498
2880	0.0065	0.495
5760	0.0134	0.488
8640	0.0215	0.480
12960	0.0300	0.472
15840	0.0303	0.471
18720	0.0315	0.470
23040	0.0419	0.460
25920	0.0426	0.459
28800	0.0441	0.457
31680	0.0485	0.453
34560	0.0531	0.448
38880	0.0657	0.436
41760	0.0607	0.441
50400	0.0706	0.431
80640	0.0936	0.408
95040	0.1184	0.383
142560	0.1408	0.361
192960	0.1472	0.354

Error for [Adduct] is $\pm 10\%$

$[7\text{-TBN}]_0 = 0.502 \text{ M}$

$R^2 = 0.992$, with a quadratic fit (Figure 1).

Table 12: Rate of disappearance of 7-TBN in a 50 mL n-hexane solution

Time Minutes	[Adduct] M	[7-TBN] M
0	0	0.251
288	0.0019	0.249
5760	0.0035	0.248
10080	0.0054	0.246
21600	0.0091	0.242
30240	0.0164	0.235
40320	0.0202	0.231
50400	0.0247	0.226
60480	0.0342	0.217
70560	0.0348	0.216
80640	0.0321	0.219
90720	0.0423	0.209
103680	0.0479	0.203
110880	0.0493	0.202
123840	0.0492	0.202
131040	0.0502	0.201
141120	0.0538	0.197
151200	0.0519	0.199
161280	0.0491	0.202
171360	0.0534	0.198
181440	0.0589	0.192

Error for [Adduct] is $\pm 10\%$

$[7\text{-TBN}]_0 = 0.251 \text{ M}$

$R^2 = 0.984$, with a quadratic fit (Figure 2).

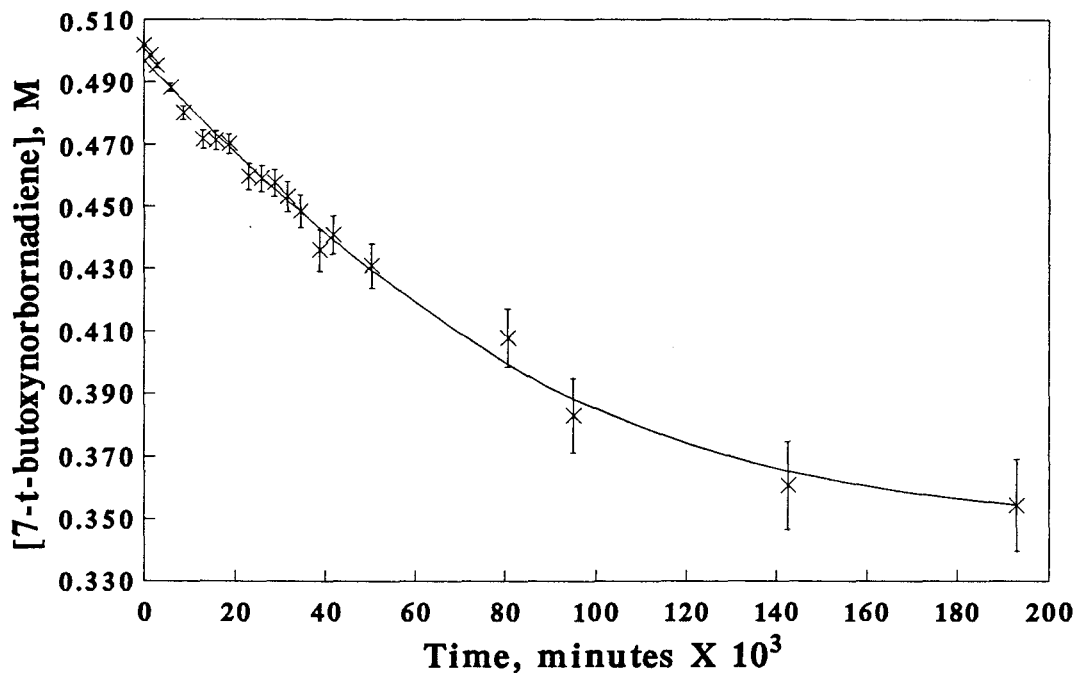


Figure 1. Rate of disappearance of 7-tert-butoxynorbornadiene in 25 mL hexane solution. (x) are experimental data points and line is the quadratic regression curve.

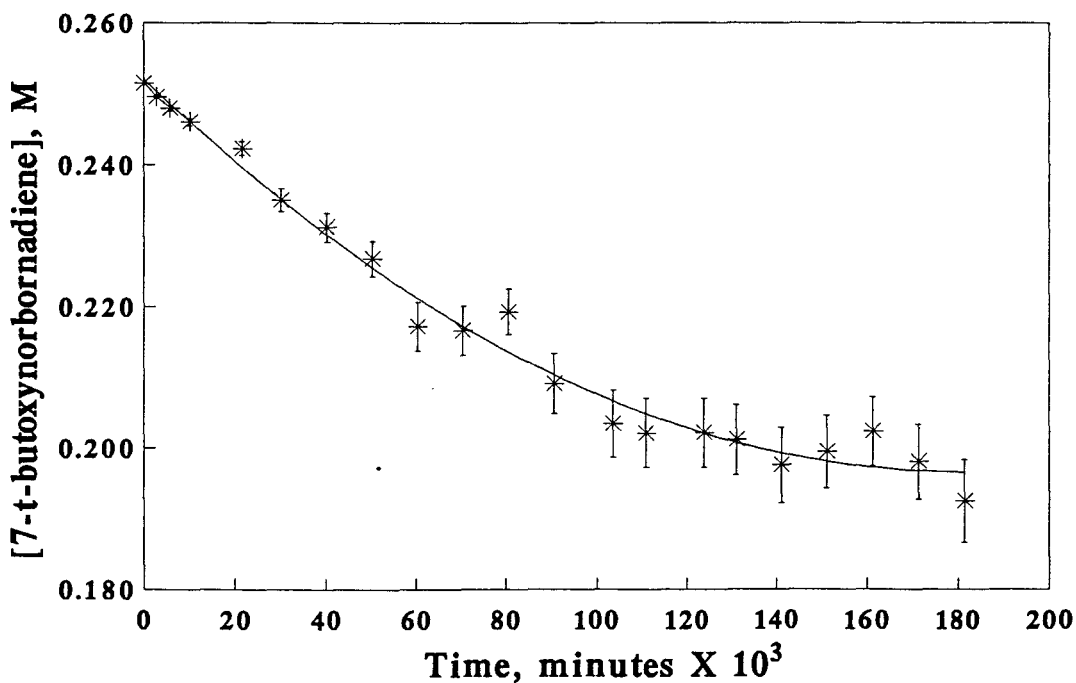


Figure 2. Rate of disappearance of 7-tert-butoxynorbornadiene in 50 mL hexane solution. (*) are experimental data points and line is the quadratic regression curve.

Table 13. Molar concentrations of monoadducts formed over time in a 25 mL CH₃CN solution ([7-TBN] = 0.502 M)

Day	[<i>endo-anti</i>]	[<i>exo-anti</i>]	[<i>endo-syn</i>]	[Total]
1	0.00126	0.00068	0.00108	0.00302
2	0.00219	0.00178	0.00146	0.00543
5	0.00529	0.00437	0.00313	0.0128
8	0.00838	0.00707	0.00512	0.0206
10	0.0100	0.00860	0.00587	0.0243
12	0.0119	0.00853	0.00649	0.0269
14	0.0144	0.0114	0.00826	0.0340
16	0.0146	0.0134	0.00851	0.0365
19	0.0184	0.0142	0.00998	0.0425
21	0.0220	0.0178	0.0134	0.0532
23	0.0212	0.0196	0.0140	0.0548
24	0.0191	0.0142	0.0198	0.0531
26	0.0245	0.0190	0.0120	0.0554
30	0.0262	0.0205	0.0152	0.0618
34	0.0300	0.0248	0.0172	0.0720
37	0.0294	0.0244	0.0178	0.0716
41	0.0334	0.0272	0.0185	0.0791
48	0.0370	0.0302	0.0173	0.0845
63	0.0421	0.0377	0.0223	0.1021
98	0.0521	0.0395	0.0258	0.1174
140	0.0590	0.0449	0.0240	0.128
159	0.0635	0.0463	0.0266	0.134

Errors are: [*endo-anti*] 6%; [*exo-anti*] 7%; [*endo-syn*] 7%; [Total Adduct] 5%

Table 14. Molar concentrations of monoadducts formed over time in a 50 mL CH₃CN solution ([7-TBN] = 0.251 M)

Day	[<i>endo-anti</i>]	[<i>exo-anti</i>]	[<i>endo-syn</i>]	[Total]
2	0.00041	0.00041	0.00056	0.00137
4	0.00114	0.00093	0.00092	0.00299
8	0.00266	0.00205	0.00183	0.00654
14	0.00412	0.00409	0.00245	0.0107
21	0.00654	0.00691	0.00364	0.0171
30	0.00906	0.00856	0.00489	0.0224
35	0.0110	0.0085	0.00517	0.0247
42	0.0122	0.0103	0.00552	0.0280
49	0.0132	0.0124	0.00562	0.0312
56	0.0148	0.0114	0.00691	0.0332
65	0.0180	0.0154	0.00774	0.0411
70	0.0204	0.0149	0.00792	0.0433
79	0.0197	0.0157	0.00896	0.0444
84	0.0185	0.0169	0.0101	0.0455
91	0.0200	0.0186	0.00903	0.0477
98	0.0224	0.0172	0.00906	0.0486
105	0.0204	0.0192	0.00932	0.0489
112	0.0214	0.0181	0.0100	0.0496
119	0.0250	0.0202	0.00984	0.0551
126	0.0213	0.0186	0.0101	0.0500
135	0.0242	0.0228	0.0119	0.0589

Errors are: [*endo-anti*] 6%; [*exo-anti*] 7%; [*endo-syn*] 7%; [Total Adduct] 5%

4. Rate of formation of monoadducts in acetonitrile.

The rate of formation of three monoadducts in acetonitrile solution was monitored and data accumulated as described for hexane in section 3 of Results. The experiment was conducted at concentrations similar to those for n-hexane. Concentration data for the three monoadducts are summarized in Tables 13 and 14.

Errors in Tables 13 and 14 expressed in \pm percentage for each monoadduct and total monoadduct were obtained by converting the standard deviations for individual and total monoadduct yields (in molar concentration, M) that were determined in the solvent study for acetonitrile (see section 2 of Results). The error bars in Figures 3 and 4 are based on these \pm percentage values.

Rate constants (k_1) were obtained via a computer program as described in section 3 of Results, and these are listed in Tables 15 and 16.

Table 15: Estimate of rate constants in a 25 mL acetonitrile solution

	<i>endo-anti</i>	<i>exo-anti</i>	<i>endo-syn</i>	total adduct
k_1 (L/mol·min) =	2.88×10^{-6}	2.26×10^{-6}	1.67×10^{-6}	$6.80(\pm 0.19) \times 10^{-6}$

Table 16: Estimate of rate constants in a 50 mL acetonitrile solution

	<i>endo-anti</i>	<i>exo-anti</i>	<i>endo-syn</i>	total adduct
k_1 (L/mol·min) =	0.440×10^{-6}	0.416×10^{-6}	0.238×10^{-6}	$1.08(\pm 0.05) \times 10^{-6}$

Rate constants for individual monoadducts were estimated by multiplying the relative

percentage yield of each monoadduct (at 30 days) with the rate constant determined for total monoadduct. These data are also listed in Tables 15 and 16.

Tables 17 and 18 provide data for the consumption of 7-*tert*-butoxynorbornadiene over time at 25 mL and 50 mL volumes in acetonitrile, respectively. Plots of these data are provided in Figures 3 and 4.

Rates of monoadduct formation were determined by substituting rate constants (Tables 15 and 16), [7-TBN] data (Tables 17 and 18), and [Ph₂CN₂] data (Tables 21 and 22) into Equation 23. Initial reaction rates (t = 0) in 25 mL acetonitrile are;

$$d[\text{Ph}_2\text{CN}_2]/dt = 6.80 \times 10^{-6} \text{ M}^{-1}\text{min}^{-1}(0.502 \text{ M})(0.532 \text{ M}) = 1.81 \times 10^{-6} \text{ M}\cdot\text{min}^{-1}$$

Initial reaction rates in 50 mL in acetonitrile are;

$$d[\text{Ph}_2\text{CN}_2]/dt = 1.08 \times 10^{-6} \text{ M}^{-1}\text{min}^{-1}(0.251 \text{ M})(0.319 \text{ M}) = 8.65 \times 10^{-8} \text{ M}\cdot\text{min}^{-1}$$

After 30 days (the interval at which the solvent study was conducted; see section 2 of Results), the reaction rate slowed in 25 mL in acetonitrile to;

$$d[\text{Ph}_2\text{CN}_2]/dt = 6.80 \times 10^{-6} \text{ M}^{-1}\text{min}^{-1}(0.440 \text{ M})(0.394 \text{ M}) = 1.18 \times 10^{-6} \text{ M}\cdot\text{min}^{-1}$$

A rate deceleration was also observed in the 50 mL volume after 30 days;

$$d[\text{Ph}_2\text{CN}_2]/dt = 1.08 \times 10^{-6} \text{ M}^{-1}\text{min}^{-1}(0.229 \text{ M})(0.263 \text{ M}) = 6.50 \times 10^{-8} \text{ M}\cdot\text{min}^{-1}$$

Table 17: Rate of disappearance of 7-TBN in a 25 mL acetonitrile solution

Time Minutes	[Adduct] M	[7-TBN] M
0	0	0.502
1440	0.0030	0.4987
2880	0.0054	0.4963
7200	0.0128	0.4889
11520	0.0206	0.4811
14400	0.0243	0.4774
17280	0.0269	0.4748
20160	0.0340	0.4677
23040	0.0365	0.4652
30240	0.0532	0.4485
33120	0.0548	0.4469
37440	0.0554	0.4463
43200	0.0618	0.4399
48960	0.0720	0.4298
53280	0.0716	0.4301
59040	0.0791	0.4226
69120	0.0845	0.4172
90720	0.1021	0.3996
141120	0.1174	0.3843
201600	0.1279	0.3738
228960	0.1364	0.3653

Error for [Adduct] is $\pm 5\%$, $[7\text{-TBN}]_0 = 0.5017 \text{ M}$
 $R^2 = 0.985$, with a quadratic fit (Figure 3)

Table 18: Rate of disappearance of 7-TBN in a 50 mL acetonitrile solution

Time Minutes	[Adduct] M	[7-TBN] M
0	0	0.2514
2880	0.0014	0.2500
5760	0.0030	0.2484
11520	0.0065	0.2449
20150	0.0107	0.2408
30240	0.0171	0.2343
43200	0.0224	0.2290
50400	0.0247	0.2267
60480	0.0280	0.2235
70560	0.0312	0.2202
80640	0.0332	0.2183
93600	0.0411	0.2103
100800	0.0433	0.2081
113760	0.0443	0.2071
120960	0.0455	0.2059
131040	0.0477	0.2037
141120	0.0486	0.2028
151200	0.0489	0.2025
161280	0.0496	0.2018
171360	0.0551	0.1963
181440	0.0500	0.2014
191520	0.0589	0.1925
201600	0.0560	0.1954

Error for [Adduct] is $\pm 5\%$, $[7\text{-TBN}]_0 = 0.2514 \text{ M}$
 $R^2 = 0.990$ with a quadratic fit (Figure 4).

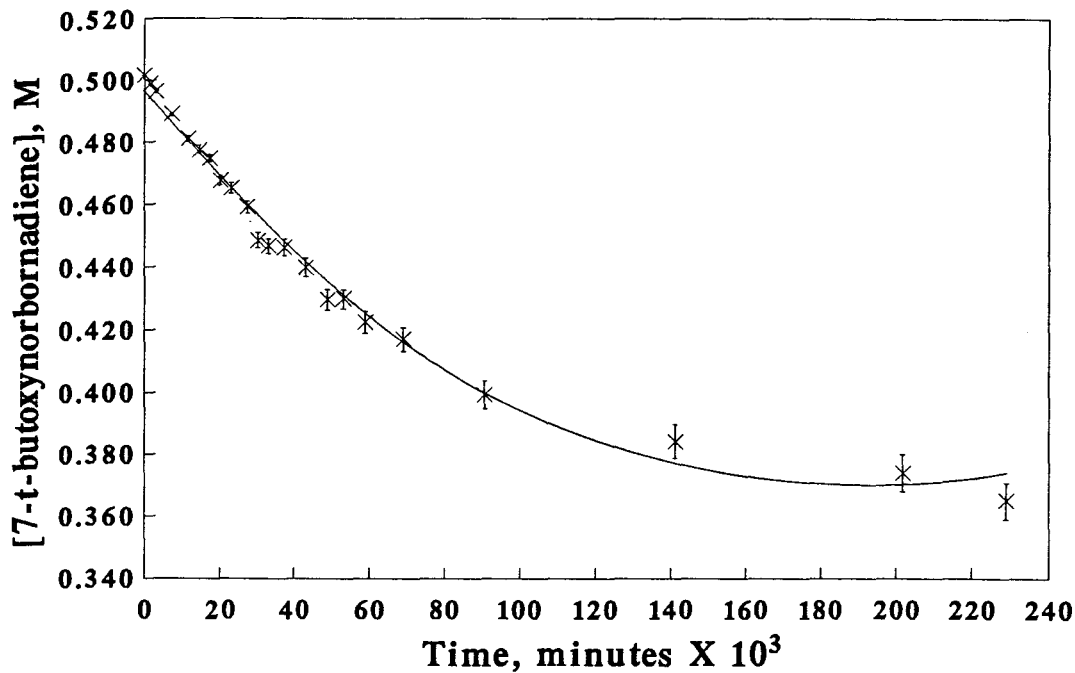


Figure 3. Rate of disappearance of 7-tert-butoxynorbornadiene in 25 mL CH_3CN solution. (\times) are experimental data points and line is the quadratic regression curve.

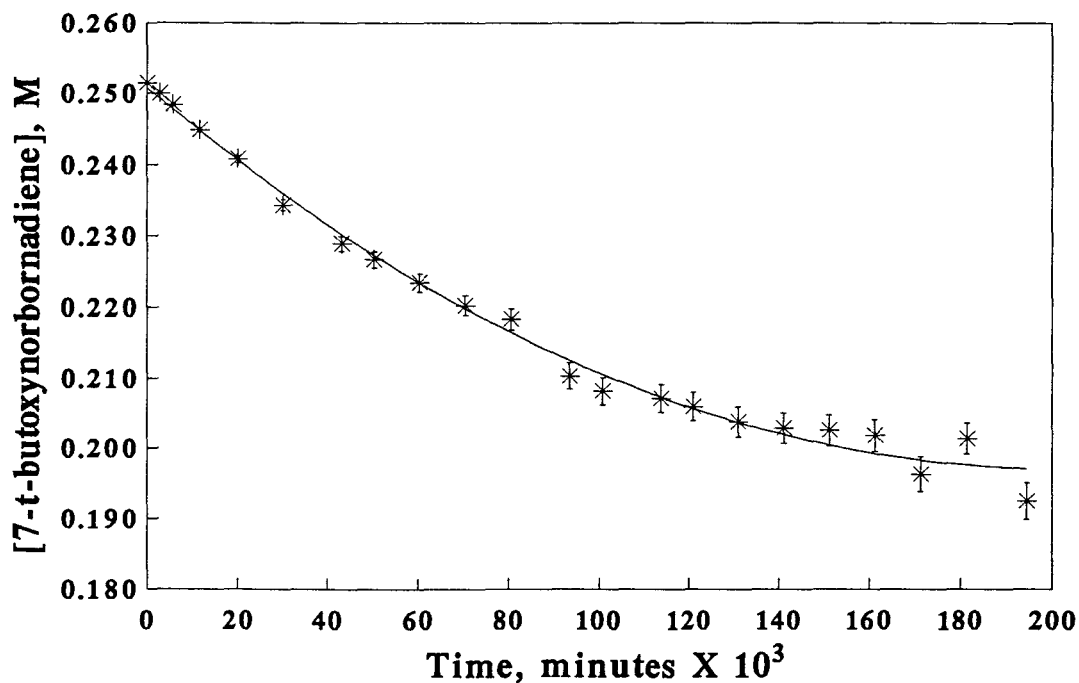


Figure 4. Rate of disappearance of 7-tert-butoxynorbornadiene in 50 mL CH_3CN solution. (*) are experimental data points and line is the quadratic regression curve.

5. Rate of disappearance of diphenyldiazomethane in hexane.

The rate of disappearance of diphenyldiazomethane in the kinetic reaction mixtures in hexane was measured by visible spectrophotometry at 525 nm. These values are listed in Tables 19 and 20. Errors are expressed in Tables 19 and 20 as \pm percentages for $1/c$ and were obtained from averaged data from the solvent study for hexane (see section 2 of Results). The error bars in Figures 5 and 6 are based on these \pm percentage values.

Rate constants (k_2 , Equation 26) were determined by computer program simultaneously with k_1 , as described in section 3 of Results. In a 25 mL hexane solution, $k_2 = 5.88(\pm 0.15) \times 10^6 \text{ M}^{-1}\text{min}^{-1}$ and in a 50 mL hexane solution, $k_2 = 6.38(\pm 0.11) \times 10^6 \text{ M}^{-1}\text{min}^{-1}$. Because the rate constants--and, thus the rate--of Ph_2CN_2 condensation (Equation 25) are marginally larger than the rate constants for monoadduct formation, the overall rate of Ph_2CN_2 disappearance (Equation 27) appears to follow 2nd order kinetics, i.e., 2nd order in Ph_2CN_2 . The observed rate constant, k_{obs} , was determined from the 2nd order rate relationship given in Equation 29,

$$1/c - 1/c_0 = kt \quad (29)$$

in which c = Molar concentration of Ph_2CN_2 after time, t

c_0 = Molar concentration of Ph_2CN_2 at $t = 0$

t = Time, minutes

Rate data used in the determinations of both k_2 and k_{obs} are given in Tables 19 and 20. Plots of $1/c$ versus time for the determination of k_{obs} are given in Figures 5 and 6. Observed rate constants are $1.02(\pm 0.31) \times 10^5 \text{ M}^{-1}\text{min}^{-1}$ in 25 mL in hexane and $9.96(\pm 0.32) \times 10^6 \text{ M}^{-1}\text{min}^{-1}$ in 50 mL in hexane.

There is reasonable agreement between the rate of Ph_2CN_2 disappearance calculated from

Equation 27 (using k_1 and k_2), and from Equation 26 (using k_{obs}). In 25 mL in hexane, the correlation between these two sets of data was excellent, with $R^2 = 0.99992$, and in 50 mL, $R^2 = 0.999761$, although the rates calculated from Equation 26 and k_{obs} were consistently larger.

A check on the goodness of fit of k_1 and k_2 was done with another BASIC computer program which used k_1 and k_2 to calculate the expected $[\text{Ph}_2\text{CN}_2]$ at each time interval (see Appendix for program). A comparison of $[\text{Ph}_2\text{CN}_2]_{calc}$ with $[\text{Ph}_2\text{CN}_2]_{exp}$ revealed good agreement, with $R^2 = 0.9676$ ($N = 19$) and $R^2 = 0.9894$ ($N = 20$) in 25 and 50 mL volumes, respectively.

Table 19: Determination of k_{obs} for the disappearance of Ph_2CN_2 in a 25 mL hexane solution

Time Minutes	$c = [\text{Ph}_2\text{CN}_2]$ M	$1/c$ M^{-1}
0	0.600	1.668
1440	0.589	1.698
2880	0.592	1.689
5760	0.574	1.743
8640	0.570	1.756
12960	0.553	1.807
15840	0.549	1.821
18720	0.543	1.843
23040	0.531	1.884
25920	0.523	1.911
28800	0.519	1.927
31680	0.507	1.972
34560	0.503	1.989
38880	0.485	2.064
41760	0.490	2.041
50400	0.469	2.135
80640	0.412	2.430
95040	0.390	2.563
142560	0.313	3.198

Error for $1/c$ is $\pm 3\%$

$c_0 = 0.600 \text{ M}$

$k_{\text{obs}} = \text{slope} = 1.02 \times 10^5 \text{ L/mol}\cdot\text{min}$ (Figure 5)

$R^2 = 0.992$

Table 20: Determination of k_{obs} for the disappearance of Ph_2CN_2 in a 50 mL hexane solution

Time Minutes	$c = [\text{Ph}_2\text{CN}_2]$ M	$1/c$ M^{-1}
0	0.316	3.170
2880	0.319	3.133
5760	0.314	3.187
10080	0.310	3.231
21600	0.301	3.323
30240	0.290	3.447
40320	0.287	3.486
50400	0.275	3.635
60480	0.268	3.737
70560	0.263	3.798
80640	0.255	3.926
90720	0.248	4.029
103680	0.243	4.117
110880	0.235	4.250
123840	0.232	4.309
131040	0.226	4.431
141120	0.222	4.496
151200	0.220	4.539
161280	0.218	4.585
171360	0.209	4.796
181440	0.193	5.171

Error for $1/c$ is $\pm 3\%$

$c_0 = 0.316 \text{ M}$

$k_{\text{obs}} = \text{slope} = 9.92 \times 10^{-6} \text{ L/mol}\cdot\text{min}$ (Figure 6)

$R^2 = 0.986$

6. Rate of disappearance of diphenyldiazomethane in acetonitrile.

The rate of disappearance of diphenyldiazomethane in acetonitrile solution was monitored and data accumulated as described for hexane in section 5 of Results. The experiment was conducted at concentration levels similar to that for hexane. Errors are expressed in Tables 21 and 22 as \pm percentages for $1/c$ and were obtained from averaged data from the solvent study for acetonitrile (see section 2 of Results). The error bars in Figures 7 and 8 are based on these \pm percentage values.

Rate constants (k_2) were found to be $8.82(\pm 0.03) \times 10^{-6} \text{ M}^{-1} \text{ min}^{-1}$ in 25 mL in acetonitrile and $1.41(\pm 0.05) \times 10^{-5} \text{ M}^{-1} \text{ min}^{-1}$ in 50 mL. Tables 21 and 22 provide data for the determination of k_{obs} by linear regression according to Equation 29. Plots of the rate data in Tables 21 and 22 are given in Figures 7 and 8, respectively. Observed rate constants were found to be $2.22(\pm 0.07) \times 10^{-5} \text{ M}^{-1} \text{ min}^{-1}$ and $1.60(\pm 0.05) \times 10^{-5} \text{ M}^{-1} \text{ min}^{-1}$ in 25 and 50 mL, respectively. As with the hexane data sets, there is reasonable agreement between rate of Ph_2CN_2 disappearance calculated from Equations 26 and 27, with $R^2 = 0.989713$ for the 25 mL data sets and $R^2 = 0.999997$ for the 50 mL data set. While the correlations are excellent, the rates determined from Equation 26 and k_{obs} are consistently larger, as expected.

The goodness of fit of k_1 and k_2 were determined by comparing $[\text{Ph}_2\text{CN}_2]_{\text{calc}}$ with $[\text{Ph}_2\text{CN}_2]_{\text{exp}}$. Again, good agreement was obtained, with $R^2 = 0.996$ ($N = 20$) for the 25 mL data set and $R^2 = 0.993$ ($N = 21$) for the 50 mL data set.

Table 21: Determination of k_{obs} for the disappearance of Ph_2CN_2 in a 25 mL CH_3CN solution

Time Minutes	$c = [\text{Ph}_2\text{CN}_2]$ M	$1/c$ M^{-1}
0	0.532	1.880
1440	0.527	1.899
2880	0.514	1.947
7200	0.500	2.001
11520	0.490	2.041
14400	0.478	2.092
17280	0.462	2.164
20160	0.461	2.169
23040	0.448	2.232
27360	0.438	2.281
30240	0.431	2.321
33120	0.427	2.344
37440	0.432	2.417
43200	0.394	2.536
48960	0.384	2.607
53280	0.375	2.667
59040	0.351	2.846
69120	0.327	3.061
90720	0.292	3.421
141120	0.212	4.724
201600	0.158	6.329
228960	0.143	6.998

$c_0 = 0.532 \text{ M}$, $R^2 = 0.98$. Error for $1/c$ is $\pm 3\%$

$k_{\text{obs}} = 2.22 \times 10^{-5} \text{ L/mol}\cdot\text{min}$ (Figure 7)

Table 22: Determination of k_{obs} for the disappearance of Ph_2CN_2 in a 50 mL CH_3CN solution

Time Minutes	$c = [\text{Ph}_2\text{CN}_2]$ M	$1/c$ M^{-1}
0	0.319	3.133
2880	0.313	3.198
5760	0.310	3.231
11520	0.299	3.348
20160	0.290	3.447
30240	0.277	3.608
43200	0.263	3.798
50400	0.256	3.909
60480	0.244	4.100
70560	0.231	4.329
80640	0.225	4.452
93600	0.218	4.585
100800	0.209	4.796
113760	0.203	4.924
120960	0.199	5.030
131040	0.196	5.113
141120	0.186	5.379
151200	0.172	5.817
161280	0.176	5.675
171360	0.177	5.640
181440	0.173	5.780
191520	0.159	6.289
201600	0.150	6.649

$c_0 = 0.319 \text{ M}$, $R^2 = 0.987$. Error for $1/c$ is $\pm 3\%$

$k_{\text{obs}} = \text{slope} = 1.60 \times 10^{-5} \text{ L/mol}\cdot\text{min}$ (Figure 8)

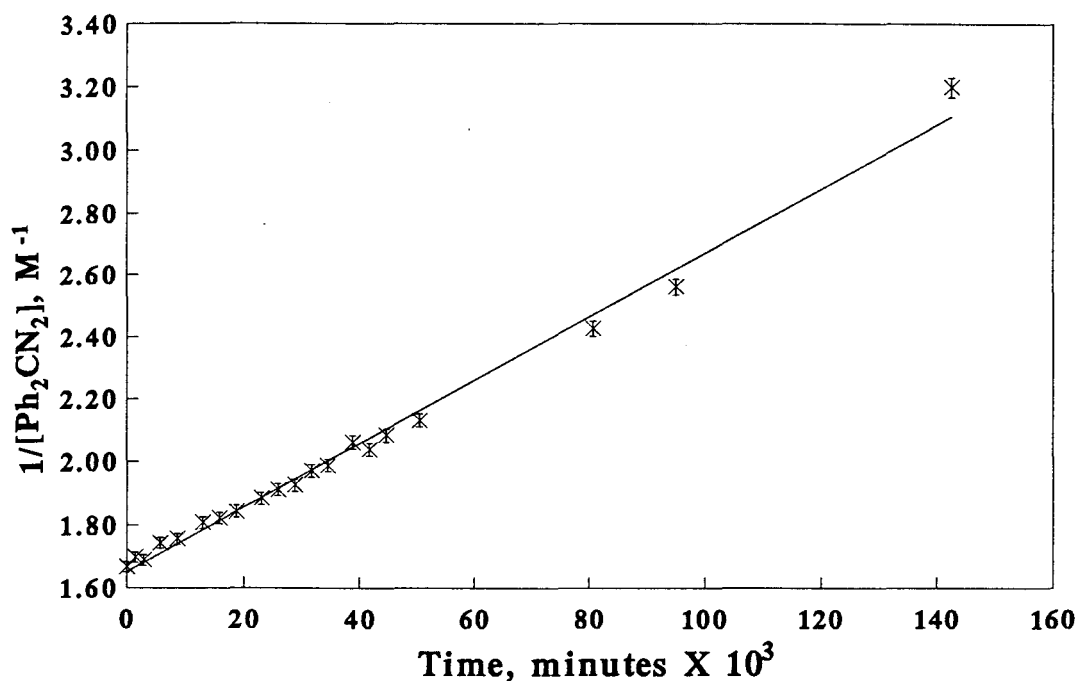


Figure 5. Plot of $1/c$ vs. time in 25 mL hexane solution. (\times) are experimental data points and line is the linear regression curve. The slope is k_{obs} for the apparent 2nd order rate of Ph₂CN₂ disappearance.

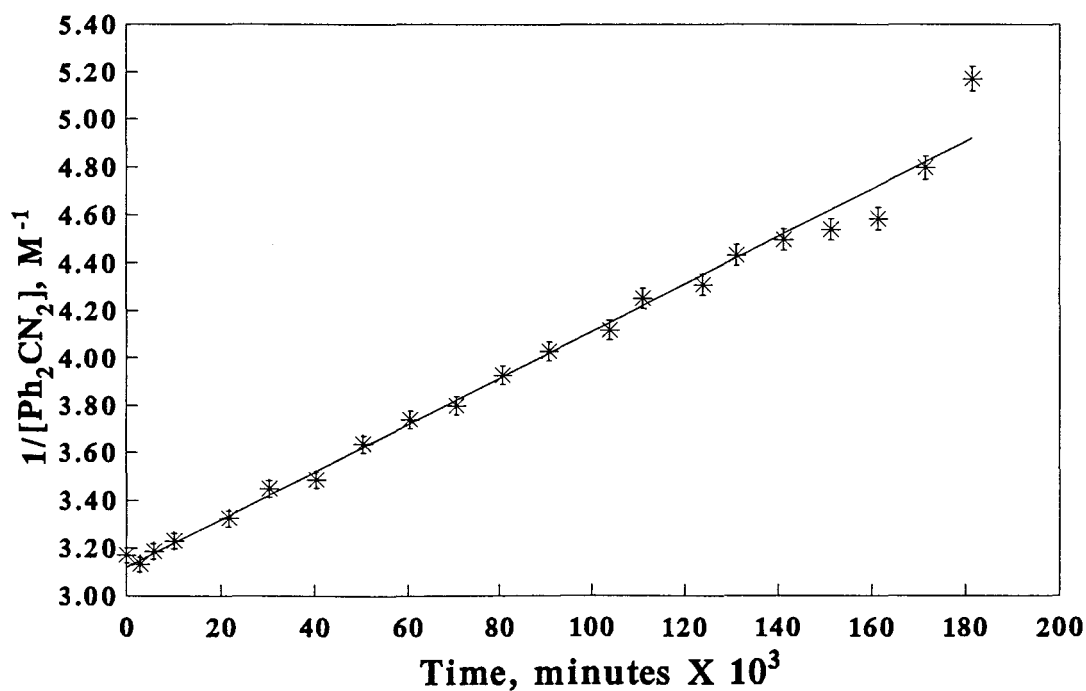


Figure 6. Plot of $1/c$ vs. time in 50 mL hexane solution. ($*$) are experimental data points and line is the linear regression curve. The slope is k_{obs} for the apparent 2nd order rate of Ph₂CN₂ disappearance.

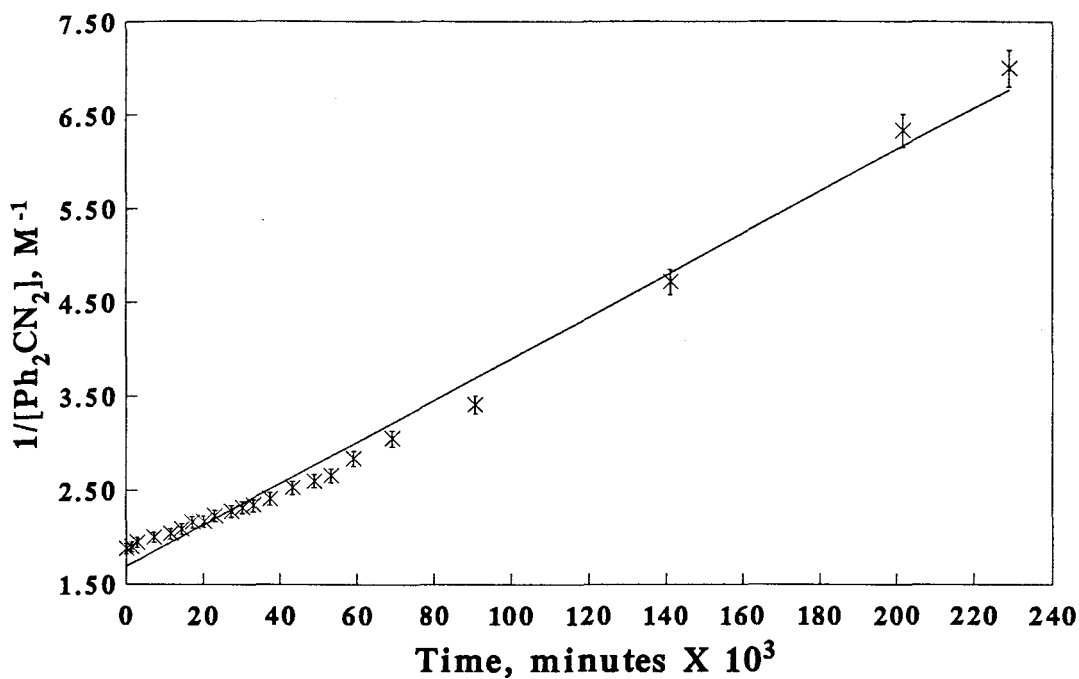


Figure 7. Plot of $1/c$ vs. time in 25 mL CH_3CN solution. (*) are experimental data points and line is the linear regression curve. The slope is k_{obs} for the apparent 2nd order rate of Ph_2CN_2 disappearance.

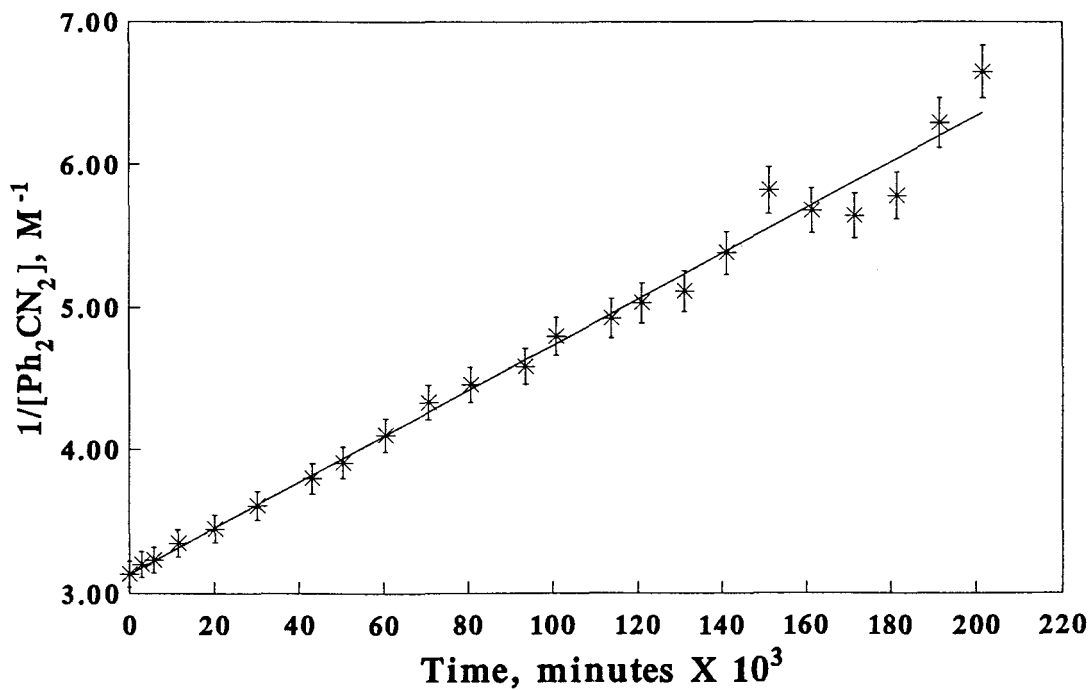
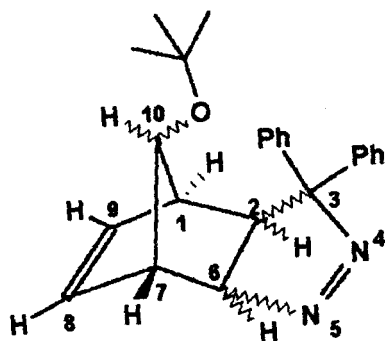
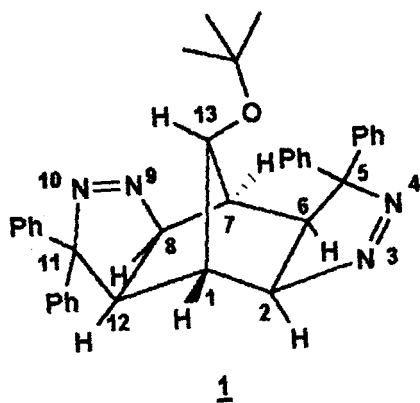
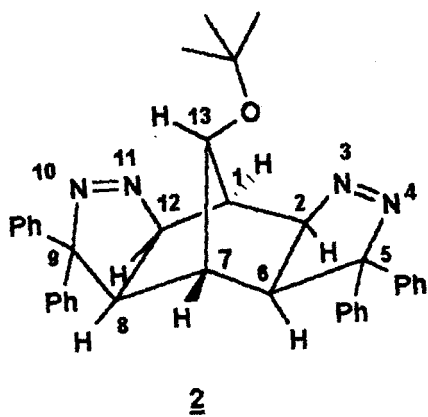


Figure 8. Plot of $1/c$ vs. time in 50 mL CH_3CN solution. (*) are experimental data points and line is the linear regression curve. The slope is k_{obs} for the apparent 2nd order rate of Ph_2CN_2 disappearance.

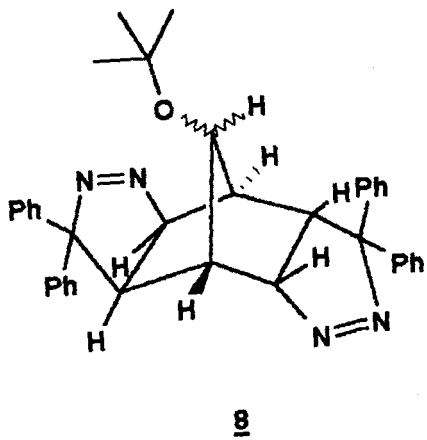
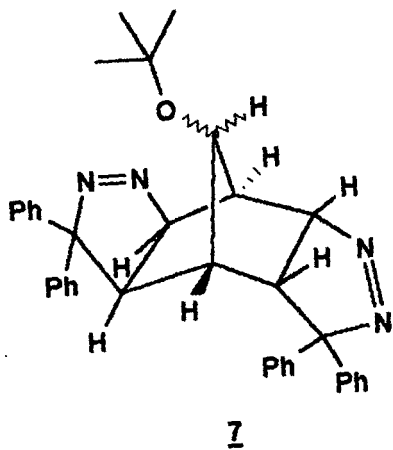
7. NMR analysis of mono- and bis-adducts.

Sullivan partially isolated the *syn-exo* monoadduct as a mixture of *syn-exo* and *anti-exo*, and his NMR analysis was based upon this mixture. The *syn-exo* adduct has presently been isolated, and the NMR peak assignments made by Sullivan have been confirmed. A total of five (out of six possible) bis adducts have been isolated, including four that have not been characterized previously. It has been determined that the structure assigned to Sullivan's *exo-exo* bis adduct is incorrect. Wilt and Sullivan assigned structure **1** to their compound based upon analysis of a 60 MHz ^1H NMR spectra, arguing that the bridgehead protons, H_1 and H_7 , at 2.59 - 2.86 ppm possessed the same chemical shift. A 300 MHz spectrum indicates that these peaks cannot be due to bridgehead protons, since, at the corresponding chemical shift of 2.78 and 2.71 ppm, the doublets are coupled to the overlapping doublets at 5.25 - 5.16 ppm as confirmed by a COSY 2D NMR experiment. The doublets at 2.78 and 2.71 are reassigned as the H_6 and H_8 protons of structure **2**, and the bridgeheads are singlets at 3.76 and 2.12 ppm corresponding to H_1 and H_7 , respectively. The COSY experiment also indicated a pronounced long-range coupling between the tert-butoxy methyl protons and H_{13} , due to the preferred orientation of the tert-butyl group away from the *exo* pyrazoline group and in close proximity to the bridgetop proton.

Exo, endo stereochemistries of the remaining bis adducts (structures **7** - **8**) were assigned by comparison of their NMR spectra with those of the parent monoadduct spectra (**3** - **6**), with emphasis on the *endo* and *exo* protons. In the ^1H NMR spectra of the monoadducts, H_2 and H_6 protons *endo* to the six-membered ring are coupled to one another, so that the corresponding peaks are doublets. The doublets of doublets corresponding to H_2 and H_6 occurs when these protons are *exo* to the ring, since H_1 - H_2 and H_6 - H_7 coupling occurs in addition to H_2 - H_6 coupling, due to the small dihedral angle between bridgehead and *exo* protons. Likewise, the *exo, endo* stereochemistries of bis adducts were based on the splitting patterns of H_2 , H_6 , H_8 ,



3-6



H₁₂.

All three proton spectra of the *exo*, *endo* bis adducts display a broad peak at 7.8 - 8.0 ppm which is absent in the *exo*, *exo* adduct and which integrates out to 1H. This peak is due to an ortho proton on an aromatic ring whose restricted rotation is due to crowding. Models of possible bis adducts suggest that such a high degree of aromatic ring crowding can occur only when pyrazoline ring formation results in a *cis*-configuration, ie., when all of the aromatic rings are on the same side of the norbornane skeleton. The *cis* isomer of the *exo*, *exo* adduct does not show a similarly restricted rotation, because the *exo*-pyrazoline rings are oriented far enough away from each other to prevent phenyl ring crowding.

¹³C NMR peak assignments for bis adducts were also based on comparisons with monoadduct spectra. In both mono- and bis adduct spectra, aromatic and vinylic carbons were downfield 125 - 145 ppm from reference tetramethylsilane. Aromatic ipso carbons were well separated at 140 - 144 ppm, with two ipso carbons in the monoadduct spectra and four ipso carbons in the bis adduct spectra. The monoadduct vinylic carbons were downfield from the remaining aromatic carbons and evident as being half the intensity of ortho and meta carbons. Vinylic carbons were distinguished from para carbon signals of equal intensity by comparison with chemical shifts of 7-*tert*-butoxynorbornadiene of 139.2 for the *anti* and 136.6 for the *syn* carbons, respectively. Para carbons were located at 126 - 128.2 ppm.

Quaternary benzylic carbons appear in the ¹³C NMR spectra of monoadducts in the range of 96.4 - 99.5 ppm (the *syn-exo* quaternary was not observed). Methine C₂'s are downfield at 96.4 - 100.3 ppm and the bridgetops are at 82.4 - 86.9 ppm. The quaternary *tert*-butoxy carbons are in a narrow range of 73.5 - 74.0 ppm. The peaks corresponding to C₁, C₆, and C₇ exist in the same range of 46.4 - 52.3 ppm and have not yet been assigned.

¹³C spectra of four of the bis adducts follow the general pattern of monoadduct spectra.

Only one quaternary benzylic carbon is evident in each of the *exo, exo* bis adduct spectra (102.5 and 101.9 ppm) based upon their peak intensities, but two are evident in each of the *endo, exo* spectra (103.7 + 97.0 and 102.7 + 98.9 ppm). Methine carbons α to the diaza group are upfield from the quaternary benzylics, at 91.0 - 99.5 ppm. Bridgetop C₁₃'s appear at 73.4 - 78.8 ppm, shifted upfield compared to monoadduct bridgetop carbons. The quaternary tert-butoxy carbons exist in the same range as the monoadduct quaternaries, around 74 ppm. Bridgehead carbons and carbons α to benzylic carbon appear in the same range as their monoadduct counterparts (C₁, C₆, and C₇), but like these, are not readily distinguished.

A HETCOR 2D NMR analysis of the *cis-exo, exo* bis adduct confirmed that the carbon peaks at 45.4 and 45.1 correspond to the ¹H NMR bridgehead singlets at 3.76 ppm and 2.12 ppm. The bridgetop carbon at 73.4 ppm corresponds to the ¹H singlet at 2.57 ppm.

CHAPTER IV

DISCUSSION

1. Overall yields of mono-pyrazoline adducts.

On reviewing Table 4, it appears that a large discrepancy exists between the percentage yields of total monoadduct calculated from limiting reagent *7-tert*-butoxynorbornadiene and from reacted diphenyldiazomethane; these differences vary dramatically from one solvent to the next. For example, in the absence of solvent (entry 1), the percentage yield when calculated from moles of diphenyldiazomethane consumed is only 1.2 times larger than when the yield is calculated from limiting reagent, but in methanol it is 3.2 times larger. The difference in calculated percentage yield calculations results from the competing side reaction of diphenyldiazomethane to form tetraphenylketazine as shown in Scheme V.

Scheme V

A very large peak attributable to tetraphenylketazine is evident in the HPLC traces of all the reaction mixtures analyzed. In all cases, tetraphenylketazine was not quantified because the size of the peak was radically off scale with respect to the internal standard. Even though the

reactants are far from completely consumed at the time of workup and analysis, the occurrence of this competing reaction complicates the analysis of overall monoadduct yield. Overall yields will henceforth refer to those which are calculated from reacted diphenyldiazomethane.

The greatest recovery of monoadduct resulted from the reaction in dimethyl sulfoxide (DMSO), entry 27, followed closely by reaction in the absence of solvent (entry 1). Of the remaining entries, the overall monoadduct yield is 1/2 to 3/4 that of the 'neat' reaction. This is consistent with a rate decrease upon dilution. There does not appear to be any discernible pattern between the total moles of monoadduct and any solvent property tested so far. In particular, it is not clear why the reaction in DMSO should produce a greater yield of monoadduct than the neat reaction. The high solvent polarity of DMSO cannot alone account for this anomaly, since dimethylformamide ($\epsilon = 36.7$, entry 25) and sulfolane ($\epsilon = 43.3$, entry 26), both highly polar solvents, do not give rise to proportionately larger yields.

In comparing the solvent parameter values listed in Table 27 to the yields in Table 4, certain trends are evident. Referring to the six simple alcohols in entries 5-10, there is an inverse relationship between ψ --the values representing cohesive energy density--and the moles of diphenyldiazomethane consumed. Since a certain amount of colinearity exists between cohesive energy density and dielectric constant ($R^2 = 0.705$ for solvents 2 - 27), it is not surprising that there is also an inverse relationship between solvent dielectric and moles of Ph_2CN_2 consumed. An inverse relationship also exists between cohesive energy density (ψ) and percentage yield of monoadduct. The chloromethyl compounds (entries 2-4) exhibit similar inverse relationships. A reasonable interpretation of these findings may be that, as the polarity of the solvent is increased, the 1,3-dipole is increasingly stabilized against condensation with itself. This would decrease the rate of consumption of Ph_2CN_2 and necessarily increase the percentage yield of monoadduct calculated from consumed Ph_2CN_2 . Similar trends are

consistently strong with protic solvents, as will be shown later, presumably because of the strong influence of intermolecular hydrogen bonding from these solvents. As for the remaining solvent families, no consistent correlation exists between the rate of disappearance of Ph_2CN_2 and Ψ , either across the entire solvent range or within solvent families. No trends are apparent when the dielectric constant, ϵ , is substituted for Ψ . There also does not appear to be any correlation between the total yield of monoadducts and either Ψ or ϵ .

Finally, the percentage yield data clearly typify a concerted reaction. Whether calculated from millimoles of 7-TBN or from millimoles of Ph_2CN_2 consumed, the percentage yield is not dependent on solvent polarity, polarizability, or hydrogen bond ability. For example, the percentage yield of monoadduct calculated from Ph_2CN_2 consumed in ethanol is 57.7% ($\epsilon = 24.55$), while in nonpolar aprotic ethyl ether ($\epsilon = 4.2$), the percentage yield is 55.6%, and in polar, aprotic benzonitrile ($\epsilon = 24.2$), the yield is 56.8%. Likewise, the percentage yields for these three solvents calculated from limiting reagent 7-*tert*-butoxynorbornadiene are very similar, at 22.4%, 24.1%, and 22.4%, respectively. The overall rates of concerted reactions are relatively insensitive to solvent polarity effects, so the yields are comparable for all solvents.

2. Relative yields and product ratios of monopyrazoline adducts.

It is obvious from the preceding discussion that overall yields of monoadduct in different solvents are not a viable indicator of the effect of solvent on 1,3-dipolar cycloadditions. Since four monopyrazoline isomers form, their relative formation in different solvents should be a better indicator of the solvent property or properties influencing the reaction. Table 5 lists the relative percentages of all four monoadducts in 26 solvents.

Upon inspection of this data, certain trends are apparent. The *syn-exo* monoadduct is consistently a minor product at less than 6.2% of the total. The *anti-exo* adduct is always less

in quantity than the *anti-endo* adduct. The *anti-endo* adduct is formed in greatest proportion in all solvents except for the nonpolar solvents, CCl_4 , hexane, cyclohexane, and decalin (entries 2, 16, 17 and 18, respectively). Nearly identical results are shared by similar solvent types; CHCl_3 , CH_2Cl_2 (entries 3 and 4), the ethers (entries 13 - 15), ethyl acetate and acetone (entries 11 and 12), and sulfolane and dimethyl sulfoxide (entries 26 and 27).

The "neat" results of Table 5 are very different from the results obtained by Wilt and Sullivan⁴ (Table 3), who performed the same reaction in the absence of solvent. In their case, the *anti-exo* adduct was the major product by a small margin. The order of product yield was *anti-exo* > *syn-endo* > *anti-endo*, opposite in order to the results currently obtained. The differences in reaction conditions are likely to be responsible for this discrepancy. Wilt and Sullivan used pseudo 1st order conditions, swamping the reaction with a 100-fold excess of 7-*tert*-butoxynorbornadiene. Their reaction was run at 25 - 30°C for 4 to 6 weeks, and their method of separation was more vigorous (steam distillation followed by repeated chromatographic separation on alumina), inviting the possibility of decomposition and product loss. Our reaction was run at 7°C for 4 weeks, using a 1:1.2 molar ratio of 7-*tert*-butoxynorbornadiene to diphenyldiazomethane, followed by chromatographic separation on silica gel.

It is apparent that changes in solvent induce fluctuations in relative percentage yield for all adducts. However, the trends observed for any individual monoadduct in a range of solvents do not correlate with any known solvent parameters. Such a data treatment also fails to provide a sound physical meaning to experimental observation. The data in Table 6 are far more suitable for comparison with solvent parameters, as shall be shown in sections 7 and 8 of this discussion.

3. Rate of formation of monoadducts in n-hexane.

The formation of monoadducts from 12.54 mmoles of 7-*tert*-butoxynorbornadiene and 16.58 mmoles of diphenyldiazomethane in 25 mL hexane solution ($[7\text{-TBN}]_0 = 0.502\text{ M}$) was monitored at regular intervals in order to confirm the assumption that the relative yields of isomers do not change over time at a concentration close to that used in the solvent study. On referring to Tables 7 and 8, that assumption was found to be valid, in that the relative percentages of three of the four monoadducts was consistent throughout the course of the experiment. The workup and analysis of the solvent study reaction mixtures at 30 ± 2 days was therefore justified.

There was some concern that, because the solvent study was conducted at a relatively high concentration ($[\text{Ph}_2\text{CN}_2] = 0.600\text{ M}$), the magnitude of the solvent effect would be obscured. A kinetic study was therefore conducted using similar mole quantities - 12.57 mmole 7-*tert*-butoxynorbornadiene and 16.03 mmole diphenyldiazomethane - in 50 mL hexane solution ($[\text{Ph}_2\text{CN}_2] = 0.316\text{ M}$) to determine whether an increase in the amount of solvent would increase the observed solvent effect. No significant dilution effects were observed on decreasing the concentration by a factor of two. Not only were the rate constants for monoadduct formation close in value ($k_1 = 4.27(\pm 0.23)$ and $3.65(\pm 0.17) \times 10^{-6}\text{ L/mol}\cdot\text{min}$), but the rate constants calculated for each monoadduct were also close (refer to Tables 9 and 10 for comparison). As expected, changes in dilution affect the rate but not the rate constant. In the present case, the initial reaction rate is reduced to 23 % (from $1.28 \times 10^{-6}\text{ M}\cdot\text{min}^{-1}$ to $2.90 \times 10^{-7}\text{ M}\cdot\text{min}^{-1}$) by doubling the dilution. This is very close to the theoretical 25 % rate reduction, where $\text{rate} = k(1/2[\text{reactant}]_{\text{initial}})^2$.

The discrepancy between rate constants is, in part, attributable to some random experimental error that occurred due to solvent evaporation, resulting in some variation in

concentration of reactants from one assay to the next. Solution concentration was more likely to occur at longer time intervals and would have been most acutely manifested in the 50 mL reaction mixture samples.

4. Rate of formation of monoadducts in acetonitrile.

A second kinetic study was conducted in acetonitrile - a solvent having much greater polarity than hexane - to ensure that the results obtained from the hexane study were not anomalous. As described in section 3 of the Discussion for the kinetic study in hexane, there was confirmation that the relative yield of each monoadduct was consistent over an extended time period (refer to Tables 13 and 14) in acetonitrile as well. The kinetic study was also conducted at two concentrations, one at a 25 mL volume and one at a 50 mL volume. The 2nd order rate constants at both concentrations ($k_1 = 6.80(\pm 0.19) \times 10^{-6}$ L/mol·min and $1.08(\pm 0.05) \times 10^{-6}$ L/mol·min at 25 mL and 50 mL, respectively) were not as close in agreement with each other as were the hexane k_1 's, i.e., while the acetonitrile k_1 values are in the same range as the k_1 values determined for hexane, there is a larger discrepancy between the acetonitrile k_1 's with increasing dilution as compared to the k_1 's from the hexane study. At the 50 mL volume, it appears that some solvent-induced rate acceleration in Ph₂CN₂ condensation (Scheme V) occurred with a concomitant rate reduction in monoadduct formation. Since the k_1 and k_2 values were determined simultaneously by an iterative procedure, the unusually sharp decrease in [Ph₂CN₂] may have created a better fit with a disproportionately larger k_2 and smaller k_1 . Indeed, the k_2 was unusually large in 50 mL in acetonitrile, at $k_2 = 1.41(\pm 0.05) \times 10^{-5}$ M⁻¹min⁻¹. It should be mentioned here that solvent evaporation did not present a problem in the acetonitrile study, probably because of its higher boiling point.

5. Rate of disappearance of diphenyldiazomethane in n-hexane.

The rate of disappearance of Ph_2CN_2 is dependent on two separate reactions (Equations 22 and 25), with the condensation to form tetraphenylketazine being the faster of the two. This is evident from the rate constants, in which k_2 is consistently larger than k_1 . At 25 mL volume, $k_2 = 5.88(\pm 0.15) \times 10^6 \text{ M}^{-1}\text{min}^{-1}$ and at 50 mL, $k_2 = 6.38(\pm 0.11) \times 10^6 \text{ M}^{-1}\text{min}^{-1}$. A comparison of rates of Ph_2CN_2 consumption due to monoadduct formation (Equation 23) versus that due to condensation (Equation 26) over time reveals the condensation rate slows down to a greater extent than the monoadduct reaction. This is not surprising, since the rate of Ph_2CN_2 condensation is dependent upon $[\text{Ph}_2\text{CN}_2]^2$.

6. Rate of disappearance of diphenyldiazomethane in acetonitrile.

As with the reaction in hexane (section 5 of Discussion), the condensation reaction is faster than the monoadduct reaction, accounting for the greater portion of Ph_2CN_2 consumed. At the 25 mL volume, the difference in k_1 and k_2 ($k_2 = 8.82(\pm 0.03) \times 10^6 \text{ M}^{-1}\text{min}^{-1}$) is slight, consistent with the hexane studies. At the 50 mL volume, the difference in k_1 and k_2 ($k_2 = 1.41(\pm 0.05) \times 10^5 \text{ M}^{-1}\text{min}^{-1}$) is much larger. The reasons for this large difference are unclear.

7. Correlations with empirical solvent parameters.

A list of Pearson correlation coefficients, R , obtained from single-parameter correlation of various intrinsic and empirical solvent parameters with $\log(\Sigma_{\text{syn}}/\Sigma_{\text{anti}})$ is given in Table 23. R is frequently used instead of R^2 in the literature concerning solvent parameter correlations, particularly in regards to multiple parameter treatments. For consistency, R is used here in the same context. Calculations were carried out on a PC using a least-squares program from Lotus

123. The correlations are the result of linear solvation free energy relationships (LSER's) of the general form of Equation 30.

$$\Delta G = \Delta G_0 + \varphi_n x_n \quad (30)$$

ΔG_0 is the Gibbs free energy change of the reaction or process in the absence of solvent, ΔG is the free energy change in a given solvent, x_n is an empirical solvent parameter, and φ_n is a coefficient relating the sensitivity of the reaction or process to the parameter. The coefficient φ_n is the slope of the line. The subscript n denotes the number of additive terms; here it is $n = 1$. The number of available data, N , for each correlation, and the solvent entry numbers (corresponding to solvent entry numbers given in Tables 4, 5 and 6) for the solvents used in the correlation are also listed in Table 23. Tables 25, 26 and 27 in the Appendix provides a compilation of some of the solvent parameter values used extensively in this text.

Table 23. Single parameter correlations with $\log(\Sigma Syn/\Sigma Anti)$

Solvent Parameter	Ref.	N	R	Solvent Entry (Tables 4-6)
ϵ	--	26	0.7456	2-27
$(\epsilon-1)/(2\epsilon-1)$	16	26	0.7590	2-27
χ_R	45	20	0.8500	2, 3, 7-17, 19-21, 23-25, 27
E_K	50	19	0.7286	2-4, 7-17, 19, 20, 24, 25, 27
$E_T^{N\dagger}$	44	15	0.9435	2, 11, 13-20, 22, 23, 25-27
E_T^N	44	26	0.6807	2-27
G	54	9	0.8902	2-4, 13, 15-17, 21, 24
$\log k_1$	34f	8	0.8618	11-14, 21, 24, 25, 27
$\log k_2$	164	18	0.7898	3, 4, 7, 9-14, 16, 17, 19-25
P	165	21	0.8869	2-4, 6, 9-15, 17-21, 23-27
Z	42, 43	12	0.5141	4, 6-10, 12, 13, 19, 24, 26, 27
$\pi^{*\dagger}$	15c	15	0.9591	2, 11, 13-20, 22, 23, 25-27
π^*	15c	26	0.8170	2-27
δ_H^2	166	26	0.7595	2-27
A_N	61	18	0.6612	2-4, 6-10, 12-16, 19, 21, 24, 25
S	43	19	0.5814	2-4, 6-13, 15-17, 19-21, 24, 25
Py	53	18	0.6544	3-5, 7-12, 14-17, 19, 22, 24, 25, 27
Py [†]	53	9	0.9230	11, 14-17, 19, 22, 25, 27
DN	167	13	0.3615	11-15, 20-27
AN	60a	22	0.5253	2-4, 6-16, 19-21, 23-27
Ω	2	7	0.6186	9, 10, 12, 18, 21, 24, 25
D_π	73	13	0.7417	3, 4, 11-15, 19-24

[†]Aprotic solvents only

The large number of solvent parameter entries in Table 23 is, perhaps, deceptive. All, save the dielectric constant, ϵ , and the dielectric constant function, $(\epsilon-1)/(2\epsilon-1)$, are empirically derived parameters, many of which presumably provide some measure of solvent polarity. The wrong approach to finding a good correlation of experimental data with a solvent property would be to collect as many parameters as possible, calculate the goodness of fit with experimental data, and pick the parameter that has the best fit. That is what appears to have occurred in Table 23. The real intention, however, is to provide the basis for an argument for the linear solvation energy relationship (LSER) ultimately chosen.

Empirical parameters are based upon some sort of model that describes a physicochemical interaction -- at either the microscopic or macroscopic level -- of a specific chemical reaction or process. The implication central to any LSER, as with a linear free energy relationship, is that the reaction or process being tested by the LSER should be directly related to the reaction or process used to develop the LSER. In this way, a meaningful physical interpretation can be extracted from the results.

The reaction being tested is a 1,3-dipolar cycloaddition. The actual quantity being measured is a set of values proportional to the difference in free energy of activation, assuming kinetic control between isomers having *syn* configuration and *anti* configuration (Equation 31).

$$\Delta\Delta G^\ddagger \propto \log(\Sigma_{syn}/\Sigma_{anti}) \quad (31)$$

$\Delta\Delta G^\ddagger$ would be expected to be somewhat sensitive to factors which stabilize charge dispersal in the transition state and factors which enhance formation of smaller transition state volumes. Evaluating the parameters in Table 23, those which are closely modeled after these

processes are ϵ , $(\epsilon-1)/(2\epsilon-1)$, E_T^N , π^* , δ_H^2 , Ω , and D_π . The dielectric constant and its function, $(\epsilon-1)/(2\epsilon-1)$ ($R = 0.7456$ and 0.7590 , respectively, $N = 26$) is a bulk solvent property and is a measure of solvent polarity. The empirical parameters E_T^N and π^* are polarity parameters derived from solvatochromic shifts. While there are other suitable solvatochromic (solvatochromic = solvent-induced spectral shift of a chromophoric compound) parameters worthy of consideration, a high degree of collinearity often exists among them. This is understandable, since the scaling of many parameters is based on a similar type of electronic transition, but using a different indicator molecule. In this case, the E_T^N and π^* parameters were chosen merely because they provided the better correlation ($R = 0.6807$ and 0.8170 , respectively, $N = 26$) and had the greater availability of solvent parameter values to choose from. The cohesive energy density parameter, δ_H^2 ($R = 0.7595$, $N = 26$), could be expected to have an effect on activation volumes, ΔV^\ddagger , of the monoadducts.

The remaining two parameters, Ω and D_π are special case parameters, designed specifically to describe solvent stabilization of Diels-Alder and 1,3-dipolar cycloadditions, respectively. Unfortunately, these parameters have a very limited set of recorded values, and correlations with these are unconvincing ($R = 0.6186$, $N = 7$ for Ω and $R = 0.7417$, $N = 13$ for D_π). These last two correlations serve to illustrate the failure of even a highly specific single parameter to adequately describe the behavior of all related reactions in solutions.

While a single solvent parameter may be very successful in describing a single, dominant solvent-solute interaction, it would be unreasonable to assert that a single parameter could adequately describe more than one such interaction, or to assume that only a single solvent-solute interaction might occur during a given process. This is reflected in the fact that, of the eligible parameters discussed so far, the correlation coefficients are nowhere near unity. Three of the entries in Table 23 (E_T^N , π^* and Py) have been recalculated after excluding protic solvents.

The correlation coefficient improves dramatically when this is done, and serves to demonstrate that different solvent 'families' have distinct properties that enable them to undergo specific interactions with the solute. In this case, protic solvents are able to hydrogen bond with the 1,3-dipole in addition to participating in polar solvent-solute interactions. Hydrogen bonding could take place between a protic solvent and the activated complex if the transition state is early, so that the complex resembles the reactants. The full negative charge of the diphenyldiazomethane-like complex alternates between two exposed centers (terminal N and benzylic C) (Scheme I), providing sites for hydrogen bonding. Hydrogen bonding would, in turn, stabilize the transition state toward cycloaddition.

8. Multiple Linear Regression Analysis.

Several multiple parameter equations have been developed which describe combinations of solvent-solute interactions, with the intention that the equations have a general application. Each parameter was created independently of the others, and represents a specific solvent-solute interaction. The generality of application of each relationship arises from the fact that each individual parameter may take on greater or lesser importance, depending upon the process being studied. The choice of those parameters, their boundary definitions, and their methods of development were subject to the inclinations of their creators. As a result, each multiple parameter relationship is distinctive in its design and construction. Of the several such equations presently available, only three are adequate (in numbers of data) for comparison here.

Multiple regression analysis was carried out by a multiple general linear hypothesis program (mglh) called SYSTAT, a revised version of a multivariate least squares mainframe program. The program calculated variable coefficients, the Pearson correlation coefficient, and analysis of variance for each of the multiple parameter relationships. Table 24a - c gives the

mgln results for three multiple parameter equations. The general equation is followed in each case by the equation with calculated coefficients inserted. The number of solvent data and correlation coefficient are included for each equation, along with analysis of variance (ANOVA). The first entry is the Koppel-Palm (KP) relationship (Table 24a), the second is the Swain-Swain-Powell-Alunni (SSPA) equation (Table 24b), and the third is the Abraham-Kamlet-Taft (AKT) equation (Table 24c).

In the KP equation, E is defined as Dimroth's E_T corrected for nonspecific solvent interactions by subtracting Y and P as shown in Equation 32.

$$E = E_T(30) - 25.1 - 14.84Y - 9.59P \quad (32)$$

Tables 25, 26, and 27 in the Appendix provide a compilation of the KP, SSAP, and AKT parameters, respectively.

Koppel-Palm equation

The Koppel-Palm expression, Table 24a, is a combination of bulk physical properties and empirical parameters reflecting nonspecific and specific solvent-solute interactions, respectively. The equation accounts for solvent polarity ($f(\epsilon)$) and polarizability ($f(\eta)$) effects, and two parameters measuring solvent electrophilicity (or Lewis acidity) and nucleophilic solvating power (or Lewis basicity). It is reasonable to envision the dispersing charges in the transition state of the model reaction being stabilized by nonspecific solvent polarity/polarization effects. Conversely, the latter two specific solvent parameters do not lend themselves to clear interpretation in terms of the model reaction, a concerted bond-forming, bond-breaking process. While it is possible to interpret the Lewis acidity parameter as being due to solvent hydrogen

Table 24a. Analysis of variance for the Koppel-Palm equation

$$A = A_0 + y \cdot Y + p \cdot P + e \cdot E + b \cdot B$$

Calculated Form: $\log(\Sigma Syn / \Sigma Anti) = 0.039 - 0.508Y^b - 0.772P^c - 0.016E_{\tau}(30)^d - 0.001B$
 $N = 18^a \quad R = 0.915$

Variable	Coefficient	Std. Error	Tolerance	T	P(2 Tail)
Constant	0.039	0.149		0.261	0.798
Y	-0.508	0.195	0.379	-2.610	0.022
P	-0.772	0.678	0.982	-1.138	0.276
E	-0.016	0.044	0.460	-3.542	0.004
B	0.001	0.000	0.246	1.859	0.086

ANOVA

Source	Sum-of-Squares	DF	Mean-Square	F-Ratio	P
Regression	0.211	4	0.053	16.739	0.000
Residual	0.041	13	0.003		

^aMaximum number of entries limited by availability of parameter data.

^bY may be one of several dielectric constant functions; here it is $Y = (\epsilon - 1)/(2\epsilon + 1)$

^cP may be one of several refractive index functions; here it is $P = (\eta^2 - 1)/(2\eta^2 + 1)$

^dE = E_τ(30), Dimroth's original solvatochromic scale.

bond donor ability, it is difficult to conceive of a solvent basicity interaction that is distinct from the bulk polarity interaction already accounted for.

There are other shortcomings with this equation, aside from the interpretive difficulties just mentioned. While a good correlation is obtained from this expression, at $R = 0.915$, only 18 out of 26 solvents were treated. In particular, no solvent data were available for the simple alcohols used in this study. A compilation of solvent parameter data is given in Table 25 in the Appendix. Five of the electrophilicity (E) values were selectively forced to zero by the authors, with the argument that these solvents are electrophilically inert. While it is true that the correlation improves from $R = 0.845$ to 0.915 when this is done, it makes the E scale somewhat arbitrary (i.e., if the E scale were truly adequate for this application, the five true E values should approach zero). The physical meaning attached to the calculated $\log(\Sigma_{syn}/\Sigma_{anti})_0$ value is that it is the logarithm of the product ratio obtained in the gas phase. This value was determined to be 0.039, and is highly unlikely. Not surprisingly, the statistical P(2 tail) value for the intercept is 0.798 and for P ($f(\eta)$) it is 0.276, indicating low statistical significance for the terms.

The Swain-Swain-Powell-Alunni Equation

Results for the SSPA treatment are given in Table 24b. Solvent parameter data are given in Table 26 in the Appendix. This is a two parameter treatment, where $A =$ "acity" value is a measure of anion solvating ability, and $B =$ "basity" is a measure of cation solvating ability. The acity + basity sums are a measure of overall solvent polarity. With 21 of the 26 solvents treated, the correlation coefficient ($R = 0.850$) is fair. The statistical P(2 Tail) values for the three coefficients indicate that they are strongly significant, and the F-ratio (23.486) is improved when compared to the Koppel-Palm treatment (F-ratio = 16.739). The physical meaning of the $\log(\Sigma_{syn}/\Sigma_{anti})_0$ is that of the results obtained for the reaction in the reference solvent heptane,

Table 24b. Analysis of variance for the SSPA equation

Variable	Coefficient	Std. Error	Tolerance	T	P(2 Tail)
Constant	-0.120	0.037		-3.259	0.004
A _j	-0.326	0.070	0.995	-4.675	0.000
B _j	-0.215	0.046	0.995	-4.673	0.000

<u>ANOVA</u>					
Source	Sum-of-Squares	DF	Mean-Square	F-Ratio	P
Regression	0.191	2	0.096	23.486	0.000
Residual	0.073	18	0.004		

^aMaximum number of entries limited by availability of parameter data.

for which $A = 0$ and $B = 0$. The cycloaddition was not run in heptane, but was run in the similar hydrocarbon solvent hexane. A comparison of calculated and experimental values are given below.

$$\log(\Sigma Syn/\Sigma Anti)_{0, calc} = -0.120 \quad (\Sigma Syn/\Sigma Anti)_{0, calc} = 0.759$$

$$\log(\Sigma Syn/\Sigma Anti)_{0, exp} = -0.142 \quad (\Sigma Syn/\Sigma Anti)_{0, exp} = 0.721$$

$$\% \text{ Difference} = (0.759 - 0.721)/0.721 \times 100 = 5.3\%$$

As measures of solute cation and anion solvating ability alone, the SSAP results can be related to the model reaction only in those terms. Solvent stabilization of the diminishing positive and negative charges of each isomeric transition state is the only physical interpretation possible. The magnitudes of the coefficients, $a_i = -0.326$ and $b_i = -0.215$, suggest that the ability to solvate electron rich moieties is slightly more important, consistent with the presence of two electron-rich sites of the 1,3-dipole versus the single electron-poor site at its center.

The Abraham-Kamlet-Taft Equation

Table 24c gives the results for the application of the AKT equation to the model reaction. Comparison on the general form of the AKT equation (Table 24c) with the form given in Equation 11 reveals that two parameters, β and ξ are missing. The flexibility of the AKT expression allows for the omission of those parameters which are not relevant to the reaction or physical process under study. The β parameter is a scale of solvent hydrogen-bond acceptor basicities. The ξ parameter is a "coordinate covalency" parameter to be used in conjunction with the β parameter. Since there is no solute hydrogen-bond donor present in the model reaction, both the β and ξ parameters are irrelevant. The equation in this form is particularly well suited to describe solvent-solute interactions in the model reaction. It describes not only solvent polarity/polarizability stabilization of dispersing charge in the transition states by the presence of the π^* and δ terms, but also solvent interaction by means of cohesive energy density, the δ_H^2

Table 24c. Analysis of variance for the AKT equation

$$XYZ = XYZ_0 + s(d\delta + \pi^*) + a\alpha + h\delta_H^2$$

Calculated Form: $\log(\Sigma Syn/\Sigma Anti) = -0.086 - 0.261(0.084\delta + \pi^*) - 0.080\alpha - 0.428\delta_H^2$

N = 26

R = 0.894

Variable	Coefficient	Std. Error	Tolerance	T	P(2 Tail)
Constant	-0.086	0.039		-2.193	0.040
π^*	-0.261	0.069	0.303	-3.761	0.001
δ	-0.022	0.039	0.718	-0.576	0.571
α	-0.080	0.050	0.448	-1.615	0.121
δ_H^2	-0.428	0.352	0.251	-1.214	0.238

ANOVA

Source	Sum-of-Squares	DF	Mean-Square	F-Ratio	P
Regression	0.268	4	0.067	20.907	0.000
Residual	0.067	21	0.003		

term. It should be mentioned that the δ_H^2 values were converted to units of Psi so that all of the solvent parameters would be of similar magnitude--numbers between 0 and 1--for ease of comparison of coefficient (s, d, a, and h) values. A correlation coefficient of 0.894 is good when all 26 solvents are considered. Table 27 in the Appendix gives a compilation of AKT parameter values for each solvent. When only aprotic solvents are considered ($\alpha = 0$, $N = 15$), the correlation improves to $R = 0.960$ and the equation reduces to Equation 33.

$$\log(\Sigma Syn/\Sigma Anti) = -0.121 - 0.266(0.030\delta + \pi^*) - 0.158\delta_H^2 \quad (33)$$

The significance of this segregation of data can best be explained by reference to Figure 9. The plot of π^* versus $\log(\Sigma Syn/\Sigma Anti)$ has been prepared such that a least-squares line is drawn through the aprotic solvents, with the remaining protic solvents existing in a scatter diagram. In developing the AKT relationship, Taft employed a rigorous definition of the term "protic", such that solvents having relatively small acidities (such as acetone, chloroform, and nitromethane) are considered to be protic. This convention must necessarily be followed when employing the AKT equation. It is immediately obvious that a linear correlation by this arrangement is much improved over a best-fitting line drawn through all of the points. The scatter of protic solvent data points is also a clear indication that a single solvent polarity scale is not adequate to describe the effect of solvent on the reaction. All of the protic solvents except for acetone are displaced below the regression line. This suggests that one or more additional solvent properties further interact with the reaction system and do so consistently from one solvent to the next. In this case the points are displaced in the direction of more negative $\log(\Sigma Syn/\Sigma Anti)$ values, corresponding to greater relative *anti*-adduct formation. Experimental error is probably responsible for displacement of the acetone data above the regression line. If

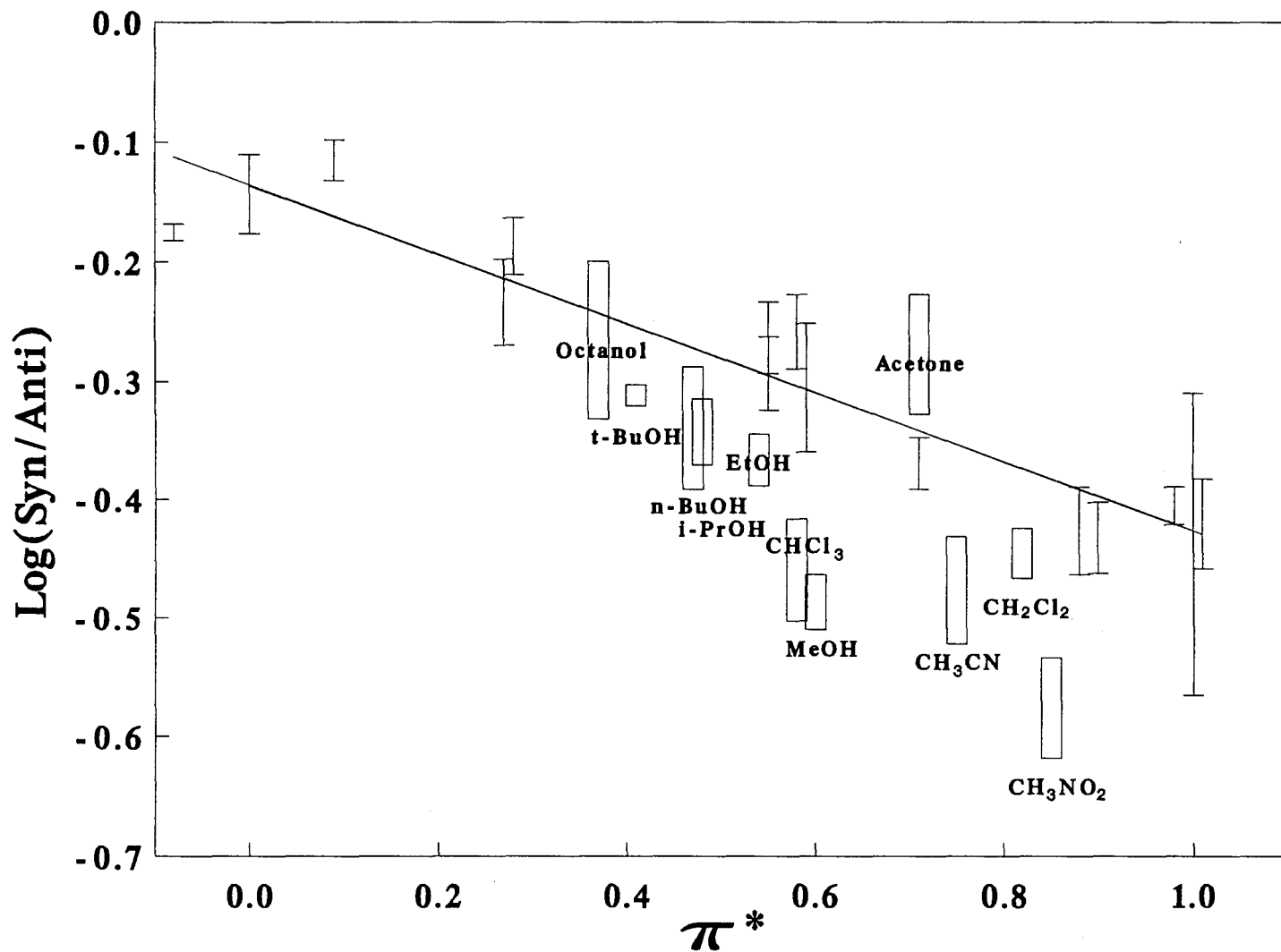


Figure 9. Plot of $\log(\text{syn}/\text{anti})$ vs. solvent polarity scale, π^* . Open error bars (I) represent aprotic solvents, closed error bars (□) represent protic solvents, and the line is the linear regression curve for the aprotic solvents.

a second solvent property were solely responsible for the protic solvent point deviations, then the individual magnitudes of all point deviations from the π^* regression line would be closely correlated to the solvent property values responsible for the deviations. It could be inferred that the responsible solvent property is hydrogen-bond donor ability, since it is the protic solvents which deviate from the line. This process, referred to as stepwise linear regression analysis, was used extensively by Taft and coworkers to develop the α and β parameter scales. In the present case, however, there is no correlation between α and $\Delta\log(\Sigma Syn/\Sigma Anti)$. This finding in turn suggests that there is yet another solvent property in addition to α and π^* interacting with the model reaction, and that it is also contributing to deviations from the π^* line. The correlation coefficient for aprotic solvents was calculated from Equation 33 instead of from π^* vs. $\log(\Sigma Syn/\Sigma Anti)$ because it was conceptually impossible to segregate δ_H^2 from π^* . All solvents have some degree of internal solvent pressure.

The intercept of Equation 33 corresponds to $\log(\Sigma Syn/\Sigma Anti)_0$ in cyclohexane solvent, since cyclohexane is the zero reference solvent for the π^* scale (DMSO is the second reference solvent, at $\pi^* = 1$). A comparison of the calculated and observed values is given below.

$$\log(\Sigma Syn/\Sigma Anti)_{0, \text{calc}} = -0.121 \quad (\Sigma Syn/\Sigma Anti)_{0, \text{calc}} = 0.757$$

$$\log(\Sigma Syn/\Sigma Anti)_{0, \text{exp}} = -0.142 \quad (\Sigma Syn/\Sigma Anti)_{0, \text{exp}} = 0.721$$

$$\% \text{ Difference} = (0.751 - 0.721)/0.721 \times 100 = 4.8\%$$

A 4.8% difference is acceptable and is slightly better than the SSAP 5.3%.

Returning to the AKT equation derived in Table 24(c), it appears that the δ_H^2 and π^* terms are more important than the other parameters in this reaction, since their coefficients are largest. An analysis of the accompanying statistical data helps to explain this. The P(2 Tail) statistic is very good for π^* at 0.001 but much poorer for δ_H^2 at 0.238. The simultaneous occurrence of π^* and δ_H^2 is in violation of one of the tenets of multiple general linear hypothesis,

since the two parameters have a significant degree of collinearity. For the 26 solvents used in this study, the correlation coefficient between π^* and δ_H^2 is $R^2 = 0.396$, and if the alcoholic solvents (entries 5-10) are omitted, it improves to $R^2 = 0.716$. The statistical significance of δ_H^2 is diminished because of this collinearity. Kamlet, Taft and Abraham have rationalized this problem, arguing as follows.^{15c} Internal solvent pressure is effectively the amount of energy required to overcome solvent-solvent attractive forces in creating a cavity for solute molecules to occupy, and those attractive forces include dipolar interactions. Thus, internal solvent pressure and polarity scales would be expected to be somewhat collinear. However, the π^* parameter is a measure of solvent-solute dipolar interactions while the δ_H^2 parameter is a measure of solvent-solvent interactions that are interrupted in forming a cavity for the solute. Inclusion of both terms in the same equation is a necessary evil.

The coefficients for α and δ are -0.080 and 0.022, respectively. The larger absolute value for the α coefficient suggests that it is a significant term, although it is less heavily weighted than either δ_H^2 or π^* . The P(2 Tail) for α is 0.121, less than that for δ_H^2 and therefore more significant. The δ term cannot be considered at all significant, but must be left in to maintain the integrity of the AKT relationship. The F-Ratio of 20.907 is better than for the Koppel-Palm equation (16.739), but poorer than the SSAP equation (23.486). Nevertheless, the use of the AKT expression is preferred for its complete set of data and its simple interpretation.

A physical interpretation of the AKT results will be given in the same order as the appearance of the AKT parameters.

π^*

ANOVA statistics suggest that solvent polarity has the most significant effect upon the *syn/anti* product ratios. The only point at which the product ratios can be influenced is at the transition state giving rise to each isomer. Prior to formation of each transition state, the dipolar

molecule, diphenyldiazomethane, experiences some charge stabilization by solvent dipole/solute charge interaction. During formation of the transition state, charge separation on the dipolar molecule is distributed or "diffused" over all the atoms of the dipole-dipolarophile activated complex. Depending upon the extent of charge diffusion in each activated complex, and of the extent of exposure of the diffused charges to the inner solvent sphere, charge stabilization by a given solvent will occur to a different extent in each complex.

Consider the effects of solvent polarity on the *syn-exo* monoadduct. During the formation of an orientation complex, the dipolar molecule must align itself with the double bond of the dipolarophile so that it is between the *tert*-butoxy group on C-7 and the double bond. The *tert*-butoxy oxygen participates in this process by electrostatic interaction of its electron pairs with the dipolar molecule charges, thereby "guiding" the dipolar molecule into place.¹⁴ Dipolar charge dispersal occurs during formation of the activated complex where partial formation of σ bonds and breakage of π bonds takes place. Charge dispersal occurs across only those atoms involved in bond formation/breakage. Stabilization by means of solvent polarity would not be expected to be very effective, since much of the region of charge dispersal is sterically inaccessible to solvent molecules.

The remaining adducts are sterically similar, are formed in similar proportions, and can be considered together. Electrostatic interaction of the overhanging *tert*-butoxy oxygen with the C-2, C-3 double bond could serve to guide diphenyldiazomethane to the *syn-endo* position to form a relatively stable orientation complex. Any interference with that interaction may reduce the frequency of *syn-endo* complex formation, such as solvent dipolar interactions with the lone pairs on oxygen. On comparing the *syn-endo* percentages in Table 5 to π^* values in Table 27, there is indeed a general trend, wherein formation of the *syn-endo* adduct is reduced in the presence of more polar solvents and is enhanced in the presence of nonpolar hydrocarbons and

ethers. In surveying the *syn-endo* percentages in chloromethyl solvents in Table 5, the proportion of *syn-endo* adduct decreases from 33.5% to 23.7% as solvent polarity increases. In hexane, cyclohexane, and decalin (entries 15 - 17), the *syn-endo* yield reaches a high range of 33.9 - 37.4%, and in very polar solvents (entries 20 - 27), the *syn-endo* yield decreases to 18.8 - 25.6%. Since the total millimolar adduct yield is noncollinear with solvent polarity and the *syn-endo* yield decreases with increasing solvent polar, it follows that *anti-endo* and *anti-exo* complex formation is more advantageous in polar solvents.

α

The apparent significance of the α parameter suggests that solvent hydrogen-bond donor ability is important. If an early transition state takes place, hydrogen bonding can occur between protic solvent and 1,3-dipole-like transition state complex, as previously discussed. If a late transition state takes place, however, the formal negative charge on diphenyldiazomethane is in the process of dispersal and elimination. In this case, solvent hydrogen bonding with diphenyldiazomethane might occur prior to activated complex formation. If the diphenyldiazomethane molecule forms a solvation complex with hydrogen-bond donor solvents, then its approach to the dipolarophile will be more hindered than that of an unencumbered diphenyldiazomethane molecule. The effect would be one of increased steric hindrance in all cases.

In entries 5 - 10 of Table 27, it is shown that α increases with decreasing chain length of alcoholic solvents. Compared with the values in Table 5, it appears that the *syn-endo* yield decreases with an increase in α . This indicates that hydrogen bonding to the t-butoxy oxygen might also occur, causing a similar interruption in interactions between the oxygen and the double bond as with the polarity effect. It should be noted that π^* displays a nearly identical trend with solvents 5 - 10; increasing with decreasing alcohol chain length. Therefore, solvent

polarity or a combination of polarity and hydrogen bonding could instead be responsible for the observed effect on relative percentage yields.

$$\delta_{\text{H}}^2$$

Internal solvent pressure, as measured by cohesive energy density, δ_{H}^2 , is the amount of energy required to break solvent-solvent interactions so that a cavity can be created for occupation by solute molecules. While this solvent effect is less significant than solvent polarity, it does operate. Figure 10 illustrates the relationship between internal solvent pressure and the $\Sigma\text{Syn}/\Sigma\text{Anti}$ product ratio. There is a general linear correlation ($R = 0.752$) for all solvents inclusive. Three distinct trends are observed when the solvents are broken up into nonpolar, polar aprotic, and protic (ie., alcoholic) groups, with correlations of $R = 0.632$, 0.761 , and 0.967 , respectively. The improvement in correlation by separating solvents into solvent property groups (with the exception of the nonpolar group) points to the fact that more than one solvent property is at work.

Internal pressure is manifested in the model reaction by enhancing frequency of formation of those isomeric transition states that have a smaller activation volume, ΔV^\ddagger . The choice of solvents having large internal pressures will tend to increase recovery of isomers having the smallest ΔV^\ddagger 's. A prediction can therefore be made for the smaller transition states by observing the trend of isomer recovery as a function of cohesive energy density. The negative slopes of Figure 10 indicates a decrease in the $\Sigma\text{Syn}/\Sigma\text{Anti}$ ratio with increasing δ_{H}^2 . This might mean that the total volume of *anti-endo* + *anti-exo* transition states are smaller than the total volume of *syn-exo* + *syn-endo* transition states. Care must be taken with such an interpretation, however. If the transition states are reached early, they will resemble the reactants more than the products, but the relative sizes of monoadducts would be impossible to predict by all but the most rigorous molecular modelling processes. Conversely, if the transition

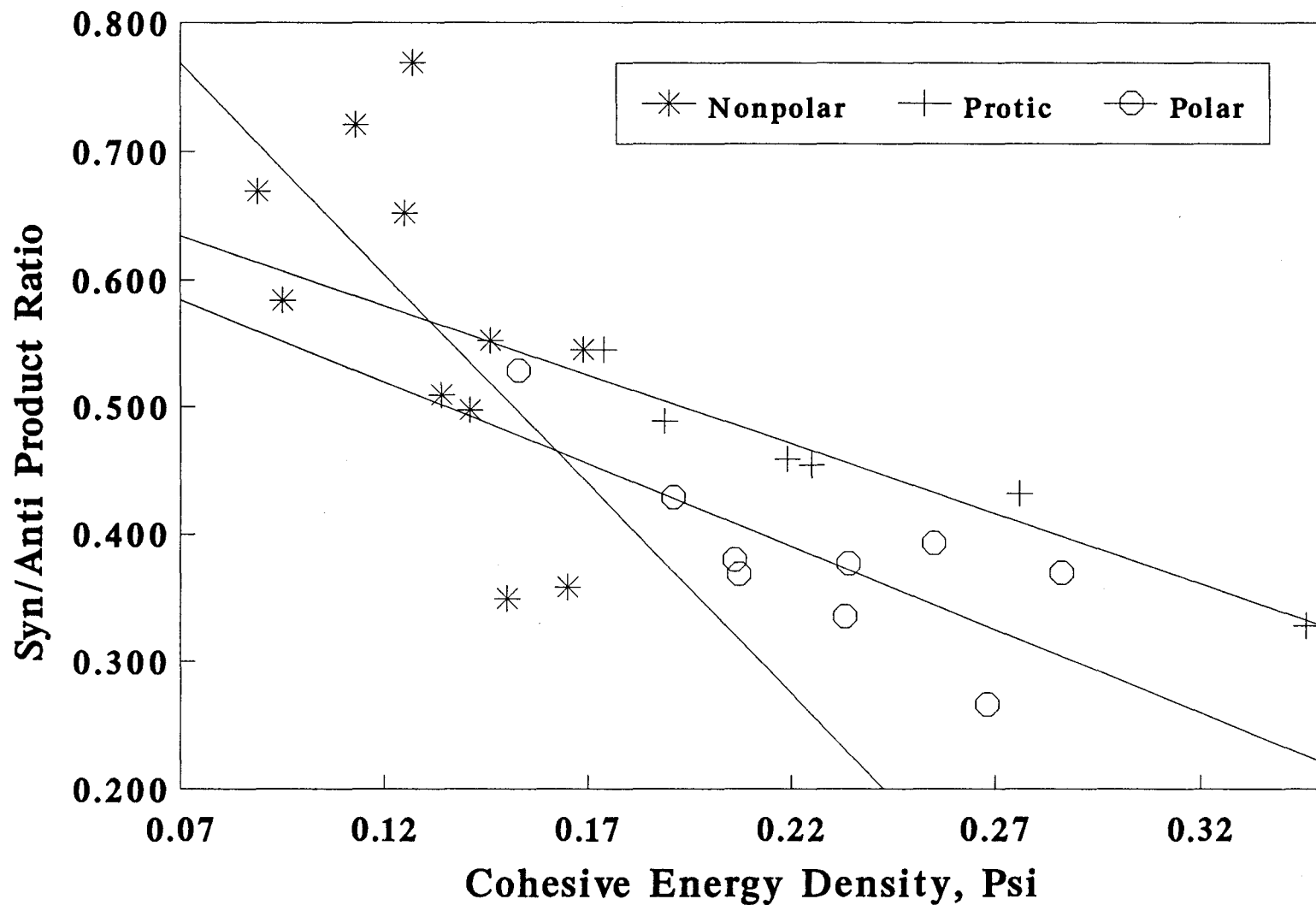


Figure 10. Cohesive energy density (δ_H^2) versus $\Sigma_{syn}/\Sigma_{anti}$ product ratio. The three straight lines are the linear regression curves when treating nonpolar, protic and polar aprotic solvents separately.

state is reached late, it will more closely resemble products, and the monoadducts themselves can serve as models for their respective transition state complexes. The calculated volumes of the four monoadducts are as follows: 299.4 Å³ for *anti-endo*, 298.9 Å³ for *syn-endo*, 298.8 Å³ for *anti-exo*, and 298.2 Å³ for *syn-exo*.¹⁶⁸ Obviously, the differences in volume are trivial, and would not account for enhanced formation of some adducts on the basis of size. In addition, it has already been pointed out that the specific solvent-solvent dipole interactions that define solvent polarity are also partly responsible for internal solvent pressure. It is therefore likely that the solvent-solute polar interactions interfere with internal solvent pressure interpretations.

From among the abundance of single- and multiple-parameter treatments that are suitable for use with these data, it is plain that multiple-parameter treatments are more successful in rendering useful correlations. This is because a variety of solvent-solute interactions are likely to occur. The best multiple parameter treatment is both the one which gives the most statistically significant correlation, and also the one which is most readily interpreted in terms of the parameters and the chemical process being studied. Of the three equations employed in this study, the Abraham-Kamlet-Taft expression is the most straightforward, since the individual parameters are derived from well defined interactions. Three solvent families were considered in this study; polar-protic, polar-aprotic, and nonpolar. Using the AKT expression as the model, it seems that polarity is the principal determining factor in the cycloaddition reaction. Internal solvent pressure is not as important as internal pressure, and this could be due to the collinearity of the cohesive energy density parameter with the polarity parameter. Hydrogen bonding by solvent is also significant, and this true for all three of the multiple-parameter equations used.

CHAPTER V

EXPERIMENTAL

1. General information.

¹H and ¹³C NMR spectra were taken on a Varian VXR 300 (7.0 T) spectrometer. Chemical shift values (δ) are reported in ppm downfield from internal tetramethylsilane. UV-visible spectrophotometry was performed on a Perkin-Elmer spectrophotometer (Coleman 575) using methanol as solvent and reference blank.

Radial, thin-layer chromatography was performed on a Chromatotron (Harrison Research). Both 1 mm and 2 mm plates were prepared with Silica Gel 60 (PF-254 with CaSO₄, EM Science). Eluting fractions were visualized using a portable UV lamp (MineralightLamp, Model UVG-11). Thin-layer chromatography was done using Eastman-Kodak company silica-gel plates (polyester or aluminum backing) with fluorescence indicator and were developed in a mixture of 1:4 ether/petroleum ether. Preparative thin-layer chromatography was carried out on precoated TLC plates (0.25mm, Silica Gel 60 F-254, EM Reagents). Melting point determinations were done on a Mel-Temp Apparatus using vacuum-sealed capillary tubes.

High-pressure liquid chromatography was performed on a Liquid Chromatograph (DuPont Instruments 850) fitted with a reverse-phase column (Ultrasphere™, 5 μ C-18, 25 cm \times 4.6 mm, Beckman, Inc.) and equipped with a UV detector (254 nm). Chromatographs were printed out on a strip-chart recorder, and peak area integration was carried out by use of a planimeter. Chromatography solvents used were ACS or HPLC grade and were prefiltered through 0.45 μ m membrane filters (Nylaflo® # 66608, Gelman Sciences). Reaction solvents

ethyl ether, dioxane, hexane, and THF were distilled from CaH_2 . Decalin (technical grade, *cis-trans* mixture) was vacuum distilled from LiAlH_4 . Octanol was predried over CaSO_4 and vacuum distilled. Ethyl acetate and propionitrile were distilled from P_2O_5 . All remaining solvents were used as received or predried over MgSO_4 as needed.

2. Preparation of diphenyldiazomethane.

Diphenyldiazomethane was not available commercially but was prepared by a modified procedure.¹⁶⁹ Very pure benzophenone hydrazone was prepared as described, with a 69% recovery. A 15 g sample of hydrazone so obtained was placed under high vacuum for 1.5 hr to remove residual water. Anhydrous Na_2SO_4 or MgSO_4 (3-5 g) was added as drying agent. Then, 200 mL anhydrous diethyl ether, and 5-6 mL ethanol saturated with KOH was added, followed by 35 g of yellow HgO. The slurry was magnetically stirred for 2.5 hr. The resultant mixture was filtered, and the solids washed with ether. The ether was removed, hexane added to dissolve the diphenyldiazomethane, and the mixture filtered to remove undissolved solids. The hexane was removed, leaving a purple-red viscous liquid, which solidified upon refrigeration to form large needles. Further recrystallization was not necessary. The extinction coefficient at $\lambda_{\text{max}} = 525 \text{ nm}$ was determined to be 93.1 in methanol (*vide infra*). m.p. = 29 - 30°C, Lit. m.p. = 29 - 30°C.¹⁶⁹

3. Reaction of diphenyldiazomethane with 7-*tert*-butoxynornornadiene.

A 0.233 g (1.12 mmol) sample of diphenyldiazomethane and 0.163 g (0.922 mmol) sample of 7-*tert*-butoxynornornadiene was weighed into a 5 mL conical reaction vial. To this was added 1.0 mL of solvent. The contents were mixed and the vial was capped and purged with argon. The vial was further sealed with parafilm and immediately refrigerated for 28-32

days at 7°C. The reaction mixture was then prepared for HPLC analysis, where monoadduct yields were determined. Yields of total monoadduct are listed in Table 4 and relative percentages of individual monoadduct yields are listed in Table 5.

4. Isolation of mono- and bis-pyrazoline adducts.

After several (7-8) cycloaddition reaction mixtures had accumulated (see Chapter V, Section 6, HPLC analysis of mono- and bis-pyrazoline adducts), they were combined and the methanol solvent removed on a rotary evaporator. The crude mixture was dissolved in a minimum amount of diethyl ether. Rough separation was achieved by radial chromatography, using a 2 mm plate. The plate was overloaded with the diethyl ether solution and eluted with petroleum ether followed by 5% Et₂O/pet. ether until the first two large bands, corresponding to diphenyldiazomethane and tetraphenylketazine eluted off. These fractions were discarded. The remainder was rapidly eluted off the plate with ether. The solvent was removed from this mixture and re-chromatographed on a 1 mm plate, using radial chromatography. A gradient elution was employed, beginning with petroleum ether, followed by 5%, 10%, 25%, and 50% Et₂O/pet ether, and finally ethyl ether. Overlapping fractions were re-chromatographed. A middle fraction, eluting after the *syn-endo* monoadduct, was composed of three compounds which resisted further separation. This diffuse fraction was collected and the solvent removed.

The solid was triturated with petroleum ether to dissolve *syn-exo* adduct plus some residual benzhydrol. The remaining solid was triturated with ether to remove the benzhydrol, leaving behind pure *endo*, *exo* bis adduct. The *syn-exo* adduct was further purified by thin-layer chromatography using a 20×20 analytical glass silica gel plate and developing it in CHCl₃.

The overall order of elution (in 1:4 Et₂O/pet ether) is Ph₂CN₂, tetraphenylketazine, *syn-endo* monoadduct, *endo*, *exo* bis adduct, *syn-exo* monoadduct, benzhydrol, *exo-anti* monoadduct,

endo-anti monoadduct, and finally the *exo, exo* bis adduct.

Monoadduct identification was confirmed by ^1H and ^{13}C NMR, and agreed with previous assignments¹⁴, and structures of four bis adducts have been partially assigned by ^1H NMR.

Anti-10-t-butoxy-5,5-diphenyl-endo-3,4-diazatricyclo[5.2.1.0^{2,6}]deca-3,8-diene, 6:¹⁴ δ 7.55 (2Hd, oAr); 7.4 - 7.12 (8Hm, Ar); 5.69 (1Hdd, J=4.9 Hz, J=7.4 Hz, H₂); 5.62 (1Hdd, J=2.9 Hz, J=5.7 Hz, H₉); 4.72 (1Hdd, J=2.9 Hz, J=5.7 Hz, H₈); 3.85 (1Hs, H₁₀); 3.66 (1Hm, H₁); 3.22 (1Hdd, J=3.9 Hz, J=7.3 Hz, H₆); 2.83 (1Hbrs, H₇); 1.16 (9Hs, tert-butoxy). ^{13}C NMR: δ 144.1, 142.1 (Ar, ipso); 131.4, 128.7 (C₈, C₉); 128.4, 128.1, 128.0, 127.4, 126.8 (Ar); 127.0, 126.9 (p Ar); 99.7 (quat. benzylic C₃); 96.4, (C₂); 86.9 (C₁₀); 73.7 (quat., t-Bu); 52.3, 50.8, 46.4 (C₁, C₆, C₇); 28.2 (methyl). HPLC retention time 38 min. HPLC Response factor = F = 3.35. m.p. = 156 - 160.5°C (lit. value 162.5 - 163.5°C).¹⁴

Syn-10-t-butoxy-5,5-diphenyl-endo-3,4-diazatricyclo[5.2.1.0^{2,6}]deca-3,8-diene, 5:¹⁴ δ 7.54 (2Hd, o Ar); 7.4 - 7.03 (8Hm, Ar); 5.85 (1Hdd, J=5.0 Hz, J=7.2 Hz, H₂); 5.58 (1Hdd, J=3.4 Hz, J=5.9 Hz, H₉); 4.67 (1Hdd, J=3.3 Hz, J=5.9 Hz, H₈); 3.64 (1Hdd, J=4.1 Hz, J=7.3 Hz, H₆); 3.5(1Hs, H₁₀); 3.42 (1Hm, H₁); 2.57 (1Hs, H₇); 1.19 (9Hs, tert-butoxy). ^{13}C NMR: δ 144.8 (Ar, ipso); 133.6, 130.6 (C₈, C₉); 128.4, 127.9, 127.2 (Ar); 128.2, 126.7 (p Ar); 100.3 (C₂); 97.5 (quat. benzylic, C₃); 86.8 (C₁₀); 74.0 (quat., t-Bu); 50.9, 50.2, 47.7 (C₁, C₆, C₇); 28.4 (methyl). HPLC retention time 78 min. F = 3.78. m.p. = 134 - 141°C (lit. value 142.5 - 143.5°).¹⁴

Syn-10-t-butoxy-5,5-diphenyl-exo-3,4-diazatricyclo[5.2.1.0^{2,6}]deca-3,8-diene, 3:¹⁴ δ 7.65 (2Hd, o Ar); 7.40 - 7.05 (8Hm, Ar); 6.29 (1Hdd, J=3.0 Hz, J=6.3 Hz, H₉); 6.12 (1Hdd, J=2.9 Hz, J=6.3 Hz, H₈); 5.11 (1Hd, J=7.4 Hz, H₂); 3.61 (1Hm, J=3.0 Hz, H₁); 3.27 (1Hs, H₁₀); 2.93 (1Hd, J=7.4 Hz, H₆); 2.73 (1Hm, J=2.9 Hz, H₇); 0.83 (9Hs, tert-butoxy). ^{13}C NMR: δ 140.2, 134.2 (C₈, C₉); 129.0, 128.4, 127.6, 126.6 (Ar); 127.0, 126.2 (p Ar); 99.8 (C₂);

84.4 (C₁₀); 74.0 (quat., t-Bu); 50.7, 49.6, 48.2 (C₁, C₆, C₇); 27.5 (Methyl). HPLC retention time 71 min. F = 4.40.

Anti-10-t-butoxy-5,5-diphenyl-exo-3,4-diazatricyclo[5.2.1.0^{2,6}]deca-3,8-diene, 4:¹⁴ δ 7.57 (2Hd, o Ar); 7.45 - 7.06 (8Hm, Ar); 6.23 (2Hs, H₈ + H₉); 5.12 (1Hd, J=7.3 Hz, H₂); 3.53 (1Hs, H₁); 3.17 (1Hs, H₁₀); 2.83 (1Hd, J=7.3 Hz, H₆); 2.37 (1Hs, H₇); 0.75 (9Hs, tert-butoxy). ¹³C NMR: δ 141.4, 143.6 (Ar, ipso); 137.2, 132.6 (C₈, C₉); 128.5, 128.4, 127.6, 127.2, 127.1, 126.5 (Ar); 128.1, 127.5 (p Ar); 99.1 (C₂); 96.4 (quat. benzylic, C₃); 82.4 (C₁₀); 73.5 (quat., t-Bu); 49.3, 49.0, 48.1 (C₁, C₆, C₇); 27.9 (methyl). HPLC retention time 44 min. F = 3.05. m.p. = 129 - 135°C (lit. value 143 - 144°).¹⁴

13-t-butoxy-5,5,9,9-tetraphenyl-exo,exo-3,4,10,11-tetraazatetracyclo[5.5.1.0^{2,6}0^{8,12}]trideca-3,10-diene, 2:¹⁴ δ 7.56 (2Hd, o Ar); 7.48 (2Hd, o Ar); 7.38 - 7.08 (16Hm, Ar); 5.26 - 5.16 (2H apparent t, J=7.4 Hz, J=8.1 Hz, H₂ + H₁₂); 3.76 (1Hs, H₁); 2.78 (1Hd, J=7.4 Hz, H₆); 2.71 (1Hd, J=8.1 Hz, H₈); 2.57 (1Hs, H₁₃); 2.12 (1Hs, H₇); 0.29 (9Hs, tert-butoxy). ¹³C NMR: δ 145.0, 143.3, 141.9, 140.4 (Ar, ipso); 128.8, 128.7, 128.5, 128.3, 127.9, 127.5, 126.8, 126.4, 126.2 (Ar); 127.9, 127.5, 127.3, 126.4 (p Ar); 102.5 (quat. benzylic); 97.5, 95.2 (C₂, C₁₂); 74.0 (quat., t-Bu); 73.4 (bridgetop, C₁₃); 51.7, 50.1 (C₆, C₈); 45.4, 45.1 (C₁, C₇); 26.7 (methyl). m.p. = 185.5 - 187°C (lit. value 186 - 186.5°).¹⁴

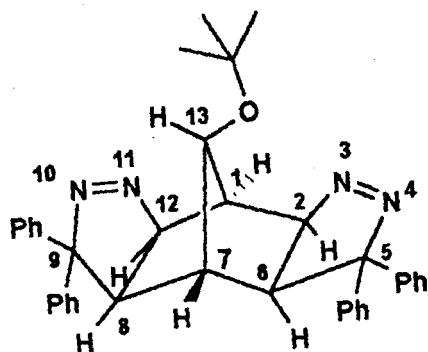
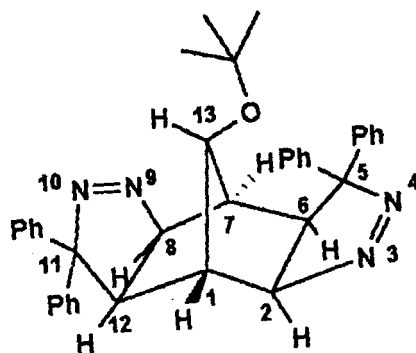
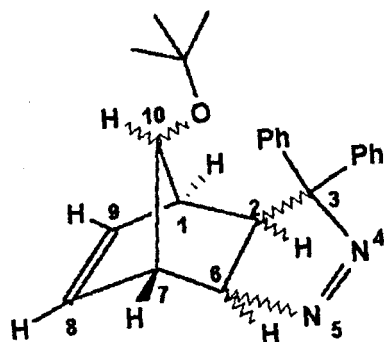
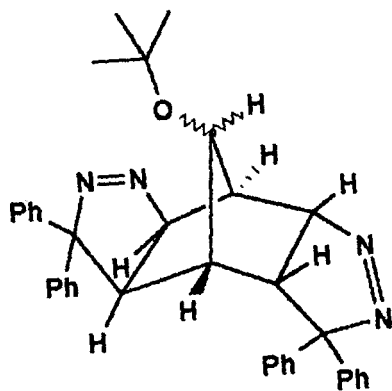
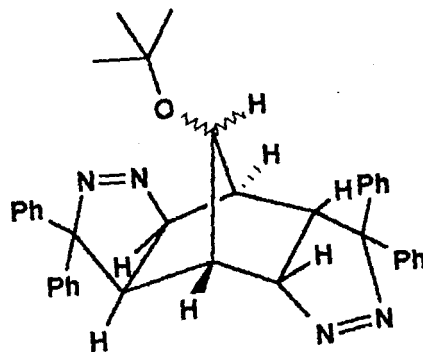
Exo, endo bis adduct #1, 7-8: δ 7.72 (2Hbrm, Ar); 7.57 - 7.03 (16Hm, Ar); 6.94 (2Hd, o Ar); 5.39 (1Hdd, J=5.8 Hz, J=8.5 Hz, *exo* to ring, α to diaza); 3.98 (1Hd, J=7.8 Hz, *endo* to ring, α to diaza); 3.69 (1Hdd, J=4.8 Hz, J=8.4 Hz, *exo* to ring, α to benzylic); 3.17 (1Hs, bridgetop, H₁₃); 2.88 (1Hd, J=4.5 Hz, bridgehead, β to diaza); 2.64 (1Hd, J=7.8 Hz, *endo* to ring, α to benzylic); 2.61 (1Hs, bridgehead, β to benzylic, H₁); 0.81 (9Hs, tert-butoxy). ¹³C NMR: δ 144.3, 142.9, 142.7, 141.2 (ipso, Ar); 129.1, 128.7, 128.5, 128.5, 127.8, 127.7, 127.1, 126.8, 126.7 (Ar); 127.6, 127.4, 127.4, 126.5 (p Ar); 103.7, 97.0 (quat. benzylic);

96.3, 92.1 (α to benzylic); 77.3 (bridgetop, C₁₃); 74.1 (quat., t-Bu); 46.5, 45.8 (C₆, C₁₂); 44.6, 39.2 (bridgeheads, C₁, C₇); 22.9 (methyl).

Exo, endo bis adduct #2, 7-8: δ 7.90 (2Hbr, Ar); 7.48 (2Ht, Ar); 7.36 (2Ht, Ar); 7.31 - 7.02 (10Hm, Ar); 6.97 (2Hd, Ar); 6.68 (2Hdd, Ar); 5.12 (1Hdd, J=6.2 Hz, J=8.0 Hz, *exo* to ring, α to diaza); 4.72 (1Hd, J=7.1, *endo* to ring, α to diaza); 4.0 (1Hm, J=6.4 Hz, bridgehead, β to diaza); 3.47 (1Hs, H₁₃); 2.95 (1Hdd, J=3.9 Hz, J=8.1 Hz, *exo* to ring, α to benzylic); 2.15 (1Hm, J=3.7 Hz, bridgehead, β to benzylic); 2.11 (1Hd, J=7.1 Hz, *endo* to ring, α to benzylic). ¹³C NMR: δ 144.3, 143.3, 142.8 (ipso, Ar); 129.0, 128.7, 128.4, 127.9, 127.6, 127.5, 127.0, 126.1, 125.7 (Ar); 126.7, 126.1 (p Ar); 102.7, 98.9 (quat. benzylic); 93.5, 91.0 (α to diaza); 78.8 (bridgetop, C₁₃); 74.7 (quat., t-Bu); 47.8, 46.3, 46.6, 41.7 (C₁, C₆, C₇, C₈); 28.0 (methyl). HPLC retention time 88 min. F = 2.65.

13-t-butoxy-5,5,11,11-tetraphenyl-*exo,exo*-3,4,9,10,-tetraazatetracyclo[5.5.1.0^{2,6}.0^{8,12}]trideca-3,9-diene 1: δ 7.65 (2Hd, o Ar); 7.52 (2Hd, o Ar); 7.47 - 7.10 (16H, Ar); 4.95 (1Hd, J=7.1 Hz, H₂); 4.91 (1Hd, J=7.7 Hz, H₁₂); 3.0 (1Hs, H₁₃); 2.99 (1Hd, J=7.0 Hz, H₆); 2.83 (1Hd, J=7.7 Hz, H₈); 2.75 (1Hs, H₁); 2.57 (1Hs, H₇). ¹³C NMR: δ 144.7, 142.8, 142.0, 140.7 (Ar, ipso); 128.8, 128.7, 128.5, 127.9, 127.8, 126.7, 126.3, (Ar); 127.9, 127.6, 127.4, 126.6 (p Ar); 101.8 (quat. benzylic); 99.4, 98.1 (α to diaza, C₂, C₈); 74.0 (bridgetop, C₁₃); 73.7 (quat.,t-Bu); 48.6, 45.9, 45.54 43.7 (C₁, C₆, C₇, C₁₂); 27.0 (methyl). HPLC retention time 82 min. F = 2.28.

Exo, endo bis adduct #3, 7-8: δ 7.88 (2Hbr, Ar); 7.47 (2Ht, Ar); 7.37 - 7.13 (10Hm, Ar); 7.10 (2Hdd, Ar); 6.90 (2Hd, Ar); 6.68 (2Hdd, Ar); 5.44 (1Hdd); 4.72 (1Hd); 3.73 (1Hm); 3.5 (1Hdd); 3.17 (1Hs); 2.07 (1Hd); 1.60 (1Hm).

213-678

5. Determination of HPLC response factors for mono- and bis-pyrazoline adducts.

Quantitative solutions of isolated mono and bis adducts were prepared by weighing 10-20 mg of each, dissolving and diluting with methanol to 10 mL in a volumetric flask containing 0.5 mL of 0.03 M E-stilbene as internal standard. A sample of the resulting solution was injected onto a reverse-phase HPLC column and eluted under the following conditions.

Gradient Elution:	Ramp	%B _{initial}	%B _{final}	Time, min.	
		B = 100% methanol, A = 50% methanol/water			
	1	40	70	75	
	2	70	95	30	
	3	95	40	10	
Flow rate:	1.0 ml/min	Pressure:	1200 - 2000 psi	Injection volume:	20 μL
Sensitivity:	0.002	Chart Speed:	20 cm/hr		

The areas of the eluting peaks were measured, and the relative response factor calculated from Equation 34.

$$[\text{adduct}] = F[\text{I.S.}] \cdot A_A / \text{A.I.S.} \quad (34)$$

F = Response factor A_A = Area of chromatographic peak for adduct

I.S. = Internal standard $A_{\text{I.S.}}$ = Area of chromatographic peak for internal standard

Since a sufficient quantity of the *syn-exo* monoadduct could not be isolated for this determination, a mixture of 1:5 *syn-exo:syn-endo* monoadduct (the ratio determined by NMR integration) was used to estimate the *syn-exo* response factor.

6. HPLC analysis of mono- and bis-pyrazoline adducts.

Reaction mixtures prepared as described in Chapter V section 3 (Reaction of diphenyldiazomethane with 7-*tert*-butoxynorbornadiene) were transferred to a 25 mL volumetric flask, 1.0 mL of 12.5 - 30.0 mM E-stilbene (in methanol) as internal standard was added and the mixture diluted to volume with methanol. If the reaction solvent was not miscible with methanol, it was removed by rotary evaporation prior to dilution with methanol. The reaction solvent was otherwise allowed to remain. Sonication (≤ 5 min) was often necessary for dissolution of the reaction mixture, and frequently tetraphenylketazine was still not completely dissolved. After a 1.0 mL aliquot was removed for spectrophotometric Ph_2CN_2 analysis, the mixture was treated with 1 drop 6 N HCl and mixed until the red color disappeared. Two to three drops of triethylamine were then added to neutralize excess HCl.

A 20 μL aliquot of the crude product mixture thus prepared was introduced onto a reverse-phase HPLC column and eluted by the same conditions specified in Chapter V, section 5. Identifiable peaks were eluted in the order of benzhydrol, *endo-anti* monoadduct, *exo-anti* monoadduct, internal standard, *syn-exo* monoadduct, *syn-endo* monoadduct, a very large tetraphenylketazine peak (overlapping two bis adducts), and remaining bis adducts.

The concentration of each monoadduct was calculated using Equation 34. Two separate reaction mixtures were prepared in each case and two injections were performed on each mixture. Averaged data is reported in Table 4 as millimoles of total monoadduct, and as relative percentages of monoadducts in Table 5.

7. Determination of residual diphenyldiazomethane.

Determination of the extinction coefficient for Ph_2CN_2 was made by preparing several

dilutions from a 0.0516 M stock solution (in methanol) and measuring the visible absorbance on a UV-vis spectrophotometer at $\lambda_{\max} = 525$ nm, using methanol as both reference and blank. A plot of absorbance vs. concentration gave a slope of 93.1 (in methanol) equivalent to the extinction coefficient according to Beer's Law, Equation 35, and in good agreement with literature values of 101 (in methanol, $\lambda_{\max} = 526$ nm)^{170a}, 100 (in n-heptane, $\lambda_{\max} = 500$ nm)^{170b}, and 89 ($\lambda_{\max} = 520$ nm)^{170c}.

$$A = \epsilon \cdot c \cdot \ell \quad (35)$$

Where ϵ is the extinction coefficient, c is molar concentration, and ℓ is the cell length, 1 cm.

A 1.0 mL sample was removed from the 25 mL methanol solution prepared for HPLC analysis and was diluted to a 10.0 mL volume with methanol. The visible absorbance was measured at 525 nm and the concentration of Ph_2CN_2 calculated from Beer's law. The mmoles of Ph_2CN_2 remaining were calculated from the concentration and dilution data so obtained, and the mmoles consumed was determined by subtraction of the mmoles of Ph_2CN_2 remaining from the mmoles of starting material.

8. Determination of rate of reaction between 7-*tert*-butoxynorbornadiene and diphenyldiazomethane in n-hexane and acetonitrile.

A 3.1126 g (15.86 mmol) sample of Ph_2CN_2 and 2.0593 g (12.54 mmol) of 7-*tert*-butoxynorbornadiene were mixed and brought to volume in n-hexane in a 25 mL volumetric flask. A total of 24 1.0 mL volumes were transferred from this bulk mixture and distributed to 2 mL vials. The vials were capped and sealed in parafilm and stored in the dark at 4°C until further use. A vial was retrieved for assay every second or third day for 1 month, then twice

per month thereafter. The contents were transferred quantitatively to a 10 mL volumetric flask. A 1.0 mL volume of 1.017 - 1.101 mM E-stilbene (in methanol) as internal standard was also added, and the contents were brought to volume in methanol.

A 1.0 mL aliquot of reaction mixture thus prepared was removed and further diluted to 10.0 mL with methanol and the absorbance measured at 525 nm. The remaining reaction mixture was treated with 1 drop of 6 M HCl to destroy residual Ph_2CN_2 . Two drops of triethylamine were then added to neutralize the HCl. The mixture was then separated and quantified as described in Chapter V section 6 (HPLC analysis of mono- and bis-pyrozoline adducts).

The entire procedure was repeated with similar concentrations of reactants (15.79 mmol Ph_2CN_2 and 12.54 mmol 7-*tert*-butoxynorbornadiene) but substituting acetonitrile as the reaction solvent. The procedure was repeated twice more with the dilution increased by a factor of two; once in n-hexane and once in acetonitrile. The stock reaction mixture for n-hexane was made by combining 3.1133 g of Ph_2CN_2 (16.028 mmol) and 2.0645 g of 7-*tert*-butoxynorbornadiene (12.569 mmol) and diluting to 50 mL with hexane. The stock reaction mixture in acetonitrile was made up of 15.965 mmol of Ph_2CN_2 and 12.570 mmol of 7-*tert*-butoxynorbornadiene in 50.0 mL acetonitrile.

APPENDIX

Table 25. Solvent parameters for the Koppel-Palm equation

Entry	Solvent	E ^a	Y ^c	P ^d	B ^e
2	CCl ₄	(0) ^b	0.2253	0.2151	31
3	CHCl ₃	6.657	0.3588	0.2105	39
4	CH ₂ Cl ₂	7.410	0.4205	0.2034	43
11	Ethyl acetate	(0) ^b	0.3850	0.1853	89 ^f
12	Acetone	8.479	0.4644	0.1803	123
13	Ethyl ether	(0) ^b	0.3404	0.1780	129
14	Tetrahydrofuran	(0) ^b	0.4072	0.1976	145
15	1,4-Dioxane	5.643	0.2232	0.2028	128
16	Hexane	(0) ^b	0.1849	0.1862	24
17	Cyclohexane	(0) ^b	0.2024	0.2040	25
19	Benzene	3.615	0.2292	0.2276	52
20	Nitrobenzene	6.662	0.4787	0.2433	63 ^g
21	Nitromethane	12.275	0.4794	0.1888	59
22	Propionitrile	9.805	0.4745	0.1829	104 ^f
23	Benzonitrile	7.155	0.4708	0.2355	97
24	Acetonitrile	11.709	0.4794	0.1748	103
25	HCON(CH ₃) ₂	9.609	0.4798	0.2055	166
27	CH ₃ SOCH ₃	10.698	0.4840	0.2210	192

$${}^a E = E_T(30) - 25.1 - 14.84Y - 9.59P$$

^bE = 0, in parentheses, refers to values for inert solvents according to Koppel and Palm. See reference 57c.

$${}^c Y = (\epsilon - 1)/(2\epsilon + 1)$$

$${}^d P = (\eta^2 - 1)/((2\eta^2 + 1))$$

^e Values taken from reference 171.

^f Values taken from reference 172.

^gB value given in reference is incorrect. The value has been corrected here.

Table 26. Swain's acity-basity parameters^a, dielectric constants and refractive indices

Entry	Solvent	A	B	ϵ^b	η^c
2	CCl ₄	0.09	0.34	2.23	1.4602
3	Chloroform	0.42	0.73	4.81	1.4459
4	CH ₂ Cl ₂	0.33	0.80	8.93	1.4242
5	1-Octanol	---	---	10.34	1.4290
6	t-Butanol	0.45	0.50	12.47	1.3877
7	1-Butanol	0.61	0.43	17.51	1.3993
8	2-Propanol	0.59	0.44	19.92	1.3772
9	Ethanol	0.66	0.45	24.55	1.3614
10	Methanol	0.75	0.50	32.66	1.3284
11	Ethyl acetate	0.21	0.59	6.02	1.3724
12	Acetone	0.25	0.81	20.56	1.3587
13	Ethyl ether	0.12	0.34	4.20	1.3524
14	THF	0.17	0.67	7.58	1.4072
15	1,4-Dioxane	---	---	2.21	1.4224
16	Hexane	0.01	-0.01	1.88	1.3749
17	Cyclohexane	0.02	0.06	2.02	1.4262
18	Decalin	---	---	2.20	1.481
19	Benzene	0.15	0.59	2.27	1.5011
20	Nitrobenzene	0.29	0.86	34.78	1.5562
21	Nitromethane	0.39	0.92	35.94	1.3819
22	CH ₃ CH ₂ CN	---	---	28.86	1.3658
23	Benzonitrile	0.30	0.87	25.2	1.5282
24	Acetonitrile	0.37	0.86	35.94	1.3441
25	HCON(CH ₃) ₂	0.30	0.93	36.71	1.4305
26	Sulfolane	---	---	43.3	1.4861
27	CH ₃ SOCH ₃	0.34	1.08	46.45	1.4793

^aacity-basity values taken from reference 67. The peculiar spellings of these parameters are intended to distinguish these parameters from a solvents acidity and basicity while at the same time indicating the similarities between. Acidity and basicity describes the ability of the solvent to ionize and thus to solvate ionic solutes, while acity and basity are measures of the ability of the solvent to solvate ionic solutes without themselves necessarily ionizing.

^bdielectric constants taken reference 173

^crefractive index values taken from reference 174

Table 27. Solvent parameters for the Abraham-Kamlet-Taft equation^a

Entry	Solvent	δ	π^*	α	δ_H^{2b}
2	CCl ₄	0.5	0.28	0	0.125
3	Chloroform ^c	0.5	0.58	0.44	0.15
4	CH ₂ Cl ₂ ^c	0.5	0.82	0.30	0.165
5	1-Octanol ^c	0	0.37	0.62	0.174
6	t-Butanol ^c	0	0.41	0.68	0.189
7	1-Butanol ^c	0	0.47	0.79	0.219
8	2-Propanol ^c	0	0.48	0.76	0.225
9	Ethanol ^c	0	0.54	0.83	0.274
10	Methanol ^c	0	0.60	0.93	0.346
11	Ethyl acetate	0	0.55	0	0.134
12	Acetone ^c	0	0.71	0.08	0.153
13	Ethyl ether	0	0.27	0	0.095
14	THF	0	0.58	0	0.146
15	1,4-Dioxane	0	0.55	0	0.169
16	Hexane	0	-0.08	0	0.089
17	Cyclohexane	0	0.0	0	0.113
18	Decalin	0	0.09	0	0.127
19	Benzene	1	0.59	0	0.141
20	Nitrobenzene	1	1.01	0	0.206
21	Nitromethane ^c	0	0.85	0.22	0.267
22	CH ₃ CH ₂ CN	0	0.71	0	0.191
23	Benzonitrile	1	0.90	0	0.207
24	Acetonitrile ^c	0	0.75	0.19	0.233
25	HCON(CH ₃) ₂	0	0.88	0	0.234
26	Sulfolane	0 ^d	0.988 ^d	0 ^d	0.255 ^c
27	CH ₃ SOCH ₃	0	1.00	0	0.285

^a δ , π^* , α , and δ_{H}^2 values taken from reference 166.

^b δ_{H}^2 values converted from kcal/liter to psi by multiplying by 0.0016875 L·lb/kcal·in²

^cProtic solvents

^dThese values taken from reference 175.

^e δ_{H}^2 calculated from $\Delta H_{\text{V}}^{\circ} = 15$ kcal/mol. See reference 173.

BASIC program for the determination of k_1 and k_2 .

```

0 LIST
1 BSUM=1E+23
10 DIM X(100),Y(100),Z(100),T(100)
15 GOTO 2000
20 INPUT "datafilename????",D$
30 GOSUB 1000
35 INPUT "initial Y-concentration????",YI
36 Y(1)=YI
40 INPUT "k1 limits (k1i,k1f,k1inc)????",K1I,K1F,K1INC
50 INPUT "k2 limits (k2i,k2f,k2inc)????",K2I,K2F,K2INC
60 FOR K1=K1I TO K1F STEP K1INC
65 PRINT (K1/K1F),BSUM,BK1,BK2
70 FOR K2=K2I TO K2F STEP K2INC
80 SUM=0
90 FOR J=2 TO N
95 DELT=T(J)-T(J-1)
100 Z(J)=X(J-1)-K1*X(J-1)*Y(J-1)*DELT-K2*X(J-1)*X(J-1)*DELT
110 SUM=SUM+(Z(J)-X(J))^2
120 Y(J)=Y(J-1)-K1*X(J-1)*Y(J-1)*DELT
130 NEXT J
140 IF SUM<BSUM THEN BSUM=SUM:BK1=K1:BK2=K2:GOTO 200
200 Y(1)=YI:SUM=0
210 NEXT K2
220 NEXT K1
300 PRINT:PRINT:PRINT
310 PRINT "best k1 equals",K1
320 PRINT "best k2 equals",K2
330 PRINT "best sum equals",BSUM
340 END
1000 OPEN"i",#1,D$
1010 INPUT#1,N
1020 FOR J=1 TO N
1030 INPUT#1,T(J),X(J)
1040 NEXT J
1050 CLOSE#1
1060 RETURN
2000 INPUT "filename????",D$
2010 INPUT "Number of data points?????",N
2020 FOR J=1 TO N
2025 PRINT J;
2030 INPUT "time,concentration",T(J),X(J)
2040 NEXT J
2045 OPEN"o",#1,D$
2050 FOR J=1 TO N
2055 T(J)=T(J)/60

```

```
2060 PRINT#1,T(J),X(J)
2070 NEXT J
2080 CLOSE#1
2090 END
^Z
```

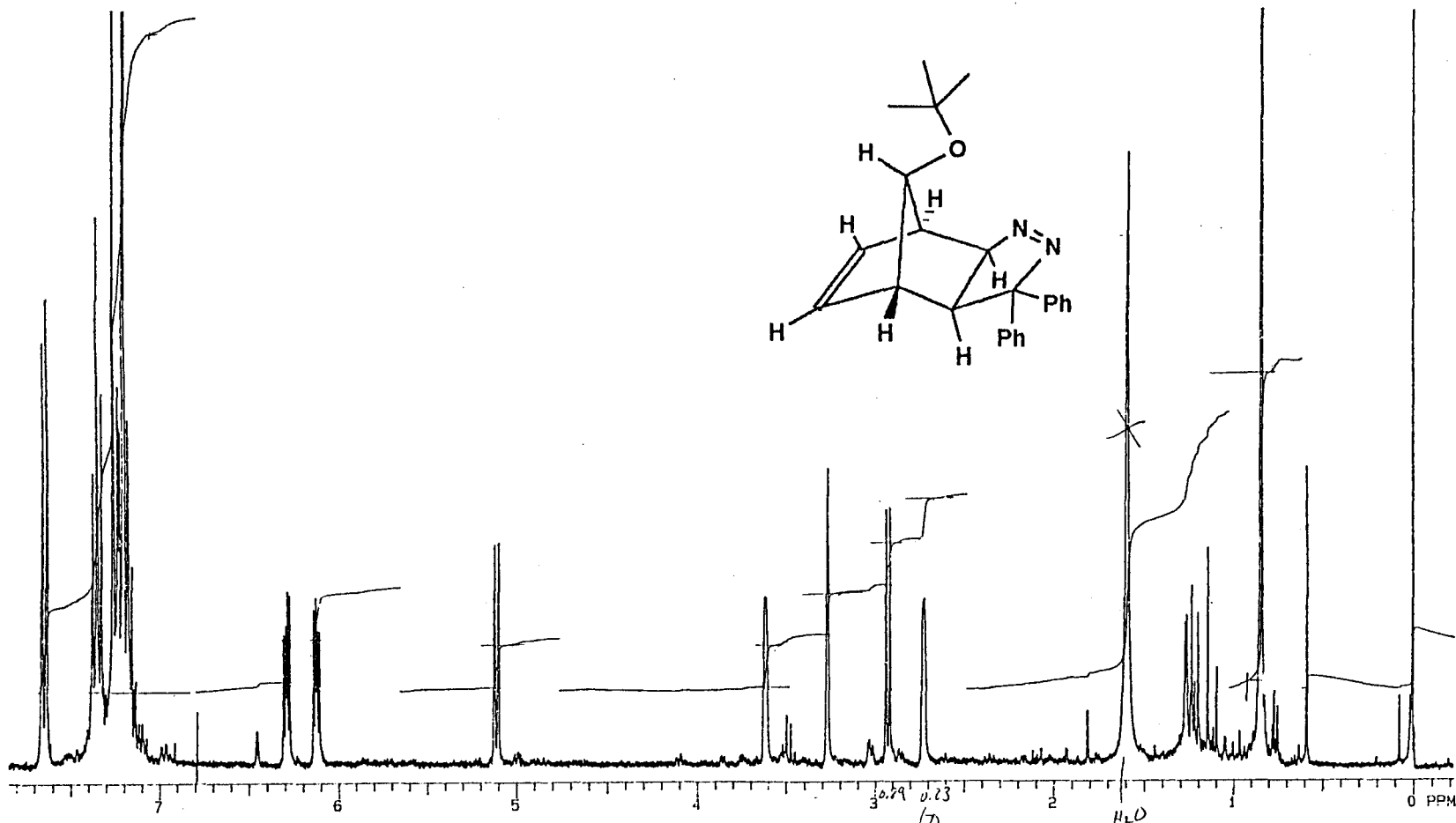
BASIC program to determine goodness of fit of k_1 and k_2

```

10 DIM X(100),Y(100),Z(100),T(100)
20 INPUT "datafilename?????",D$
25 INPUT "number of data points?????",N
30 GOSUB 1000
35 INPUT "initial Y-concentration????",YI
36 Y(1)=YI
37 INPUT "do you want a printout (Y=1,N=0)????",ANS
40 INPUT "best k1?????",K1
50 INPUT "best k2????????",K2
60 Z(1)=X(1)
70 PRINT T(1),Z(1),X(1)
90 FOR J=2 TO N
95 DELT=T(J)-T(J-1)
100 Z(J)=X(J-1)-K1*X(J-1)*Y(J-1)*DELT-K2*X(J-1)*X(J-1)*DELT
120 Y(J)=Y(J-1)-K1*X(J-1)*Y(J-1)*DELT
125 PRINT T(J),Z(J),X(J)
126 IF ANS=1 THEN LPRINT T(J),Z(J),X(J)
130 NEXT J
340 END
1000 OPEN "i",#1,D$
1020 FOR J=1 TO N
1030 INPUT#1,T(J),X(J)
1040 NEXT J
1050 CLOSE#1
1060 RETURN
2000 INPUT "filename?????",D$
2010 INPUT "Number of data points?????",N
2020 FOR J=1 TO N
2025 PRINT J;
2030 INPUT "time,concentration",T(J),X(J)
2040 NEXT J
2045 OPEN "o",#1,D$
2050 FOR J=1 TO N
2055 T(J)=T(J)/60
2060 PRINT#1,T(J),X(J)
2070 NEXT J
2080 CLOSE#1
2090 END
^Z

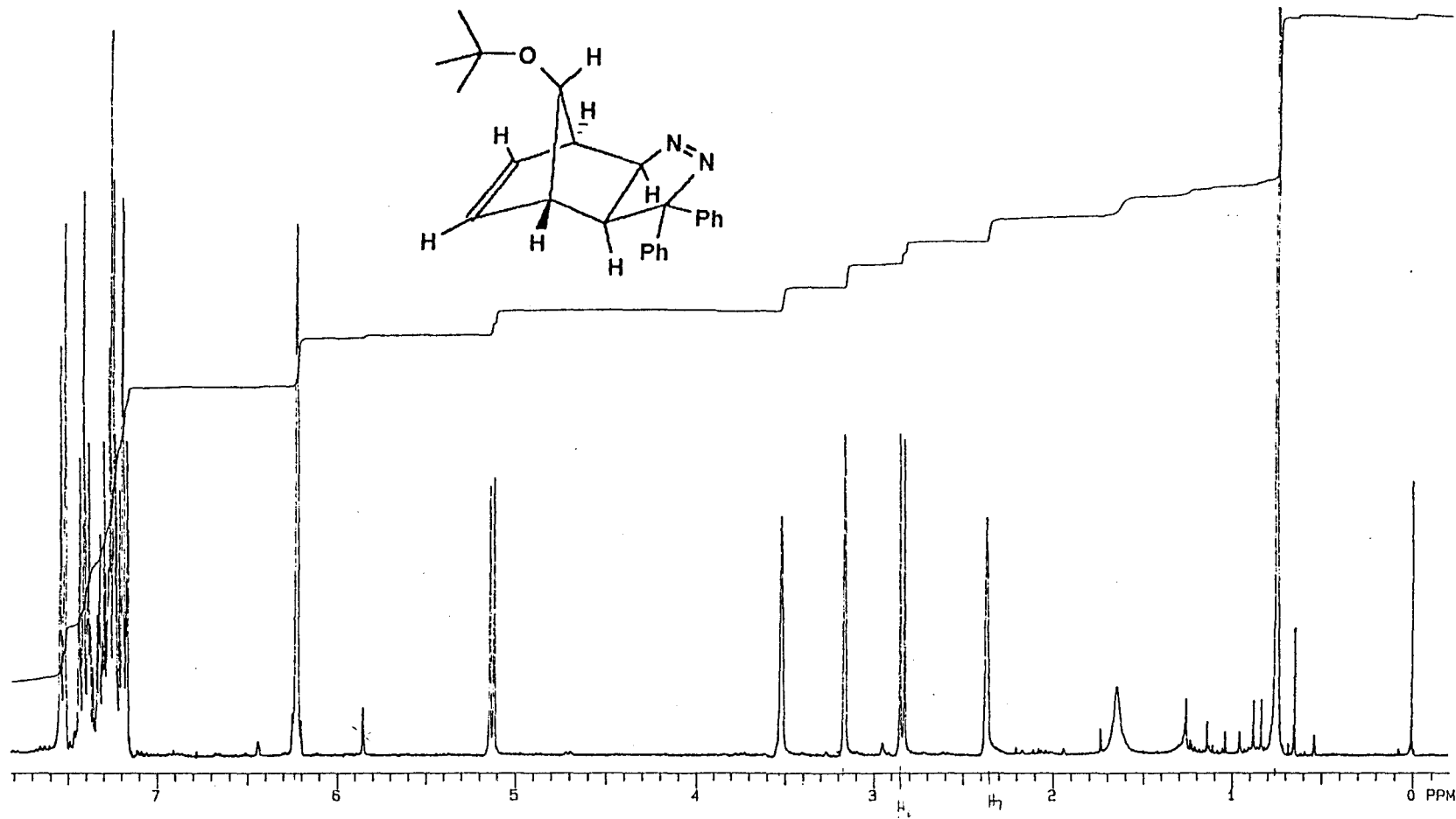
```

SPECTRA



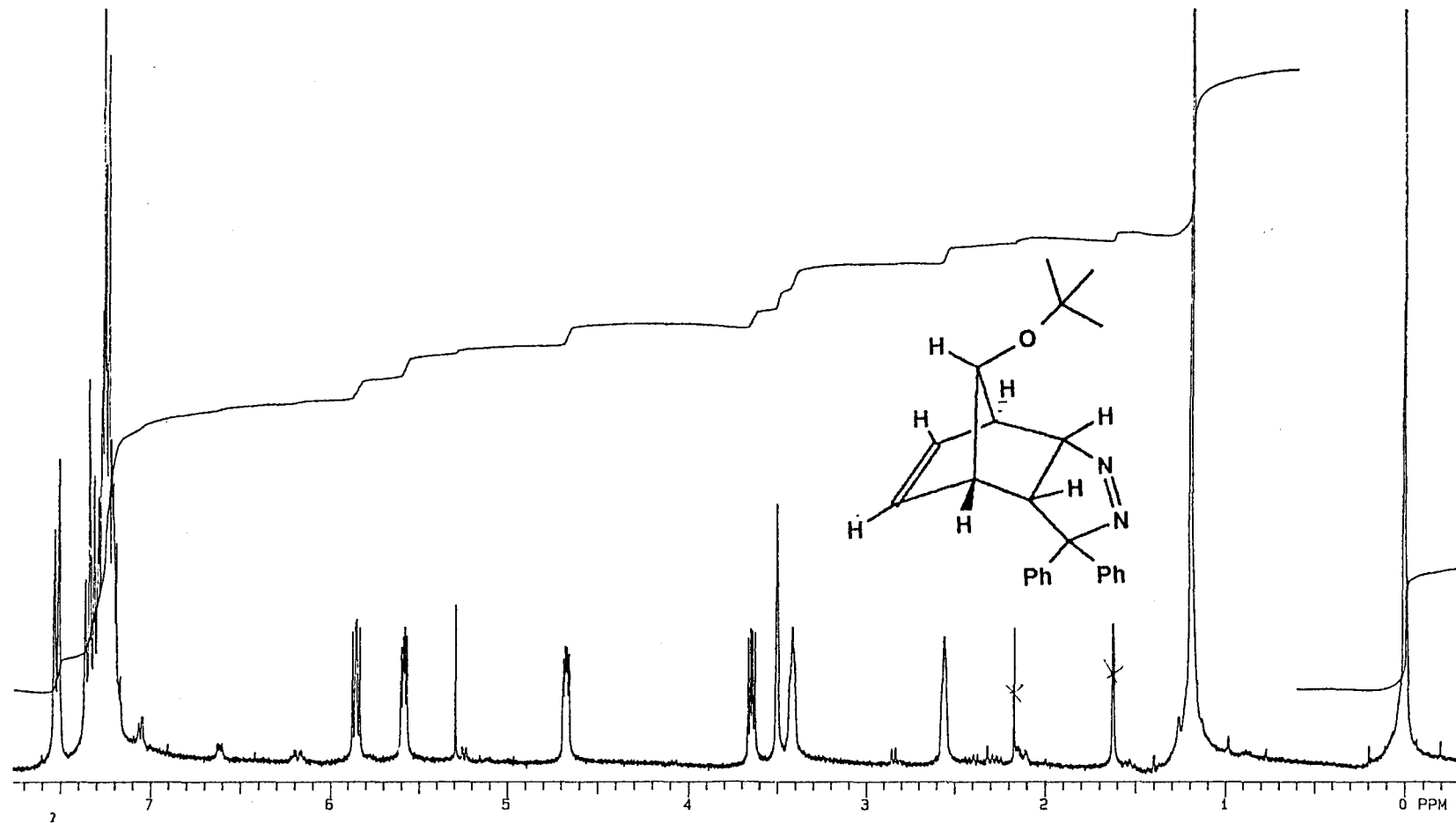
1.750	300	1.750	350.3	32	---	---	ST01H	H
4000.0	700	NNN	20	---	---	---	---	08-22-90
3.752	0	C	200	2418.6	-66.4	---	---	VXR 300
7.0	128	---	---	---	---	---	CDCL3	

¹H NMR of *Syn*-10-*t*-butoxy-5,5-diphenyl-*exo*-3,4-diazatricyclo[5.2.1.0^{2,6}]deca-3,8-diene (3)



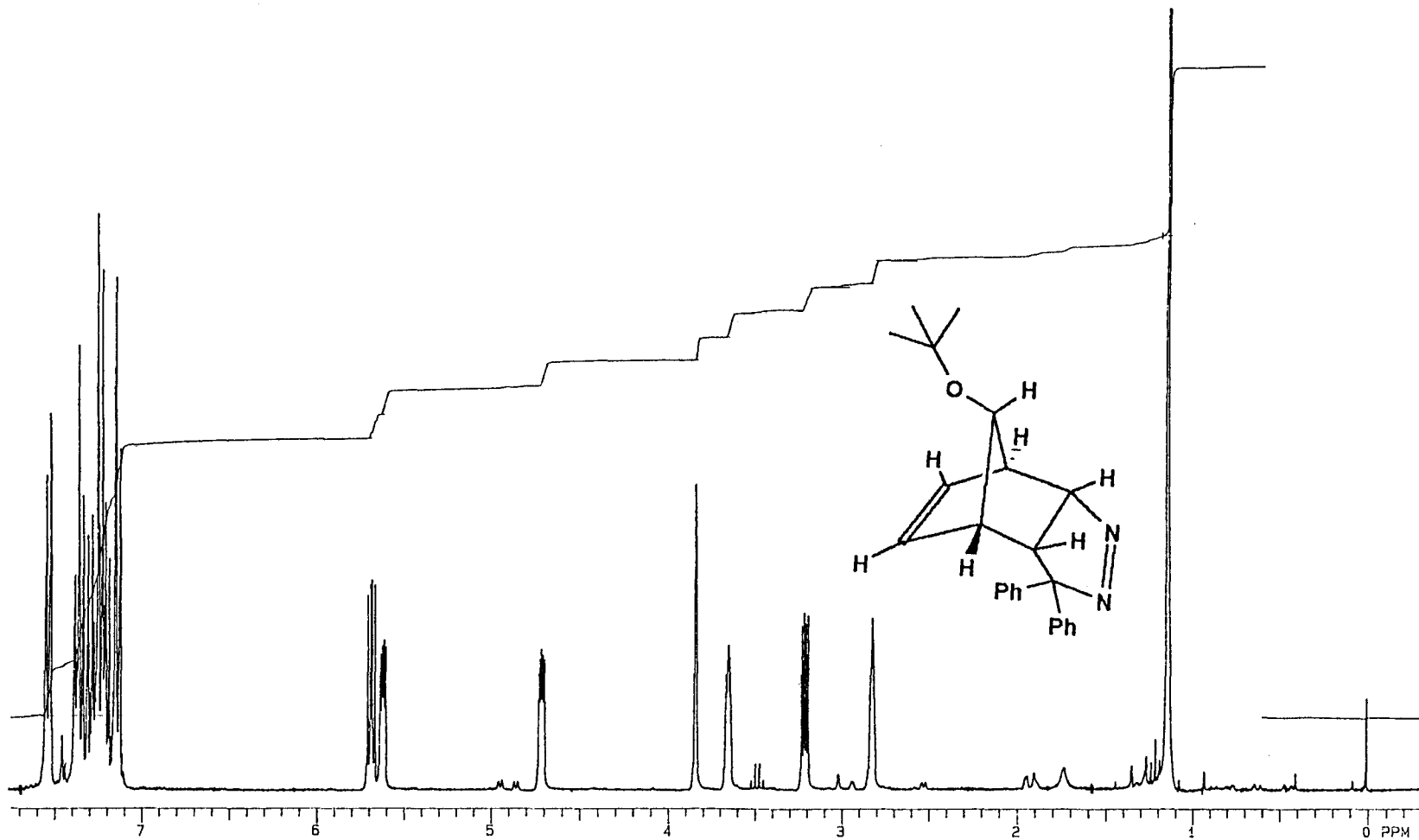
1.750	300	1.750	350.3	32	---	---	ST01H	
4000.0	700	NNN	20	---	---	---	EXO, ANTI PYRAZOLINE MONOADDUCT	EXOAN
3.752	0	C	200	2403.2	-58.6	---		08-29-80
7.0								VXR 300

¹H NMR of *Anti*-10-*t*-butoxy-5,5-diphenyl-*exo*-3,4-diazatricyclo[5.2.1.0^{2,6}]deca-3,8-diene, (4)



1.750	300	1.750	350.3	32	--	--	STD1H	
4000.0	700	NNN	20	--	--	--	BIIP107 5-17-90	FXN8
3.752	0	C	200	2417.6	-89.6		FXN8 CYCLOADDITION OF	05-17-90
7.0	64						T-BUTOXYNORADIENE+PH2CH2	VXR 300
							CDCL3	

¹H NMR of *Syn*-10-t-butoxy-5,5-diphenyl-*endo*-3,4-diazatricyclo[5.2.1.0^{2,6}]deca-3,8-diene, (5)



1.750
4000.0

300
700

1.750
NNN

350.3
20

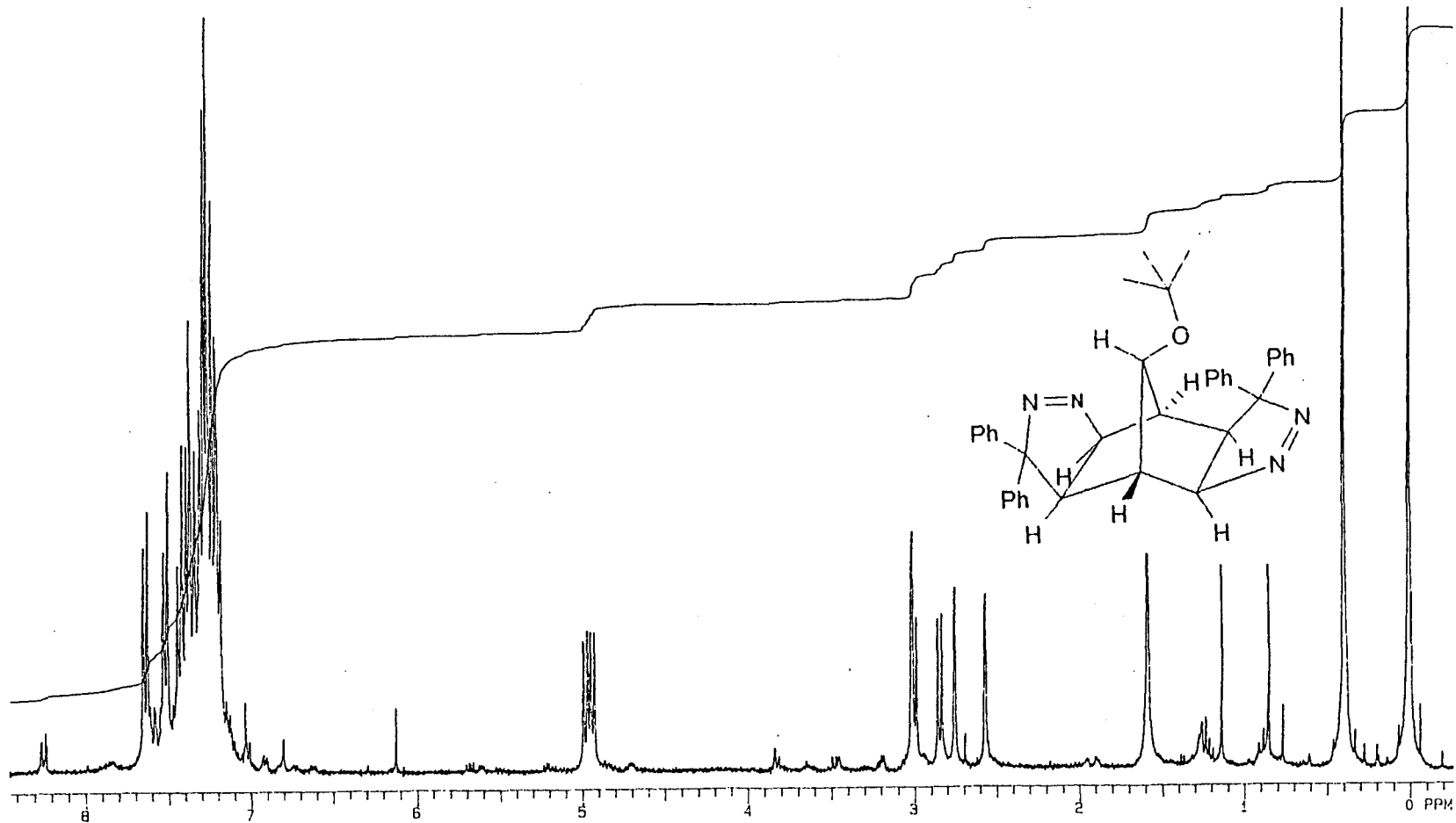
32

STD1H

ANTI, ENDO

H

¹H NMR of *Anti*-10-*t*-butoxy-5,5-diphenyl-*endo*-3,4-diazatricyclo[5.2.1.0^{2,6}]deca-3,8-diene, (6)



1.750
4000.0
2.000
7.0

300
700
0
97

1.750
NNN
C

350.3
20
200

16
2609.2

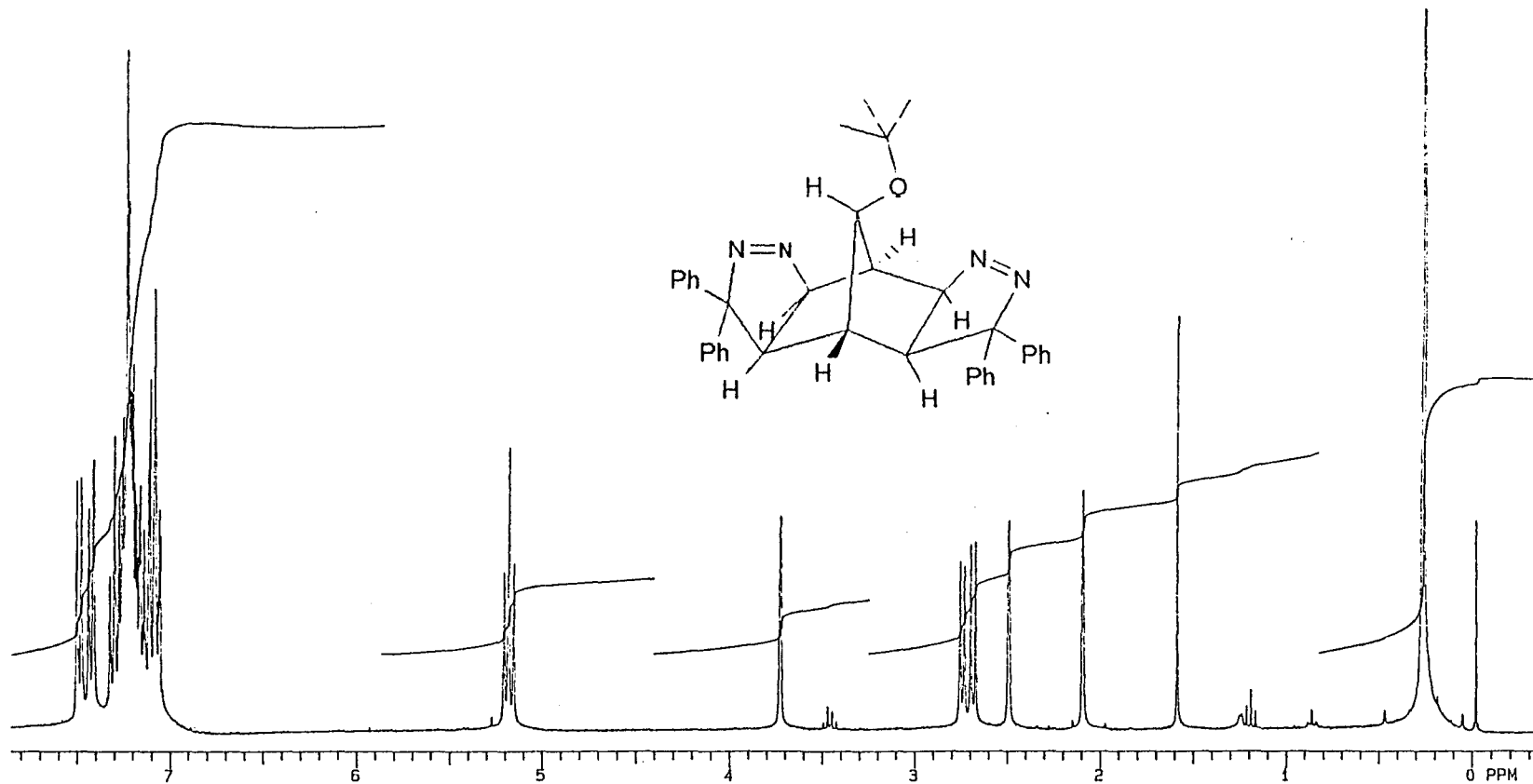
ST01H

6-28-91 BIS ADDUCT #4

CDCL3

H
06-28-91
VXR 300

¹H NMR of 13-t-butoxy-5,5,11,11-tetraphenyl-*exo,exo*-3,4,9,10-tetraazatetracyclo[5.5.1.0^{2,6}.0^{8,12}]trideca-3,9-diene (1)



1.500

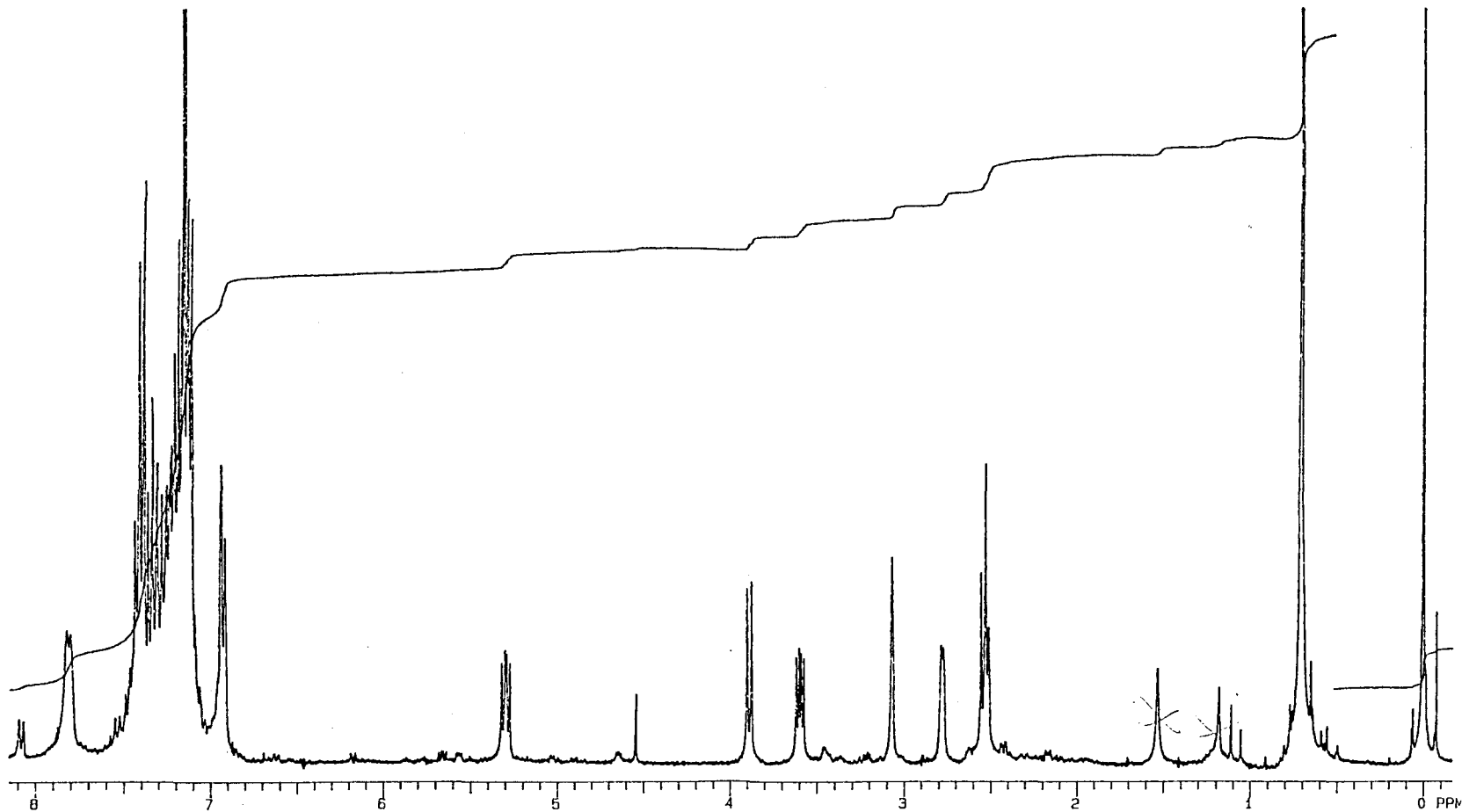
337

1000.0

2.018

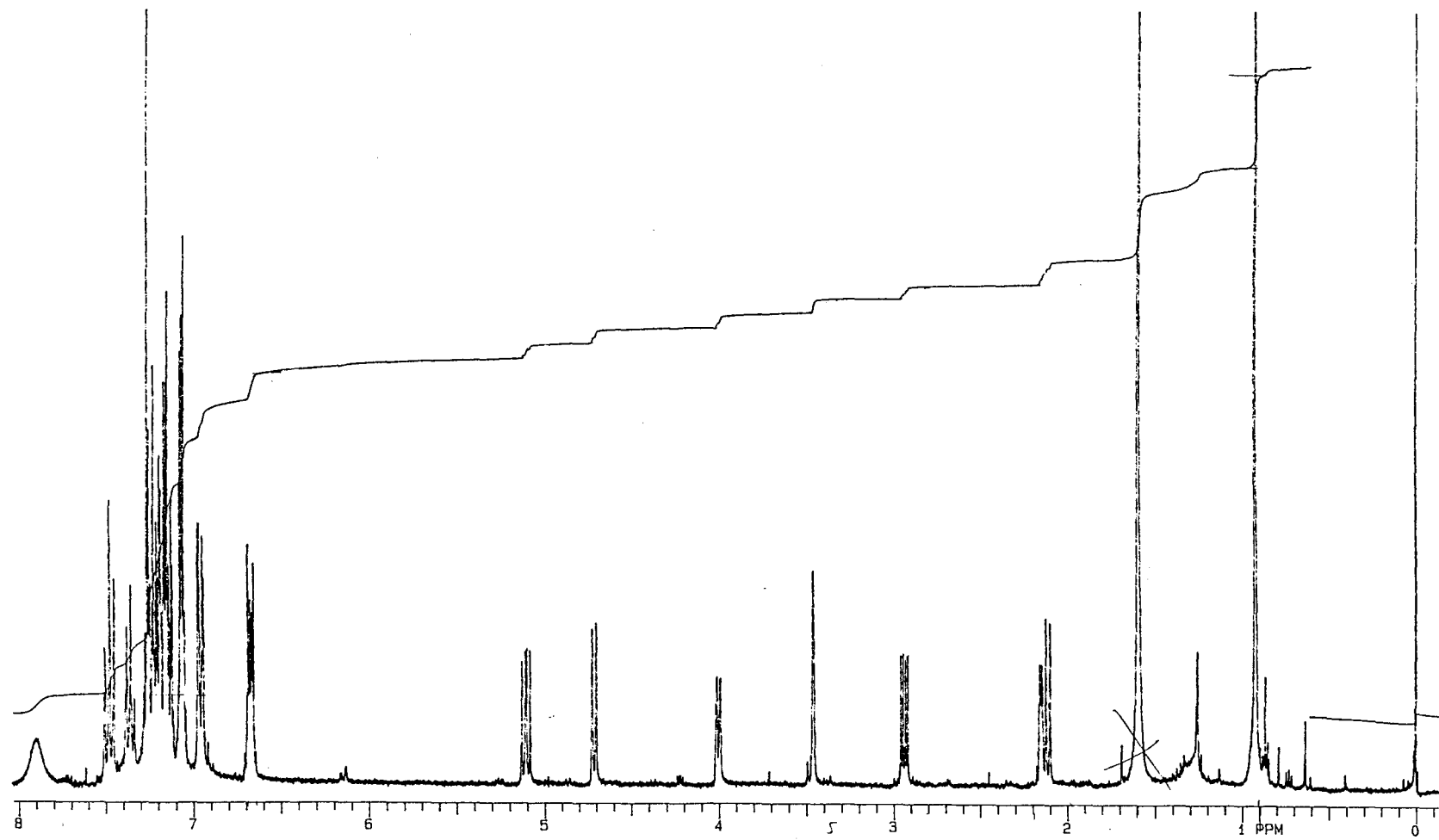
915 570-620 22.3%0 IN CDCl₃

¹H NMR of 13-t-butoxy-5,5,9,9-tetraphenyl-*exo,exo*-3,4,10,11-tetraazatetracyclo[5.5.1.0^{2,6}.0^{8,12}]trideca-3,10-diene, (2)



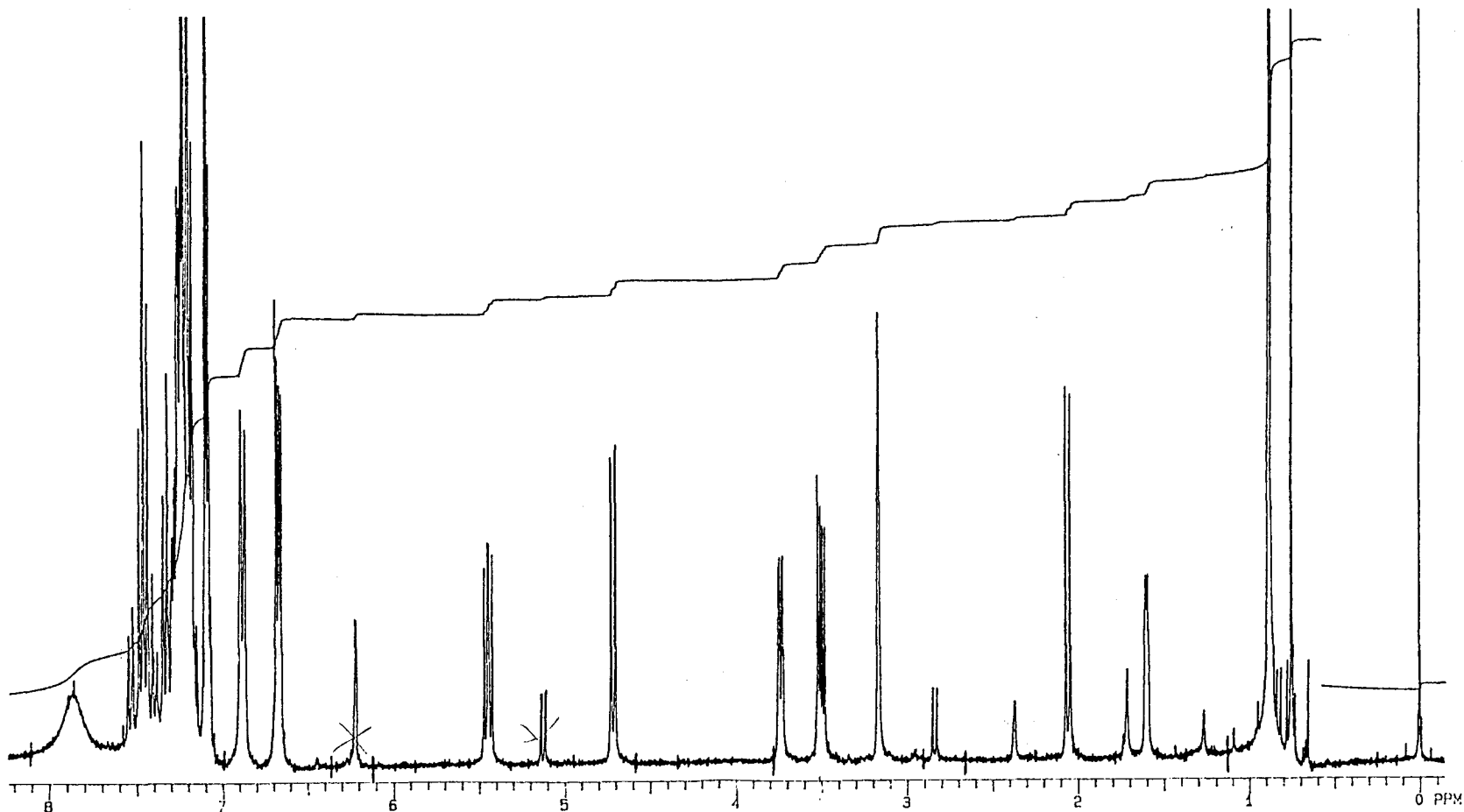
1.750	300	1.750	350.3	32	---	---	STD1H	
4000.0	700	NSN	20	---	---	---	2-27-91 FRACTION 1	H
3.752	0	C	200	2494.5	-50.8	---		02-27-91
7.0	82					CDCL3		VXR 300

¹H NMR of *Exo, endo* bis adduct #1, (7-8)



1.1480 300 1.750 350.3 32 --- --- 3701H
 400000 790 NIN 20 --- --- ---
 300 MHz 790 MHz 300 MHz 790 MHz 300 MHz 790 MHz 300 MHz 790 MHz

¹H NMR of *Exo, endo* bis adduct #2, (7-8)



1.750
4000.0
3.752
7.0

300
700
0
64

1.750
NNN
C

350.3
20
200

32
2511.1

-43.0

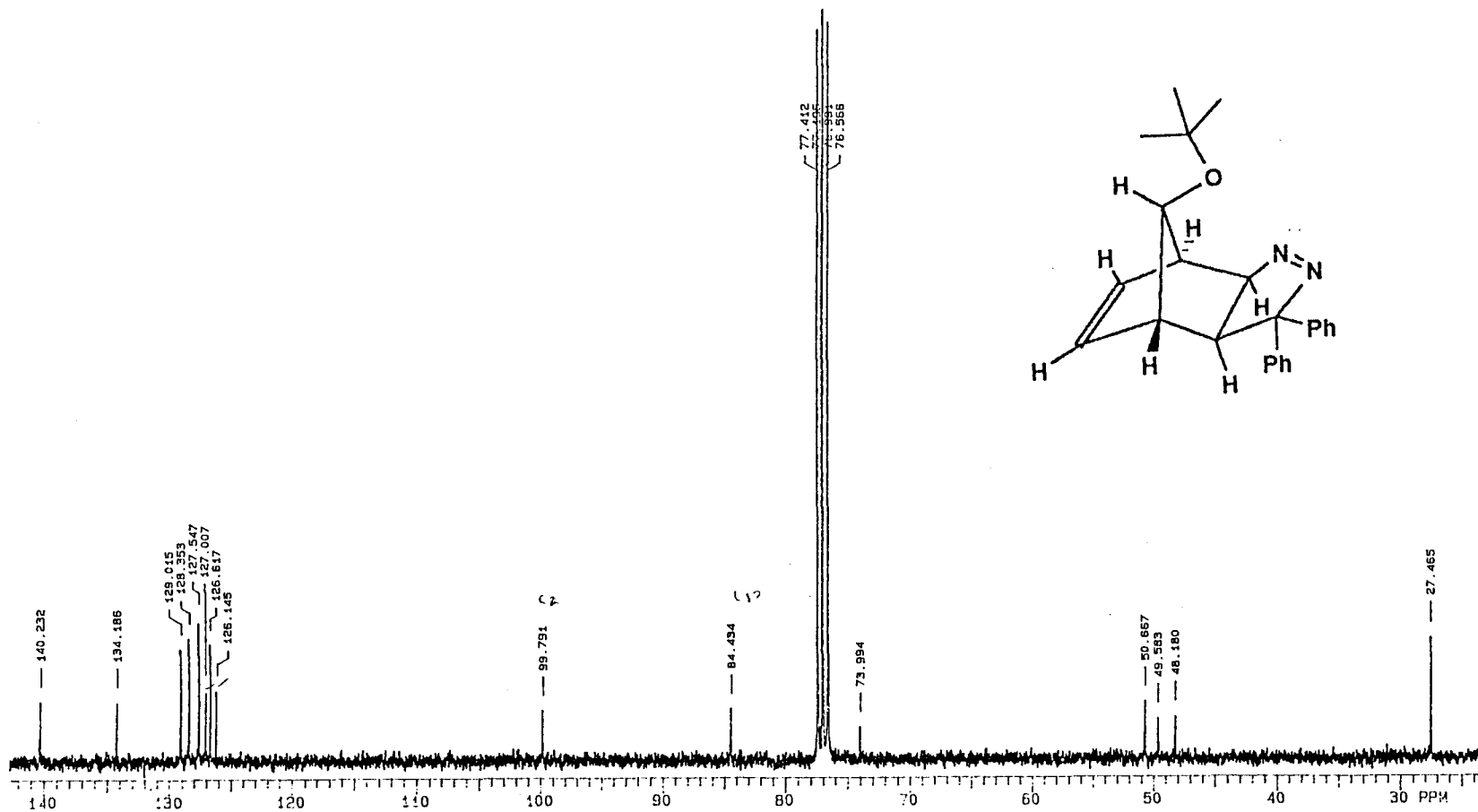
ST01H

CDCL3

6-28-91 SEE BIIP239
6-19 ENTRY PARTIALLY
ISOLATED A/X IMPURITY

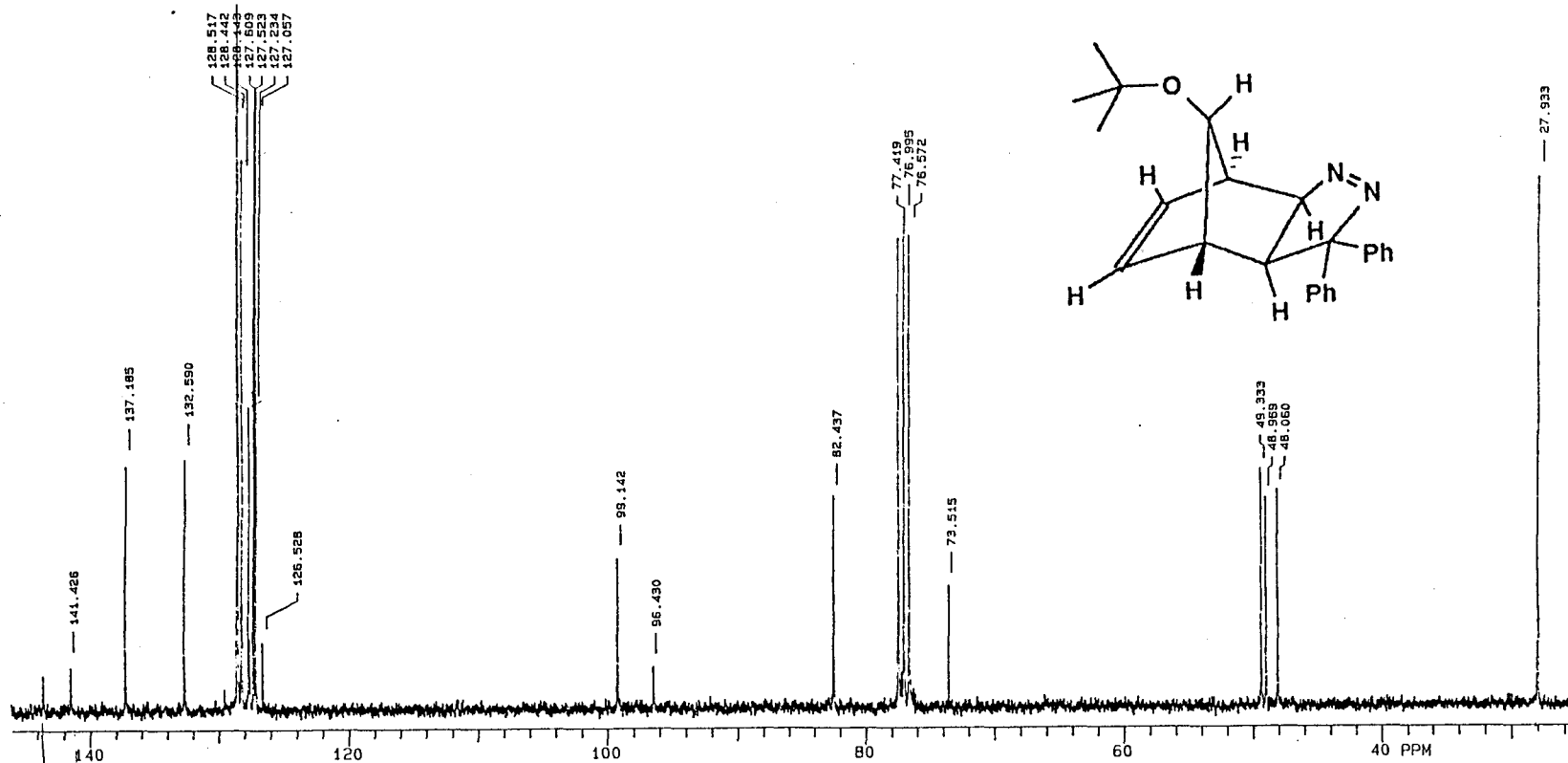
H
08-27-91
VXR 300

¹H NMR of *Exo, endo* bis adduct #3, (7-8)



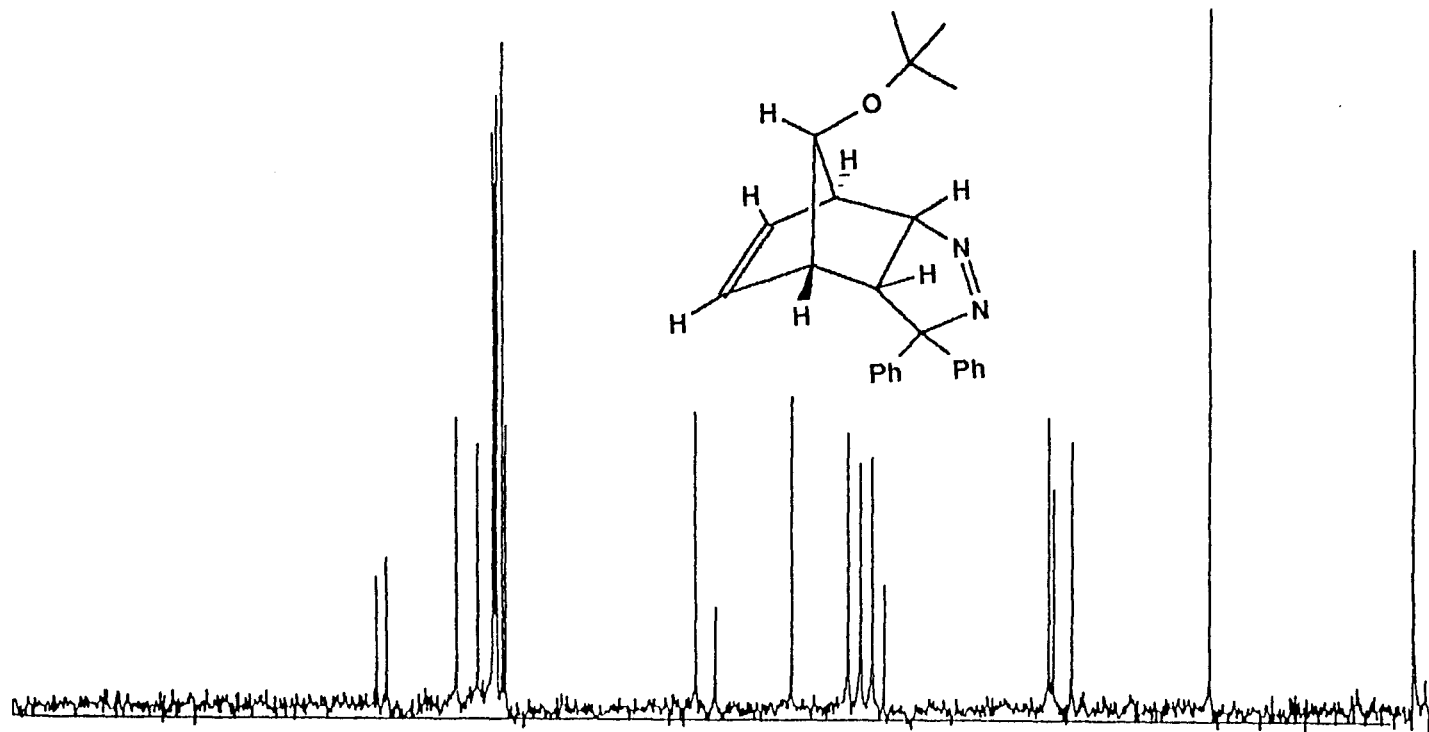
13.750	75	1.750	350.3	64	---	---	ST013C	
16501.7	700	YYY	5	1.000	---	---	SYN. EXO	C
1.639	0	S	9900	8973.3	1779.2			08-22-90
8.7	2241	17.5	64.0				CDCL3	VXR 300

¹³C NMR of *Syn*-10-*t*-butoxy-5,5-diphenyl-*exo*-3,4-diazatricyclo[5.2.1.0^{2,6}]deca-3,8-diene, (3)

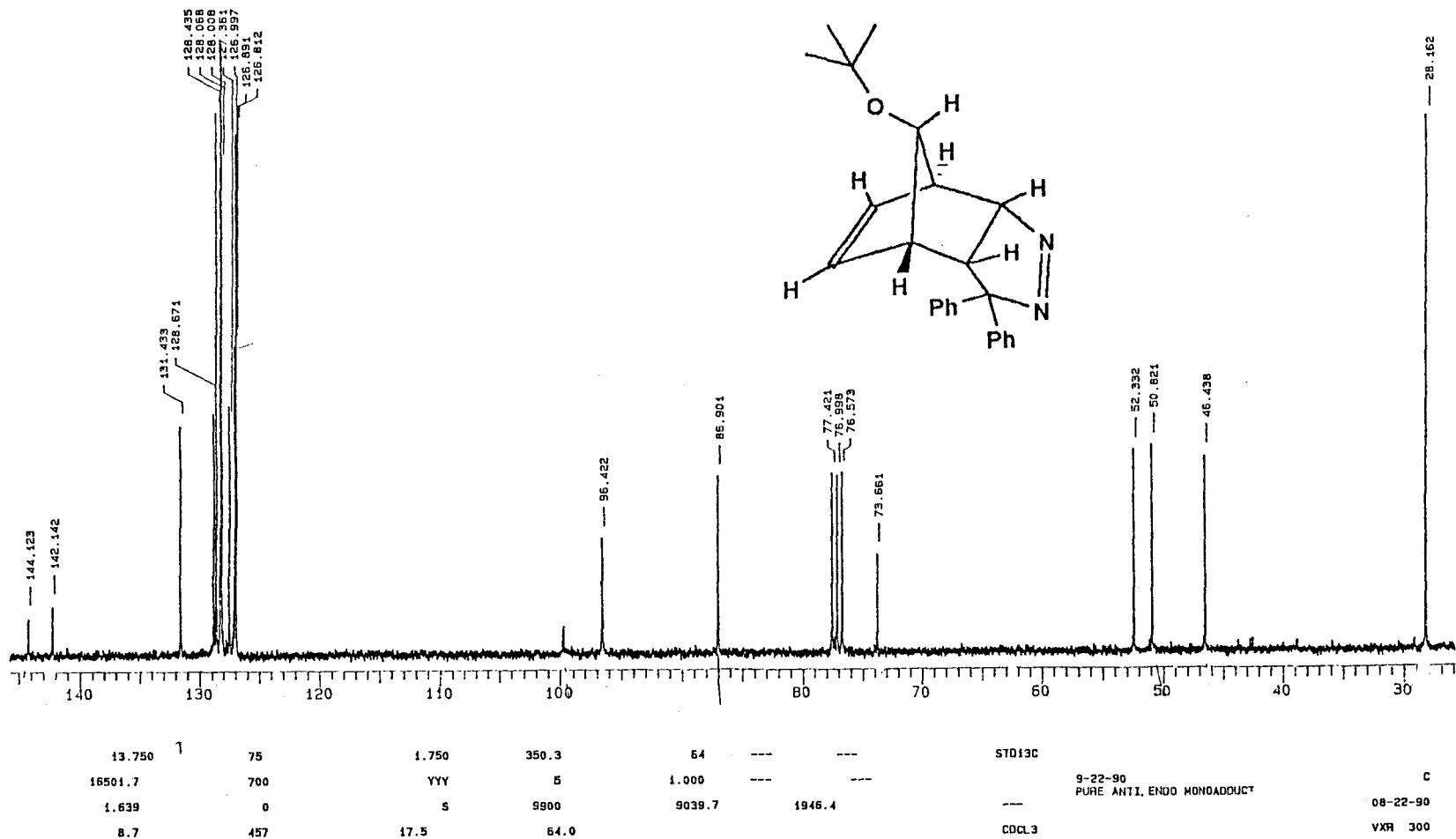


13.750	75	1.750	350.3	64	---	---	STD13C	
16501.7	700	YYY	5	1.000	---	---		ANTI, EXO MONOADDUCT
1.639	0	S	9900	9125.3	1882.5	---		08-29-90
0.7	1730	17.5	64.0				CDCL3	VXR 300

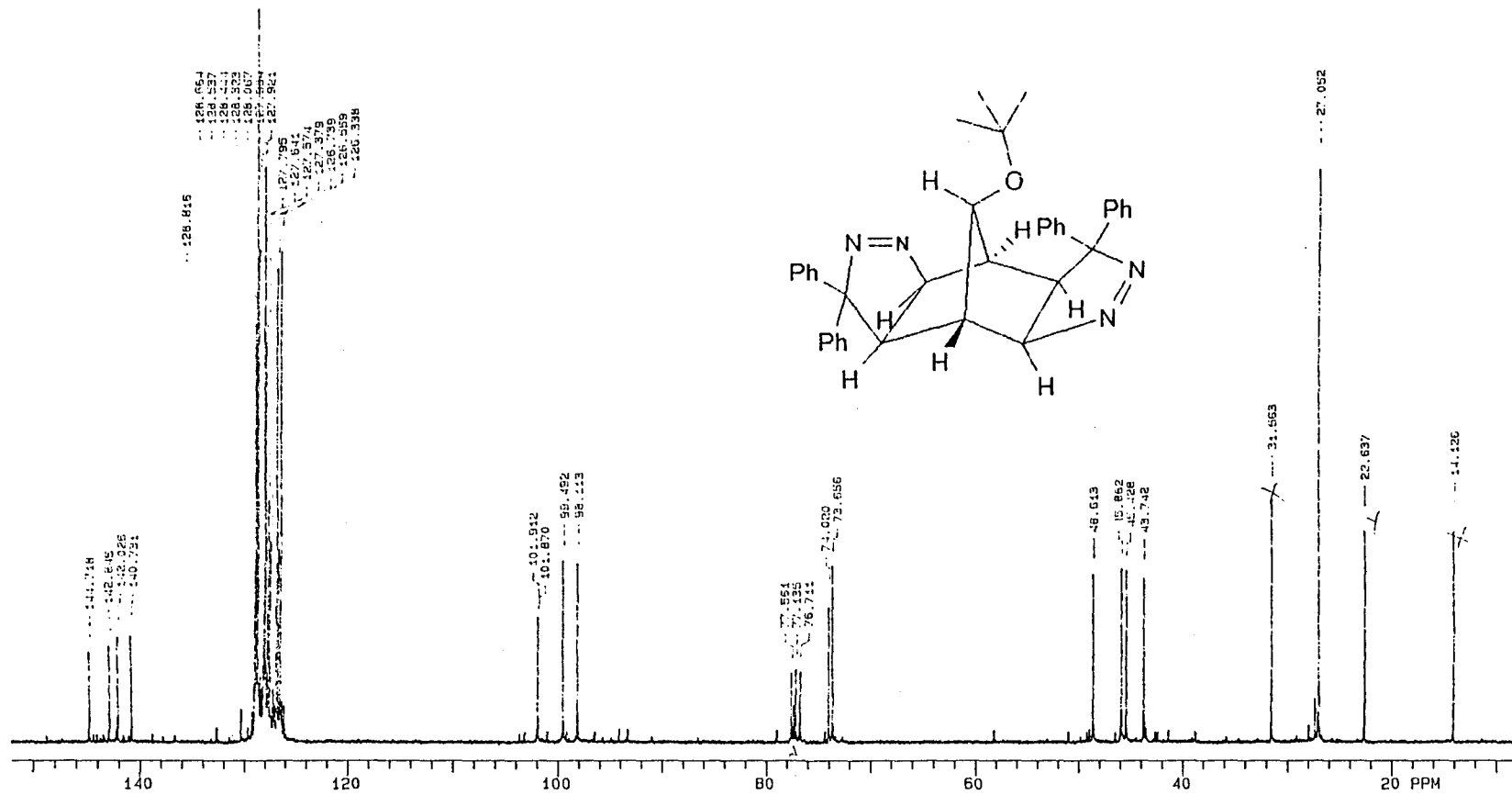
^{13}C NMR of *Anti*-10-*t*-butoxy-5,5-diphenyl-*exo*-3,4-diazatricyclo[5.2.1.0^{2,6}]deca-3,8-diene, (4)



^{13}C NMR of *Syn*-10-*t*-butoxy-5,5-diphenyl-*endo*-3,4-diazatricyclo[5.2.1.0^{2,6}]deca-3,8-diene, (5)

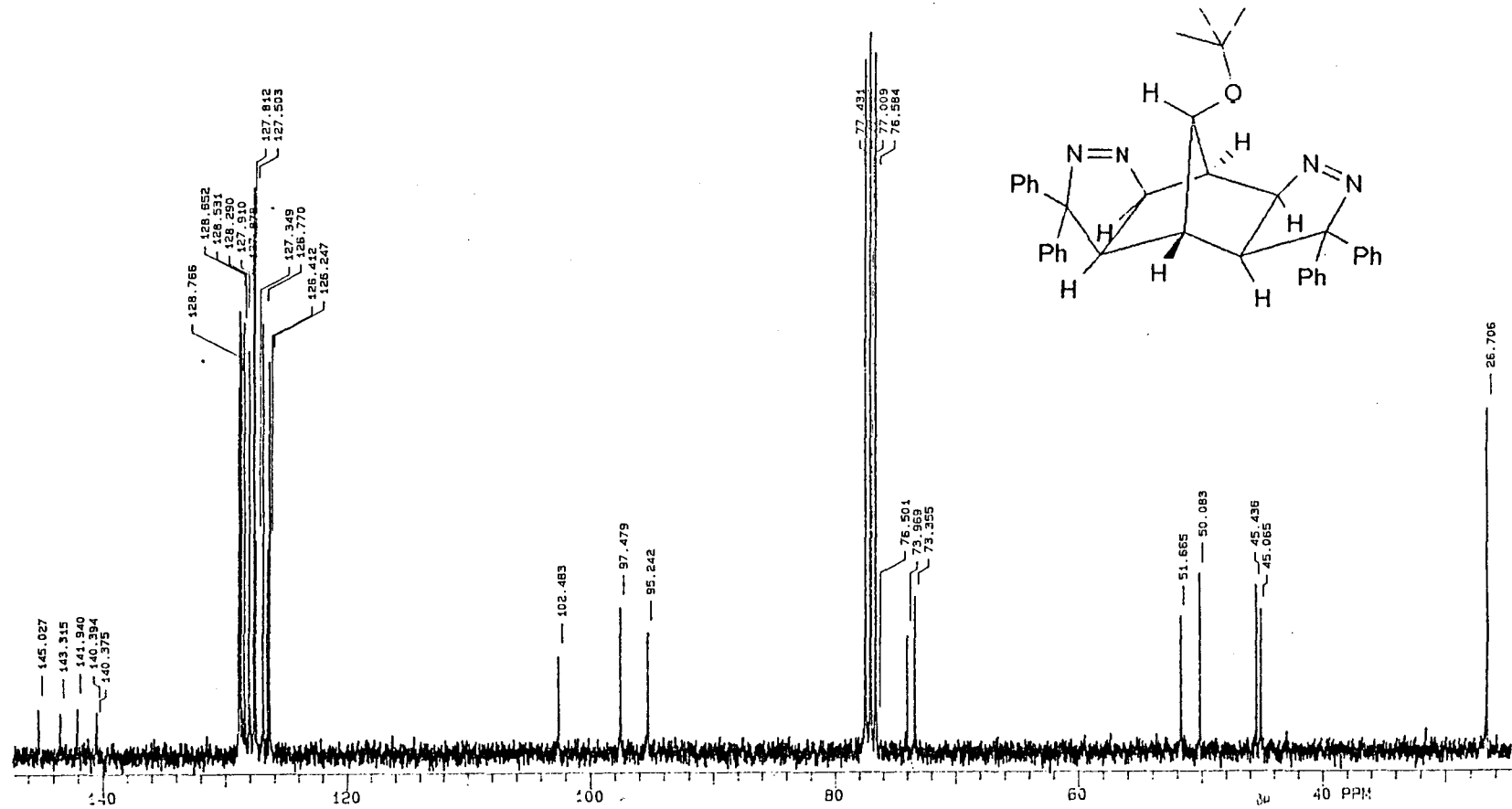


¹³C NMR of *Anti*-10-*t*-butoxy-5,5-diphenyl-*endo*-3,4-diazatricyclo[5.2.1.0^{2,6}]deca-3,8-diene, (6)



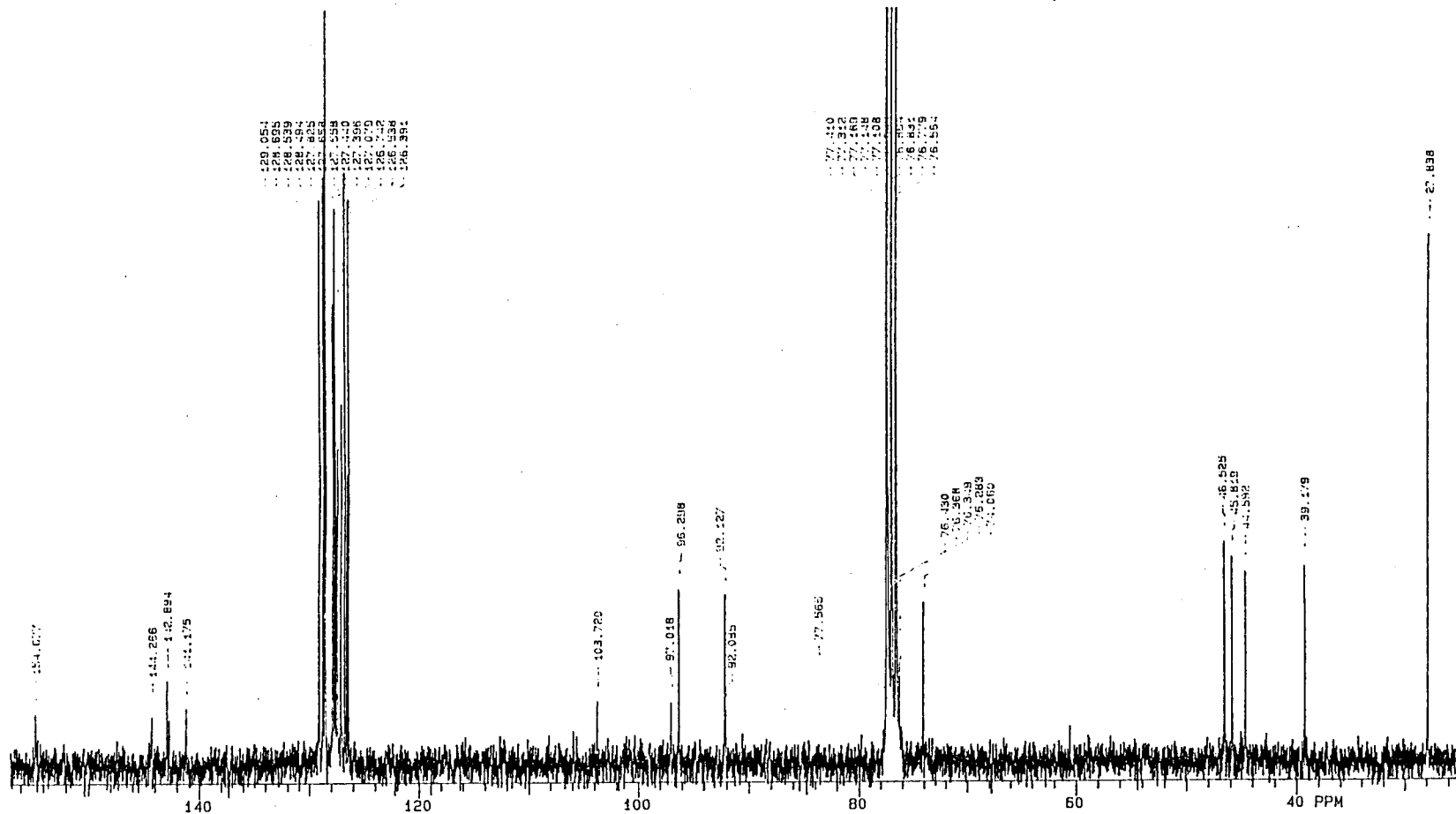
13.750	75	1.750	350.3	64	---	---	STD13C		
16501.7	700	YYY	0	1.000	---	---		7-21-91 SECOND EYE, EXO	BISXX2
1.639	0	S	8800	10839.1	619.4			BIS PRODUCT	07-24-91
8.7	1320	17.5	---				CDCL3		VXR 300

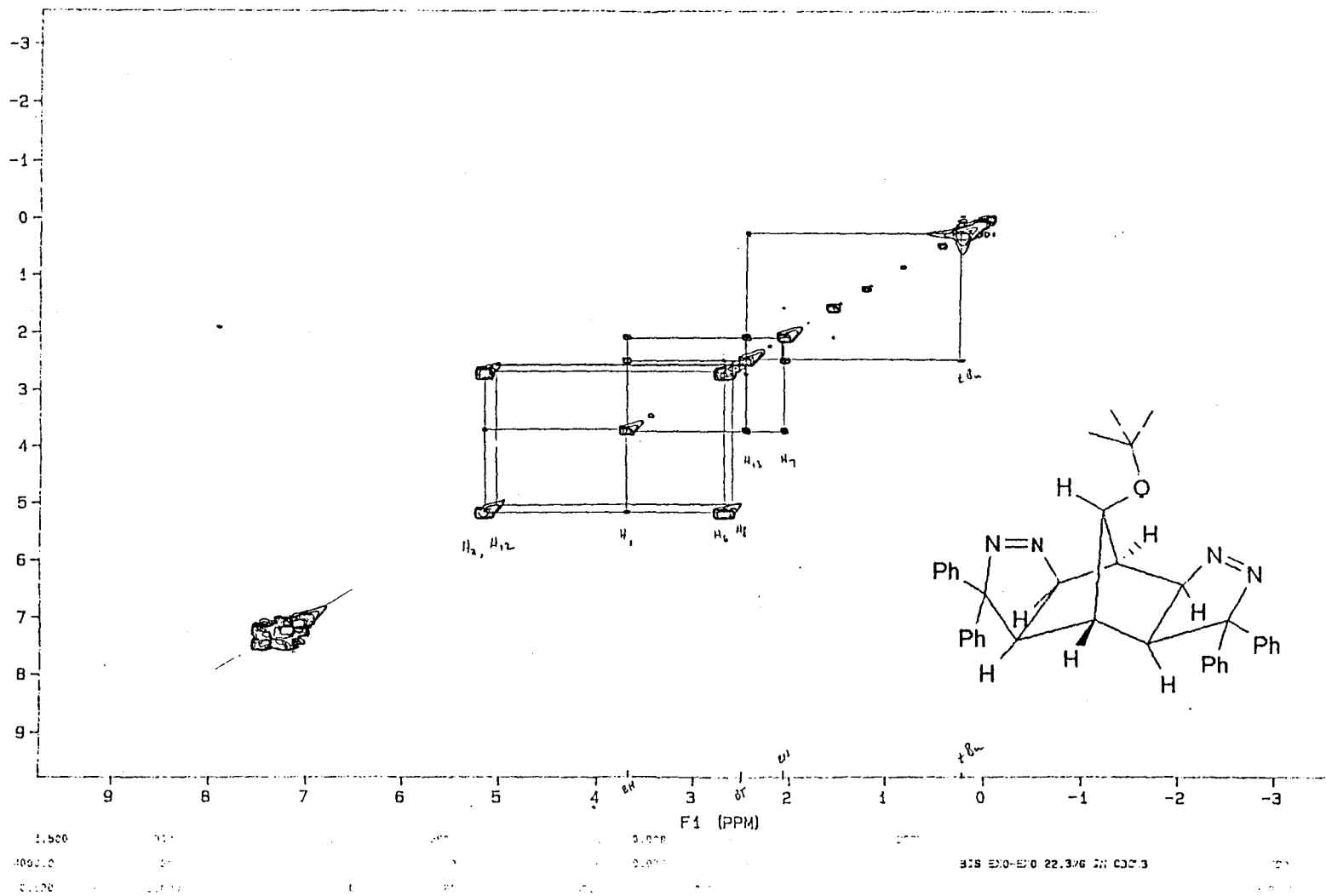
¹³C NMR of 13-t-butoxy-5,5,11,11-tetraphenyl-*exo,exo*-3,4,9,10-tetraazatetracyclo[5.5.1.0^{2,6}.0^{8,12}]trideca-3,9-diene (1)



13.750	75	1.750	350.3	64	---	---	ST013C	
16501.7	700	YYY	5	1.000	---	---	EXO,EXO BIS ADDUCT	C
1.639	0	S	9900	9234.6	1861.8	---	---	08-22-90
8.7	833	17.5	64.0			CDCL3		VXR 300

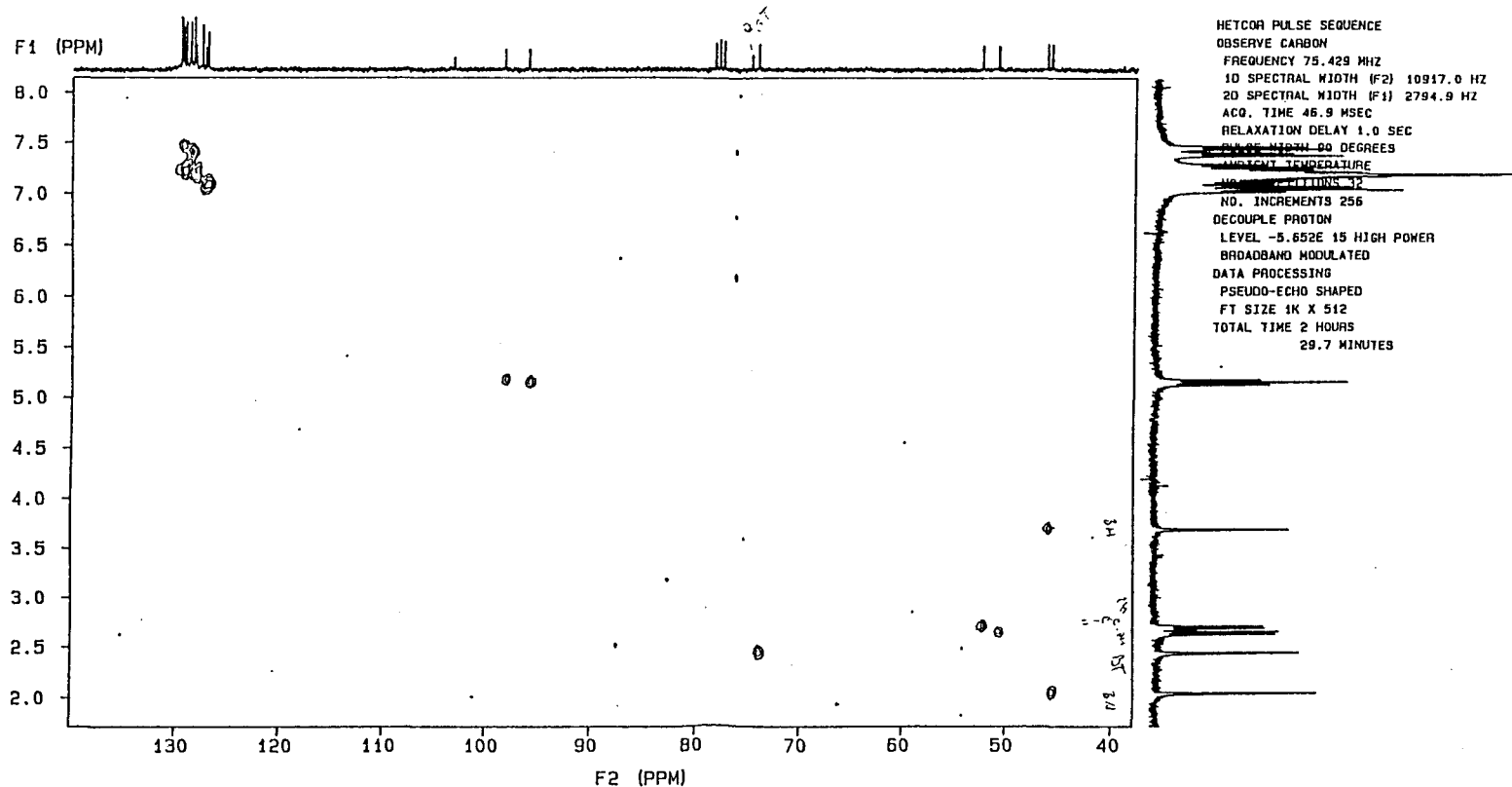
¹³C NMR of 13-t-butoxy-5,5,9,9-tetraphenyl-*exo,exo*-3,4,10,11-tetraazatetracyclo[5.5.1.0^{2,6}.0^{8,12}]trideca-3,10-diene, (2)





COSY 2D NMR of 13-t-butoxy-5,5,9,9-tetraphenyl-*exo,exo*-3,4,10,11-tetraazatetracyclo[5.5.1.0^{2,6}.0^{8,12}]trideca-3,10-diene, (2)

BIS-EXO-EXO-ADDUCT
EXP5 PULSE SEQUENCE: HETCOR
DATE 11-05-92
SOLVENT CDCL3
FILE HETCOR



HETCOR 2D NMR of 13-t-butoxy-5,5,9,9-tetraphenyl-*exo,exo*-3,4,10,11-tetraazatetracyclo[5.5.1.0^{2,6}.0^{8,12}]trideca-3,10-diene, (2)

REFERENCES

1. Huisgen, R. Angew. Chem. Int. Ed. Engl., **1963**, 2, 633.
2. Berson, J.A.; Hamlet, Z.; Mueller, W.A. J. Am. Chem. Soc., **1962**, 84, 297.
3. Schneider, H.-J.; Sangwan, N.K. Angew. Chem. Int. Ed. Engl., **1987**, 896.
4. Sangwan, N.K.; Schneider, H.-J. J. Chem. Soc. Perkin Trans. II., **1989**, 1223.
5. Cativiela, C.; Mayoral, J.A.; Avenoza, A.; Peregrina, J.M.; Roy, M.A. J. Phys. Org. Chem., **1990**, 3, 414.
6. Cativiela, C.; Garcia, J.I.; Mayoral, J.A.; Avenoza, A.; Peregrina, J.M.; Roy, M.A. J. Phys. Org. Chem., **1991**, 4, 48.
7. Braun, R.; Schuster, F.; Sauer, J. Tetrahedron Lett., **1986**, 27, 1285.
8. (a) Gajewski, J.J.; Grieco, P.A.; Gee, K.R.; Olson, L.P.; Montgomery, L.K., Department of Chemistry, Indiana University, Bloomington IN, 47405, Personal Communication. (b) Gajewski, J.J. J. Org. Chem., **1992**, 57, 5500.
9. Huisgen, R. Angew. Chem. Int. Ed. Engl., **1963**, 2, 565.
10. (a) Sustmann, R. Tetrahedron Lett., **1971**, 2717. (b) Sustmann, R. Tetrahedron Lett., **1971**, 2721. (c) Salem, L. J. Am. Chem. Soc., **1968**, 90, 543, 553.
11. Turner, R.B.; Meador, W.R.; Winkler, R.E. J. Am. Chem. Soc., **1957**, 79, 4116.
12. Huisgen, R. *1,3-Dipolar Cycloaddition Chemistry*; Padwa, A., Ed.; John Wiley: New York, 1984; Vol.1, p 3.
13. McLean, S.; Findlay, D.M. Tetrahedron Lett., **1969**, 2219.
14. (a) Wilt, J.W.; Sullivan, D.R. J. Org. Chem., **1975**, 40, 1036. (b) Sullivan, D.R., Ph.D. Dissertation, 1973, Loyola University of Chicago.
15. (a) Kamlet, M.; Taft, R.W. J. Am. Chem. Soc., **1976**, 98, 377. (b) Taft, R.W.; Kamlet, M. J. Am. Chem. Soc., **1976**, 98, 2886. (c) Kamlet, M.J.; Abboud, J.-L.M.; Taft, R.W. J. Am. Chem. Soc., **1977**, 99, 6027. (d) Taft, R.W.; Abboud, J.-L.M.; Kamlet, M.J. J. Am. Chem. Soc., **1981**, 103, 1080. (e) Kamlet, M.J.; Carr, P.W.; Taft, R.W.; Abraham, M.H. J. Am. Chem. Soc., **1981**, 103, 6062. (f) Taft, R.W., "Linear Solvation Energy Relationships" In *Progress in Physical Organic Chemistry*; Taft, R.W., Ed; Wiley-Interscience: New York, 1981; Vol. 13, p 485ff. (g) Taft, R.W.; Shuely, W.J.; Doherty, R.M.; Kamlet, M.J. J. Org. Chem., **1988**, 53, 1737.

16. (a) Kirkwood, J.G. J. Chem. Phys., **1934**, 2, 351 (b) This equation is actually only one of the terms in a more extensive equation given in reference 1(a), with $n = 1$, but it is in this form that it is widely known.
17. (a) Laidler, K.J.; Eyring, H. Ann. N. Y. Acad. Sci., **1940**, 39, 303. (b) Laidler, K.J. *Chemical Kinetics*; McGraw-Hill: New York, 1950; Chapter 5.
18. Kwart, H.; Lilley, T.H. J. Org. Chem., **1978**, 43, 1978.
19. (a) Steiner, G.; Huisgen, R. Tetrahedron Lett., **1973**, 3759. (b) Huisgen, R.; Steiner, G. J. Am. Chem. Soc., **1973**, 95, 5056.
20. Richardson, M.; Soper, F.G. J. Chem. Soc., **1929**, 1873.
21. Glasstone, S. J. Chem. Soc., **1936**, 723.
22. (a) Hildebrand, J.H.; Scott, R.L. *The Solubility of Nonelectrolytes* 3rd ed.; Dover: New York, 1964. (b) Hildebrand, J.H.; Prausnitz, J.M.; Scott, R.L. *Regular and Related Solutions*; Van Nostrand-Reinhold: Princeton, 1970.
23. (a) Scatchard, G. Chem. Rev. **1931**, 8, 321. (b) Scatchard, G. Chem. Rev., **1932**, 10, 229.
24. Wong, K.F.; Eckert, C.A. Trans. Farad. Soc., **1970**, 66, 2313.
25. (a) Meyer, K.H. Chem. Ber., **1914**, 47, 826. (b) Meyer, K.H. Chem. Ber., **1920**, 53, 1410. (c) Meyer, K.H. Chem. Ber., **1921**, 54, 579.
26. (a) Gutmann, V.; Wychera, E. Inorg. Nucl. Chem. Lett., **1966**, 2, 257. (b) Gutmann, V., Coordination Chem. Rev., **1967**, 2, 239. (c) Gutmann, V.; Scherhauser, A. Monatsh. Chem., **1968**, 99, 335. (d) Gutmann, V. Chimia, **1969**, 23, 285. (e) Gutmann, V. *Coordination Chemistry in Non-Aqueous Solvents*; Springer, Wien: New York, 1968.
27. (a) Eliel, E.L. Pure Appl. Chem., **1971**, 25, 509. (b) Eliel, E.L. Supplement to Pure Appl. Chem., **1971**, p219ff. (c) Eliel, E.L.; Hofer, O. J. Am. Chem. Soc., **1973**, 95, 8041.
28. (a) Maria, P.-C.; Gal, J.-F. J. Phys. Chem., **1985**, 89, 1296. (b) Elégant, L.; Fratini, G.; Gal, J.-F.; Maria, P.-C. J. Calorim. Anal. Therm., **1980**, 11, 3/21/1...3/21/9.
29. Persson, I. Pure Appl. Chem., **1986**, 58, 1153.
30. Drago, R.S.; Wayland, B.B. J. Am. Chem. Soc., **1965**, 87, 3751.
31. (a) Leo, A.; Hansch, C.; Elkins, D. Chem. Rev., **1971**, 71, 525. (b) Hansch, C.; Leo, A. *Substituent Constants for Correlation Analysis in Chemistry and Biology*; Wiley-Interscience: New York, 1979. (c) Leo, A. J. Chem. Soc. Perkin Trans. II, **1983**, 825.

32. (a) Abraham, M.H.; Grellier, P.L.; McGill, R.A. J. Chem. Soc. Perkin Trans. II, 1988, 339. (b) Abraham, M.H. J. Am. Chem. Soc., 1982, 104, 2085.
33. Marcus, Y. J. Phys. Chem., 1987, 91, 4422.
34. (a) Grunwald, E.; Winstein, S. J. Am. Chem. Soc., 1948, 70, 846. (b) Winstein, S.; Grunwald, E.; Jones, H.W. J. Am. Chem. Soc., 1951, 73, 2700. (c) Fainberg, A.H.; Winstein, S., J. Am. Chem. Soc., 1956, 78, 2770. (d) Fainberg, A.H.; Winstein, S. J. Am. Chem. Soc., 1957, 79, 1597, 1602, 1608. (e) Winstein, S.; Fainberg, A.H.; Grunwald, E. J. Am. Chem. Soc., 1957, 79, 4146, 5937. (f) Smith, S.G.; Fainberg, A.H.; Winstein, S. J. Am. Chem. Soc., 1961, 83, 618.
35. (a) Winstein, S.; Grunwald, E.; Jones, H.W. J. Am. Chem. Soc., 1951, 73, 2700. (b) Winstein, S.; Fainberg, A.H.; Grunwald, E. J. Am. Chem. Soc., 1957, 79, 4146.
36. (a) Bentley, T.W.; Schadt, F.L.; Schleyer, P.v.R. J. Am. Chem. Soc., 1972, 94, 992. (b) Bentley, T.W.; Bowen, C.T.; Morten, D.H.; Schleyer, P.v.R. J. Am. Chem. Soc., 1981, 103, 5466.
37. Swain, C.G.; Mosely, R.B.; Bown, D.E. J. Am. Chem. Soc., 1955, 77, 3731.
38. (a) Peterson, P.E.; Walter, F.J. J. Am. Chem. Soc., 1972, 94, 991. (b) Peterson, P.E.; Vidrine, D.W.; Waller, F.J.; Henrichs, P.M.; Magaha, S.; Stevens, B. J. Am. Chem. Soc., 1977, 99, 7968.
39. Smith, S.G.; Fainberg, A.H.; Winstein, S. J. Am. Chem. Soc., 1961, 83, 618.
40. Drougard, Y.; Decroocq, D. Bull. Soc. Chem. Fr., 1969, 2972.
41. (a) Gielen, M.; Nasielski, J. J. Organomet. Chem., 1963, 1, 173. (b) Gielen, M.; Nasielski, J. J. Organomet. Chem., 1967, 7, 273.
42. (a) Kosower, E.M. J. Am. Chem. Soc., 1958, 80, 3253. (b) Kosower, E.M. *An Introduction to Physical Organic Chemistry*; Wiley: New York, 1968; p 293ff.
43. Brownstein, S. Can. J. Chem., 1960, 38, 1590.
44. (a) Dimroth, K.; Reichardt, C.; Siepman, T.; Bohlmann, F. Liebigs Ann. Chem., 1963, 661, 1. (b) Reichardt, C. Liebigs Ann. Chem., 1971, 752, 64. (c) Reichardt, C.; Harbusch-Görnet, E. Liebigs Ann. Chem., 1983, 721.
45. Brooker, L.G.S.; Craig, A.C.; Heseltine, D.W.; Jenkins, P.W.; Lincoln, L.L. J. Am. Chem. Soc., 1965, 87, 2443.
46. (a) Dähne, S; Schob, F.; Nolte, K.-D.; Radeaglia, R. Ukr. Khim. Zh. (Russ Ed.), 1975, 41, 1170. (b) Chem Abstr., 84, 43086j (1976).
47. (a) Dubois, J.-E.; Goetz, E.; Bienvenüe, A. Spectrochim. Acta, 1964, 20, 1815. (b) Dubois, J.-E.; Bienvenüe, A. J. Chim. Phys., 1968, 65, 1259.

48. (a) Janowski, A.; Turowska, -Tyrk, I.; Wrona, P.K. J. Chem. Soc. Perkin Trans. II **1985**, 821. (b) Mukerjee, P.; Ramachandran, C.; Pyter, R.A. J. Phys. Chem., **1982**, 86, 3189.
49. Walter, W.; Bauer, O.H. Liebigs Ann. Chem., **1977**, 421.
50. Walther, D. J. Prakt. Chem., **1974**, 316, 604.
51. Manuta, D.M.; Lees, A.J. Inorg. Chem., **1983**, 22, 3825.
52. (a) Zhmyreva, I.A.; Zelinskii, V.V.; Kolobkov, V.P.; Krasnitskaya, N.D. Dokl. Akad. Nauk SSSR, Ser. Khim., **1959**, 129, 1089. (b) Chem Abstr. 55, 26658e (1961). (c) Langhals, H. Tetrahedron, **1987**, 43, 1771.
53. Dong, D.C.; Winnik, M.A. Can. J. Chem., **1984**, 62, 2560.
54. Allerhand, A.; Schleyer, P.v.R. J. Am. Chem. Soc., **1963**, 85, 371.
55. Kagiya, T.; Sumida, Y.; Inoue, T. Bull. Chem. Soc. Jpn., **1968**, 41, 767.
56. Burden, A.G.; Collier, G.; Shorter, J. J. Chem. Soc. Perkin Trans. II, **1976**, 1627.
57. (a) Koppel, I.A.; Paju, V.A. Reakts. Sposobnost. Org. Soedin., **1974**, 11, 121. (b) Chem Abstr. 82, 42805q (1975). (c) Koppel, I.A.; Palm, V.A. *The Influence of Solvent on Organic Reactivity*; In *Advances in Linear Free Energy Relationships*; Chapman, N.B. and Shorter, J., Eds.; Plenum Press: New York, 1972; Chapter 5, p 203ff.
58. Nicolet, P.; Laurence, C.; Lucon, M. J. Chem. Soc. Perkin Trans. II, **1987**, 483.
59. Brownlee, R.T.C.; Dayal, S.K.; Lyle, J.L.; Taft, R.W. J. Am. Chem. Soc., **1972**, 94, 7208.
60. (a) Mayer, U.; Gutmann, V.; Gerger, W. Monatsh. Chem., **1975**, 106, 1235. (b) Mayer, U.; Gutmann, V.; Gerger, W. Monatsh. Chem., **1977**, 108, 489, 757. (c) Gutmann, V. Electrochimica Acta, **1976**, 21, 661. (d) Gutmann, V. CHEMTECH, **1977**, 7, 255. (e) Schmid, R. J. Solution Chem., **1983**, 12, 135. (f) R. Schmid, R.; Sapunov, V.N. *Non-Formal Kinetics in Search of Chemical Reaction Pathways*; Verlag Chemie: Weinheim, 1982. (g) Schmid, R. J. Solution Chem., **1983**, 12, 135. (h) Mayer, U. *NMR Spectroscopic Studies on Solute-Solvent and Solute-Solute Interactions In Ions and Molecules in Solution*; Tanaka, N.; Ohtaki, H.; Tamamushi, R., Eds.; Elsevier: Amsterdam, 1983; p 219ff.
61. Knauer, B.R.; Napier, J.J. J. Am. Chem. Soc., **1976**, 98, 4395.
62. Fowler, F.W.; Katritzky, A.R.; Rutherford, R.J.D. J. Chem. Soc. Part B, **1971**, 460.

63. (a) Koppel, A.; Palm, V.A. Reakts. Sposobnost. Org. Soedin., **1971**, 8, 291. (b) Koppel, I.A.; Palm, V.A. *The Influence of the Solvent on Organic Reactivity In Advances in Linear Free Energy Relationships*; Chapman, I.A.; Shorter, J., Eds.; Plenum Press: New York, 1972; Chapter 5, p 203ff.
64. (a) Krygowski, T.M.; Fawcett, W.R. J. Am. Chem. Soc., **1975**, 97, 2143. (b) Krygowski, T.M.; Fawcett, W.R. Aust. J. Chem., **1975**, 28, 2115. (c) Krygowski, T.M.; Fawcett, W.R. Can. J. Chem., **1976**, 54, 3283.
65. Buncl, E.; Rajagopal, S. Acc. Chem. Res., **1990**, 23, 226.
66. Mayer, U. Monatsh. Chem., **1978**, 109, 421, 775.
67. Swain, C.G.; Swain, M.S.; Powell, A.L.; Alunni, S. J. Am. Chem. Soc., **1983**, 105, 502.
68. Dougherty, R.C. Tetrahedron Lett., **1975**, 385.
69. Glikberg, S.; Marcus, Y. J. Solution Chem., **1983**, 12, 255.
70. (a) Heublin, G.; Hallpap, P.; Wondraczek, R.; Akler, P. Z. Chem., **1980**, 20, 11. (b) Heublin, G. J. Macromol. Sci. Part A, **1985**, 22, 1277.
71. Kupfer, M.; Abraham, W. Z. Phys. Chem.(Liebig), **1986**, 267, 705.
72. For a thorough discussion of single and multiple solvent parameter treatments, see Reichardt, C. *Solvents and Solvent Effects in Organic Chemistry*, 2nd ed. VCH Verlag: Weinheim, 1988.
73. Oshima, T.; Arikata, S.; Nagai, T. Chem Res.(S), **1981**, 204.
74. (a) Huisgen, R. Pure Appl. Chem., **1980**, 52, 2283. (b) k_2 refers to a bimolecular rate constant.
75. Breslow, R.; Rideout, D. J. Am. Chem. Soc., **1980**, 102, 7816.
76. Breslow, R.; Rizzo, C.J. J. Am. Chem. Soc., **1991**, 113, 4340.
77. Breslow, R.; Maitra, U.; Rideout, D. Tetrahedron Lett., **1983**, 24, 1901.
78. Breslow, R. Acc. Chem. Res., **1991**, 24, 159.
79. Grieco, P.A.; Garner, P.; He, Z. Tetrahedron Lett., **1983**, 24, 1897.
80. Grieco, P.; Yoshida, K.; Garner, P. J. Org. Chem., **1983**, 48, 3137.
81. (a) Grieco, P.A.; Nunes, J.J.; Gaul, M.D. J. Am. Chem. Soc., **1990**, 112, 4595. (b) Forman, M.A.; Dailey, W.P. J. Am. Chem. Soc., **1991**, 113, 2761.

82. Breslow, R.; Guo, T. J. Am. Chem. Soc., **1988**, 110, 5613.
83. Kadaba, P.K. Tetrahedron, **1969**, 25, 3053.
84. Burrage, M.E.; Cookson, R.C.; Gupte, S.S.; Stevens, I.D.R. J. Chem. Soc. Perkin Trans. II, **1975**, 1325.
85. Huisgen, R.; Reissig, H.-U.; Huber, H.; Voss, S. Tetrahedron Lett., **1979**, 32, 2987.
86. (a) Firestone, R.A.; Christensen, B.G. Tetrahedron Lett., **1973**, 389. (b) Firestone, R.A.; Vitale, M.A. J. Org. Chem., **1981**, 46, 2160. (c) Firestone, R.A.; Saffar, S.G. J. Org. Chem., **1983**, 48, 4783.
87. Blake, J.F.; Jorgenson, W.L. J. Am. Chem. Soc., **1991**, 113, 7430.
88. Van Eldik, R.; Asano, T.; LeNoble, W.J. Chem. Rev., **1989**, 89, 549.
89. McCabe, J.R.; Eckert, C.A. Acc. Chem. Res., **1974**, 7, 251.
90. Swieton, G.; Jouanne, J.v.; Kelm, H. J. Org. Chem., **1983**, 48, 1035.
91. Raistrick, B.; Sapiro, A.H.; Newitt, D.M. J. Chem. Soc., **1939**, 1761.
92. Walling, C.; Peisach, J. J. Am. Chem. Soc., **1958**, 80, 5819.
93. Dauben, W.G.; Kozikowski, A.D. J. Am. Chem. Soc., **1974**, 96, 3664.
94. Issacs, N.S.; Rannala, E. J. Chem. Soc. Perkin Trans. II, **1975**, 1555.
95. Ouellette, R.J.; Williams, S.H. J. Am. Chem. Soc., **1971**, 93, 466.
96. Snyder, J.P.; Harpp, D.N. J. Am. Chem. Soc., **1976**, 98, 7821.
97. Huisgen, R.; Reissig, H.-U.; Huber, H. J. Am. Chem. Soc., **1979**, 101, 3647.
98. (a) Firestone, R.A. J. Org. Chem., **1968**, 33, 2285. (b) Firestone, R.A. Tetrahedron, **1977**, 33, 3009.
99. Huisgen, R. J. Org. Chem., **1968**, 33, 2291.
100. Buchner, E. Chem. Ber., **1888**, 21, 2637.
101. Smith, L.I. Chem. Rev., **1938**, 23, 193.
102. (a) Eistert, B. Angew. Chem., **1941**, 54, 124. (b) Young, W.G., Andrews, L.J.; Lindenbaum, S.L.; Cristol, S.J. J. Am. Chem. Soc., **1944**, 66, 810. (c) Huisgen, R. Angew. Chem., **1955**, 67, 439.

103. (a) Hoffmann, R.; Woodward, R.B. J. Am. Chem. Soc., 1965, **87**, 2046, 4388. (b) Woodward, R.B.; Hoffmann, R. Angew. Chem. Int. Ed. Engl., 1969, **8**, 781.
104. (a) Houk, K.N. Acc. Chem. Res., 1975, **8**, 361. (b) Houk, K.N.; Sims, J.; Watts, C.R.; Luskus, L.J. J. Am. Chem. Soc., 1973, **95**, 7303.
105. Bastide, J.; Ghandour, N.EL.; Henri-Rousseau, O. Tetrahedron Lett., 1972, **41**, 4225.
106. Koga, N.; Ozawa, T.; Morokuma, K. J. Phys. Org. Chem., 1990, **3**, 519.
107. Alder, K.; Stein, G.; Scheider, S. Liebigs Ann. Chem., 1935, **515**, 185.
108. Huisgen, R.; Möbius, L.; Müller, G.; Stangl, H.; Szeimies, G.; Vernon, J.M. Chem. Ber., 1965, **98**, 3992.
109. The authors chose a different nomenclature such that syn=exo and anti=endo. This author has converted their nomenclature for the sake of clarity.
110. DeMicheli, C.; Gandolfi, R.; Oberti, R. J. Org. Chem., 1980, **45**, 1209.
111. Klumpp, G.W.; Veeffkind, A.H.; deGraaf, W.; Bickelhaupt, F. Liebigs Ann. Chem., 1967, **706**, 47.
112. Halton, B.; Woolhouse, A.D. Aust. J. Chem., 1973, **26**, 619.
113. Franck-Neumann, M.; Sedrati, M. Angew. Chem. Int. Ed. Engl., 1974, **13**, 606.
114. Wilt, J.W.; Peeran, M. J. Org. Chem., 1986, **51**, 2618.
115. Wilt, J.W.; Roberts, W.N. J. Org. Chem., 1978, **43**, 170.
116. Saito, T.; Motoki, S. J. Org. Chem., 1979, **44**, 2493.
117. Wilt, J.W.; Malloy, T.P. J. Org. Chem., 1973, **38**, 277.
118. Filipescu, N.; DeMember, J.R. Tetrahedron, 1968, **24**, 5181.
119. (a) McLean, S.; Findlay, D.M. Tetrahedron Lett., 1969, **27**, 2219. (b) Findlay, D.; Roy, M.; McClean, S. Can. J. Chem., 1972, **50**, 3186.
120. Stille, J.K.; Frey, D.A. J. Am. Chem. Soc., 1959, **81**, 4273.
121. (a) Lidov, R., Chem. Abstr., 1954, **48**, 2769, (1953). (b) Delacey, T.P.; Kennard, C.H.L. J. Chem. Soc. Perkin Trans. II, 1972, 2153. (x-ray structure).
122. Fliege, W.; Huisgen, R. Liebigs Ann. Chem., 1973, 2038.
123. Battiste, M.A.; Timberlake, J.F.; Malkus, H. Tetrahedron Lett., 1976, 2529.

124. Byrne, L.T.; Rye, A.R.; Wehe, D. Aust. J. Chem., 1974, 27, 1961.
125. Mazzaocchi, P.H.; Stahly, B.; Dodd, J.; Rondan, N.G.; Domelsmith, L.N.; Rozeboom, M.D.; Caramella, P.; Houk, K.N. J. Am. Chem. Soc., 1980, 102, 6482.
126. Houk, K.N.; Mueller, P.H.; Wu, Y.-D. Tetrahedron Lett., 1990, 7285.
127. Houk, K.N.; Wu, Y.-D.; Mueller, P.H. Tetrahedron Lett., 1990, 7289.
128. DalBola, L.; DeAmicila, M.; DeMicheli, C.; Gandolfi, R.; Houk, K.N. Tetrahedron Lett., 1989, 30, 807.
129. Freeman, F. Chem. Rev., 1975, 75, 439, and references therein.
130. Wilt, J.W.; Narutis, V.P. J. Org. Chem., 1979, 44, 4899.
131. Baird, W.C.; SurrIDGE, J.H. J. Org. Chem., 1972, 37, 1182.
132. Ph.D. dissertation, Ramakrisnan Subramanian, Loyola University of Chicago, 1990.
133. Cieplak, A.S. J. Am. Chem. Soc., 1981, 103, 4540.
134. (a) Hahn, J.M.; le Noble, W.J. J. Am. Chem. Soc., 1992, 114, 1917. (b) see also Cheung, C.K.; Tseng, L.T.; Lin, M.-H.; Srivastava, S.; le Noble, W.J. J. Am. Chem. Soc., 1986, 108, 1598.
135. Suzuki, T.; Li, Q.; Khemani, K.C.; Wudl, F.; Almarsson, Ö. Science, 1991, 254, 1186.
136. Bianchi, G.; DeMicheli, C.; Gandolfi, R. Angew. Chem. Int. Ed. Engl., 1979, 18, 721, and references cited therein.
137. Texier, F.; Bourgois, J. Heterocycl. Chem., 1975, 505.
138. Bougois, J.; Tonnard, F.; Texier, F. Bull. Soc. Chim. Fr., 1976, 2025.
139. (a) Regitz, M. Angew. Chem., 1967, 79, 786. (b) Regitz, M. Angew. Chem. Int. Ed. Engl., 1967, 6, 733. (c) Regitz, M. Synthesis, 1972, 351.
140. Franck-Neumann, M.; Buchecker, C. Tetrahedron Lett., 1969, 2659.
141. Aue, D.H.; Helwig, G.S. Tetrahedron Lett., 1974, 721.
142. Carpenter, W.R.; Haymaker, A.; Moore, D.W. J. Org. Chem., 1966, 31, 789.
143. (a) Pocar, D.; Stradi, R. Ann. Chim (Rome), 1971, 61, 161. (b) Pocar, D.; Trimarco, P. J. Chem. Soc. Perkin Trans., 1976, 622. (c) Dalla Croce, P.; Stradi, R. Tetrahedron, 1977, 33, 865.
144. Kucera, J.; Janousek, Z.; Arnold, Z. Collect. Czech. Chem. Comm., 1970, 35, 3618.

145. Paquette, L.A.; Berk, H.C.; Degenhardt, C.R.; Ewing, G.D. J. Am. Chem. Soc., **1977**, 99, 4764.
146. (a) Berlin, K.D.; Khayat, M.A.R. Tetrahedron, **1966**, 22. (b) Gompper, R.; Schelbe, J.; Schneider, C.S. Tetrahedron Lett., **1978**, 3897. (c) Hoffmann, R.W.; Bressel, U.; Gelhaus, J.; Hauser, H.; Möhl, G. Chem. Ber., **1971**, 104, 2611. (d) Jackson, A.H.; Matlin, S.A.; Rees, A.H.; Towill, R. J. Chem. Soc. Chem. Comm., **1978**, 646.
147. Huisgen, R.; Möbius, L.; Müller, G.; Stangl, H.; Szeimies, G.; Vernon, J.M. Chem. Ber., **1965**, 98, 3992.
148. (a) Brisdon-Jones, F.S.; Buckley, G.D.; Cross, L.H.; Driver, A.P. J. Chem. Soc., **1951**, 2999. (b) Brisdon-Jones, F.S.; Buckley, G.D. J. Chem. Soc., **1951**, 3009.
149. Reimlinger, H.K.; Skattelbol, L. Chem. Ber., **1961**, 94, 2429.
150. (a) Micheida, C.J. Tetrahedron Lett., **1968**, 2281. (b) Kellog, R.M., In *Photochemistry of Heterocyclic Compounds*; Buchardt, O. Ed.; Wiley: New York, 1976; pp 385, 386.
151. (a) Lee, S.L.; Cameron, A.M.; Warkentin, J. Can. J. Chem., **1972**, 50, 2326. (b) Meier, H.; Zeller, K.P. Angew. Chem., **1977**, 89, 876. (c) Meier, H.; Zeller, K.P. Angew. Chem. Int. Ed. Eng., **1977**, 16, 835.
152. Back, Th.G.; Barton, D.H.R.; Britten-Kelly, M.R.; Guziec, F.S. J. Chem. Soc. Perkin Trans. I, **1976**, 2079.
153. (a) Thijs, L.; Wagenaar, A.; Van Rens, E.M.M.; Zwanenburg, B. Tetrahedron Lett., **1973**, 3589. (b) Bonini, B.F.; Maccagnani, G.; Wagenaar, A.; Thijs, S.; Zwanenburg, B. J. Chem. Soc. Perkin Trans. I, **1972**, 2490. (c) Vernier, C.G.; Gibbs, C.G. Tetrahedron Lett., **1972**, 2293.
154. Ykman, P.; L'abbé, G.; Smets, G. Tetrahedron, **1973**, 29, 195, and references cited therein.
155. Paulissen, R. J. Chem. Soc. Chem. Comm., **1976**, 219.
156. Saunier, Y.M.; Danion-Bougot, R.; Danion, D.; Carri Tetrahedron, **1976**, 32, 1995.
157. Gagneux, A.; Winstein, S.; Young, W.G. J. Am. Chem. Soc., **1960**, 82, 5956.
158. (a) Vandensavel, J.M.; Smets, G.; L'abbé, G. J. Org. Chem., **1973**, 38, 675. (b) L'abbé, G. Bull. Soc. Chim. Fr., **1975**, 1127.
159. Pocar, D.; Ripamonti, M.C.; Stradi, R.; Trimarco, P. J. Heterocycl. Chem., **1977**, 14, 173.
160. Vandensavel, J.-M.; Smets, G.; L'abbé, G. J. Org. Chem., **1973**, 38, 675.

161. Grashey, R.; Adelsberger, K. Angew. Chem. Int. Ed. Engl., 1962, 1, 267.
162. Grashey, R.; Lutermann, H.; Schmidt, R.; Adelsberger, K. Angew. Chem. Int. Ed. Engl., 1962, 1, 406.
163. There is no evidence to suggest that the 1,3-dipolar cycloaddition between 7-*tert*-butoxynorbornadiene and diphenyldiazomethane is reversible (see Reference 14), and thus under thermodynamic control, although cycloreversion processes of similar reactions have been well documented (Ref. 136-162). The *syn-endo*, *anti-endo*, and *anti-exo* adducts are known to be very stable at ambient temperatures, as solids or in most solutions. To confirm the absence of reversibility in the reaction, the *syn-exo*, *anti-exo* and *syn-endo* adducts were stored in CDCl₃ at 24 ± 2°C for 79 days. NMR analysis revealed that no cycloreversion occurred.
164. Lussan, C.; Jungers, J.C., Bull. Soc. Chim. Fr., 1968, 2678.
165. Uschold, R.E.; Taft, R.W., Org. Mag. Res., 1969, 1, 375.
166. Abraham, M.; Grellier, P.L.; Abboud, J.-L.; Doherty, R.M.; Taft, R.W. Can. J. Chem., 1988, 66, 267.
167. Marcus, Y. J. Sol. Chem., 1984, 13, 599.
168. Total volumes of each monoadduct were calculated using the Discover molecular modelling program from BIOSYM.
169. Smith, L.I.; Howard, K.L. *Organic Synthesis*, Vol. 3; Wiley: New York, 1955; pp 351-352.
170. (a) Calvert, J.G.; Pitts, J.N. *Photochemistry*; Wiley: New York, 1966, p 467. (b) DeMore, W.B.; Pritchard, H.O.; Davidson, N., J. Am. Chem. Soc., 1959, 81, 5874. (c) Lardy, G.C., J. Chim. Phys., 1924, 21, 288.
171. Burden, A.G.; Collier, G.; Shorter, J. J. Chem. Soc. Perkin Trans. II, 1976, 1627.
172. Kagiya, T.; Sumida, Y.; Inoue, T. Bull. Chem. Soc. Jpn., 1968, 41, 767.
173. Riddick, J.A.; Bunger, W.B.; Sakano, T.K., *Techniques of Chemistry Organic Solvents. Physical Properties and Methods of Purification* 4th ed., Wiley: New York, 1982.
174. Aldrich Chemical Company catalog, 1991.
175. Kamlet, M.J.; Abboud, J.-L.M.; Abraham, M.H.; Taft, R.W. J. Org. Chem., 1983, 48, 2877.

Acknowledgements

I wish to thank Dr. David Crumrine for his advice, participation, and encouragement over the years. I am grateful for the opportunity and financial support provided by Loyola University. I also wish to thank Dr. Jaselskis for allowing me the long term use of his equipment. Many thanks to Chandra Srinivasan for obtaining some very useful NMR spectra. Thanks to Dr. David Ricketts for taking the time to compute some essential data for this research and to Dr. Gerald Funk for giving his time to clarify some aspects of statistical analysis. My heartfelt thanks goes to Gary Madsen for his enduring patience, generosity and technical skills in helping to produce this manuscript.

I am grateful to the members of the dissertation committee, Dr. James Babler, Dr. Mary Boyd, Dr. Daniel Graham, and Dr. Robert Walter for consenting to be on the committee, with all of the time and effort that it entails. Additional thanks goes to Dr. Graham for writing some computer programs for me.

VITA

The author, Sheila Louise Celsor, was born on June 26, 1959 in Chicago, Illinois.

In September 1977, Ms. Celsor entered Northeastern Illinois University, and graduated in 1982 with a Bachelor of Science degree in Chemistry and Biology. Ms. Celsor was employed as a quality assurance chemist at Diosynth Inc. from September 1982 to January 1987.

In August 1987, she joined the Chemistry Department at Loyola University of Chicago to pursue a Doctor of Philosophy degree in Chemistry. She was awarded a graduate assistantship from September 1987 to September 1991, and from April 1992 to August 1992, and was awarded a teaching fellowship from September 1991 to April 1992, enabling her to complete the degree of Doctor of Philosophy in 1993.

APPROVAL SHEET

The dissertation submitted by **Sheila L. Celsor** has been read and approved by the following committee:

Dr. David S. Crumrine, Director
Associate Professor, Chemistry
Loyola University of Chicago

Dr. James H. Babler
Professor, Chemistry
Loyola University of Chicago

Dr. Mary K. Boyd
Assistant Professor, Chemistry
Loyola University of Chicago

Dr. Daniel Graham
Assistant Professor, Chemistry
Loyola University of Chicago

Dr. Robert I. Walter
Professor Emeritus, Chemistry
University of Illinois, Chicago

The final copies have been examined by the director of the dissertation and the signature which appears below verifies the fact that any necessary changes have been incorporated and that the dissertation is now given final approval by the Committee with reference to the content and form.

The dissertation is, therefore, accepted in partial fulfillment of the requirements for the degree of Doctor of Philosophy.

15 January 1993
Date

David Crumrine
Directors Signature

Sheila L. Celsor

Loyola University of Chicago

EFFECT OF SOLVENT ON 1,3-DIPOLAR CYCLOADDITION TRANSITION STATES

1,3-dipolar cycloadditions are concerted, pericyclic reactions which are synthetically useful since they provide a facile route to heterocyclic ring systems. Because these reactions do not involve a charge-separated intermediate there is usually an absence of large, solvent-induced rate changes, except when water is used as solvent or cosolvent. However, among those cycloadditions resulting in tricyclic ring systems, stereospecificity is either enhanced or altered in the presence of different solvents. Identification of the solvent properties giving rise to stereochemical preferences would contribute to an understanding of the mechanism including activated complex formation as well as a means by which stereoselectivities can be manipulated and optimized.

In this study, the cycloaddition of 7-*tert*-butoxynorbornadiene and diphenyldiazomethane in various solvents resulted in significant solvent dependence of stereoselectivity, as shown by shifts in distribution of the four pyrazoline adducts. Correlation of the shifts in syn-anti stereoselectivity with solvent parameters that reflect a range of solvent polarity, hydrogen-bond donor-acceptor ability, polarizability, Lewis acidity-basicity, etc., has been accomplished. A good correlation between a solvent parameter and experimental outcome is a strong indication that the parameter is directly involved in the reaction transition state. Multiple solvent parameter treatments were more successfully correlated than single solvent polarity parameter treatments. The multiple parameter correlations employed were the Koppel-Palm equation (4 parameters),

the Swain-Swain-Powell-Alunni equation (2 parameters), and the Abraham-Kamlet-Taft expression (4 parameters).

A strongly competing side reaction of diphenyldiazomethane condensation complicated the cycloaddition by rapidly consuming the 1,3-dipole. As a result, although the overall yields of the model reaction were also monitored, these results did not correlate with solvent parameters. Rates of reaction for cycloaddition in hexane and acetonitrile were determined over a 4 month period. These results confirmed that the stereoselectivity in a given solvent does not shift over time, and that the cycloaddition is classically second order (first order in both reactants).